

The Sirtuins and SMCs: Regulators of Heterochromatin in Time and Space

Ryan D. Fine

New Eagle, Pennsylvania

B.S., Pennsylvania State University, 2013

M.S., University of Virginia, 2015

A Dissertation Presented to the Graduate Faculty of the University of Virginia in

Candidacy for the Degree of Doctor of Philosophy

Department of Biochemistry and Molecular Genetics

University of Virginia

April, 2019

Abstract

With average length of human healthspan not matching the average length of lifespan, aging is perhaps the biggest obstacle facing modern society due to the economic and social burdens of dealing with chronic disease. Thus, it has become essential to discover mechanistic causes behind the aging process itself to devise strategies and eliminate this gap. In this regard, a large body of research has been conducted on the sirtuin family of NAD⁺-dependent protein deacetylases conserved from bacteria to humans. These fascinating enzymes link a cell's metabolic state to protein acetylation status and epigenetic silencing of heterochromatin. General activation of sirtuins increases lifespan across a range of model organism from yeast to mice through increased stabilization of heterochromatic loci. Furthermore, dietary supplementation of precursors to the sirtuin activator, NAD⁺, increases healthspan in mice, suggesting a route for therapeutic interventions in humans. However, the seven human sirtuins play a wide array of roles and, in some cases, counter-act the effects of one another, warranting more investigation into their regulatory functions.

An equally conserved family of proteins known as the structural maintenance of chromosomes (SMCs) have been studied for roles in segregation of mitotic chromosomes. Yet, throughout the years of sirtuin driven heterochromatin research, the SMCs have time and time again displayed a number of roles in helping the nuclear sirtuins establish and maintain heterochromatic loci. While the SMCs generally work independently, there is extensive interplay between family members in driving chromosomal structural changes, especially within the nucleolus of a cell. More importantly, several SMC mutations cause a wide range of diseases in patients due to defects in heterochromatin as opposed to sister chromatid segregation. This thesis attempts to explore the mechanistic roles of both families within the context of heterochromatin.

Publications

The following articles correspond to material presented in the respective chapters. I do not claim sole credit for any information contained within.

Chapter II:

Li, M.*, Fine, R. D.*, Dinda, M., Bekiranov, S. and Smith, J. S. (2019) A Sir2-regulated locus control region in the recombination enhancer of *Saccharomyces cerevisiae* specifies chromosome III structure. PLoS Genet. (in revision at time of writing)

Chapter III:

Fine, R.D., Maqani, N., Li, M., Franck, E., and Smith, J.S. (2019). Depletion of limiting rDNA structural complexes triggers chromosomal instability and replicative aging of *Saccharomyces cerevisiae*. Genetics. (in press)

Table of Contents

	Page
Title Page	i
Abstract	ii
Publications	iii
Table of Contents	iv
List of Figures	vi
List of Abbreviations	ix
Chapter I: Introduction	1
<i>Budding Yeast Heterochromatin</i>	2
<i>Fission Yeast and Beyond</i>	13
<i>The Sirtuin Family of NAD⁺ Deacetylases</i>	15
<i>The SMC Super Family</i>	21
<i>Cohesin</i>	22
<i>Condensin</i>	25
<i>Smc5/6 Complex</i>	27
<i>Dysregulation of Sirtuins and SMCs during Aging: A Heterochromatin Malfunction?</i>	29
Chapter II: Sir2 and Condensin Regulation of <i>RDT1</i> and Chromosome III Structure	36
<i>Introduction</i>	37
<i>Materials and Methods</i>	40
<i>Results</i>	47
<i>Discussion</i>	65
<i>Supplemental Data</i>	71
Chapter III: Sir2 and Cohesin Regulation of Genome Stability	74
<i>Introduction</i>	75

<i>Materials and Methods</i>	79
<i>Results</i>	87
<i>Discussion</i>	107
<i>Supplemental Data</i>	114
Chapter IV: Conclusions and Future Directions	116
Appendix A: Future Directions Supporting Data	126
Acknowledgements	131
References	132

List of Figures

Figure 1.1. Model of heterochromatin formation at <i>HM loci</i> .	3
Figure 1.2. Hi-C reveals spatial features of budding yeast genome organization	10
Figure 1.3. Hi-C reveals <i>cis</i> and <i>trans</i> telomeric interactions.	12
Figure 1.4. Phylogenetic distance tree of sirtuin deacetylases.	16
Figure 1.5. The SMC super family of complexes in budding yeast.	22
Figure 2.1. <i>MATa</i> -specific binding of Sir2 and condensin to the recombination enhancer (RE)...	48
Figure 2.2. <i>RDT1</i> is a novel Sir2 regulated gene.	50
Figure 2.3. <i>MATa</i> -specific transcription of <i>RDT1</i> is repressed by Sir2 and Hst1.	51
Figure 2.4. Identification of a 100bp sequence that recruits Sir2/condensin and represses <i>RDT1</i> expression.	53
Figure 2.5. Deletion of Sir2 or the <i>RDT1</i> promoter Sir2/condensin binding site does not affect protein levels of Sir2 or Myc-tagged condensin subunits.	54
Figure 2.6. The <i>RDT1</i> -proximal Mcm1/a2 binding site (DPS2) is important for Sir2 and condensin recruitment.	54
Figure 2.7. Dynamics of Sir2 and condensin binding at the <i>RDT1</i> promoter and <i>MATa</i> locus during mating-type switching.	57
Figure 2.8. The Sir2/condensin binding site controls chromosome III architecture.	59
Figure 2.9. Deleting the Sir2/condensin binding site within the RE (100bp Δ) does not alter Sir2 function at <i>HMLα</i> .	60
Figure 2.10. Loss of Sir2 and the Sir2/condensin binding site alters mating-type switching.	62

Figure 2.11. Auxin inducible degron (AID)-mediated depletion of Brn1 does not derepress <i>RDT1</i> or <i>HMLα</i>	63
Fig 2.12. Effects of condensin depletion on mating-type switching.	64
Figure 3.1. Depletion of Sir2 complexes and elevated chromosome instability in replicatively aging cells.	89
Figure 3.2. Chromosome instability is linked to rDNA stability and cohesin redistribution	91
Figure 3.3. The Lrs4 subunit of cohibin/monopolin is depleted in aged yeast cells.	92
Figure 3.4. RLS of the cohesion visualization strains is normal and unaffected by position of the lacO array.	94
Figure 3.5. Sister chromatid cohesion is weakened in aged yeast cells.	95
Figure 3.6. Modulation of RLS and CIN by manipulating <i>MCD1</i> and <i>SIR2</i> expression levels....	97
Figure 3.7. Galactose shortens yeast RLS in the common yeast BY4741/4742 strain background.	99
Figure 3.8. Doxycycline-induced <i>MCD1</i> overexpression in WT and <i>mcd1Δ</i> strains....	100
Figure 3.9. Doxycycline-induced <i>MCD1</i> overexpression in BY Background.	101
Figure 3.10. CR suppresses the CIN and RLS defects of <i>sir2Δ</i> and <i>mcd1</i> mutants.	103
Figure 3.11. Chromosomal instability during replicative aging is linked to the rDNA.	105
Figure 3.12. Deleting Sir2 had no effect on the left rDNA flank chromatin loop interaction with centromere XII.	106
Figure S3.1. Detailed western blot and bud scar count quantification.	114
Figure S3.2. rDNA stability does not affect sister chromatid cohesion.	115
Figure A.1. Cohibin, condensin, and Sir2 genome-wide transcriptional regulation.	126
Figure A.2. Deletion of <i>SIR2</i> predominantly affects budding yeast heterochromatin structure.	127

Figure A.3 Sir2 is required for cohesin binding within the rDNA array.	128
Figure A.4. Model of condensin loop-extrusion at the RE locus on chromosome III.....	129
Figure A.5. Model of cohibin recruitment of condensin to the <i>RDT1</i> promoter.	130
Figure A.6. Cohibin physically interacts with Mcm1.	130

List of Common Abbreviations

3C	Chromosome Conformation Capture
ChIP	Chromatin Immunoprecipitation
ChIP-seq	Chromatin Immunoprecipitation Sequencing
CIN	Chromosome Instability
CLS	Chronological Lifespan
CR	Calorie Restriction
DNA	Deoxyribonucleic Acid
GAL	Galactose
GLU	Glucose
Hi-C	High Throughput Chromosome Conformation Capture
HML	Homothallic Mating Left
HMR	Homothallic Mating Right
mRNA	Messenger Ribonucleic Acid
NAD ⁺	Nicotinamide Adenine Dinucleotide
NTS1	Non-Transcribed Spacer 1
RAF	Raffinose
rDNA	Ribosomal DNA; Nucleolus
RE	Recombination Enhancer
RENT	Regulator of Nucleolar Silencing and Telophase
RLS	Replicative Lifespan
RNA	Ribonucleic Acid
rRNA	Ribosomal Ribonucleic Acid
SCC	Sister Chromatid Cohesion
SIR	Silent Information Regulator
SMC	Structural Maintenance of Chromosomes
TPE	Telomere Position Effect
qPCR	Quantitative Polymerase Chain Reaction
qRT-PCR	Quantitative Reverse Transcriptase Polymerase Chain Reaction

Chapter I

Introduction

In early 2001, the first public releases of the human genome sequencing project were published for all the world to explore (LANDEN *et al.* 2001; VENTER *et al.* 2001), yet to this very day, a significant portion of the human genome, 5-10%, has remained elusive and refused to yield the entirety of its DNA alphabetical sequence (ALTEMOSE *et al.* 2014). This remaining portion is composed of highly repetitive DNA sequences that can span entire megabases. Thus, the cause of this sequencing problem lies in the limitations of modern-day sequencing technology, which is either unable to reproduce the entirety of a single repeat during the sequencing process itself or an inability to be assembled by algorithms, which require long stretches of unique sequence (TREANGEN AND SALZBERG 2014). This repetitive DNA, or more precisely described chromatin, composed of DNA, histones, and non-histone proteins, often belongs in the category of “different” chromatin, otherwise known as heterochromatin, and first defined by Emil Heitz in 1928 (HEITZ 1928). Heterochromatin has often remained in the shadows of its brethren, euchromatin, which is responsible for encoding the genetic information necessary to produce RNA and proteins as part of a process generally described as the central dogma of biology (CRICK 1970). However, it has become quite clear that failure to maintain the distinct characteristics of heterochromatin, namely transcriptional gene silencing, DNA compaction, and spatial compartmentalization within the nucleus of a cell, results in a wide array of human diseases and increased cancer susceptibility (reviewed in (HAHN *et al.* 2010). Researchers have been quite fortunate over the past several decades to elucidate the mechanisms of this unruly chromatin by studying the humble and genomically simplified model organism

budding yeast, *Saccharomyces cerevisiae*, as well as its distant relative, the fission yeast, *Schizosaccharomyces pombe*.

Budding Yeast Heterochromatin

Between the two species of yeast, *Saccharomyces cerevisiae* is considered simpler in terms of general heterochromatin mechanisms owing to a lack of methylation modifications and associated proteins often found in higher Eukaryotes. This includes direct DNA methylation, trimethylation of H3K9, and trimethylation of H3K27, which are respectively recognized by heterochromatin protein 1 (HP1) and Polycomb repressive complex 1 (PRC1) to induce heterochromatin domains and gene silencing in humans (NESTOROV *et al.* 2013). Additionally, budding yeast lacks pericentric heterochromatin probably due to lack of a regional centromere (for more detail; see *Fission Yeast and Beyond*). Yet arguably no other model organism other than *Drosophila melanogaster* has provided us with a richer detail about the governing principles of heterochromatin formation and regulation.

In budding yeast, there are three classes of heterochromatin located at the silent mating-type loci, telomeric loci, and rDNA array (reviewed in (GARTENBERG AND SMITH 2016). The silent mating-type loci, *HMR* and *HML*, and the telomeres form similar domains of heterochromatin and have led the way in the development of a minimum two-step model of formation. Heterochromatin inducing proteins are first nucleated to a DNA locus by sequence specific DNA binding factors and then “spread” in a processive and directional manner (Figure 1.1A). The ribosomal DNA (rDNA) is more distinct owing to its complex nature of being both transcriptionally silent and transcriptionally active at the same time throughout the entire cell cycle (GERKE AND SEUFORT 2019). Indeed, the 35s rRNA transcribed by RNA polymerase I and

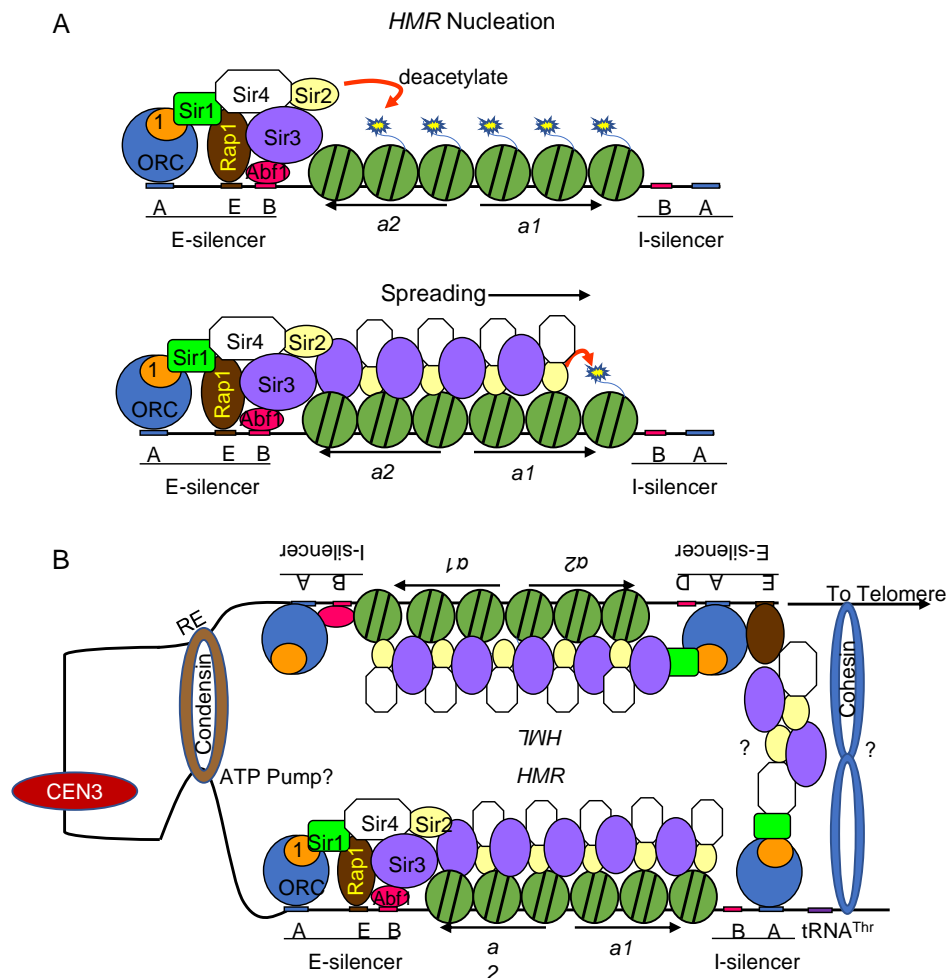


Figure 1.1. Model of heterochromatin formation at *HM loci*. (A) Basic model of silencing. The E and I silencers have DNA motifs recognized by ORC, Rap1, and ABF1 in varying combinations. The Sir1-4 proteins are then nucleated, positioning the histone deacetylase, Sir2, in proximity to acetylated side chains (tails) of histones H3 and H4 on nearby nucleosomes. Sir2 catalyzed removal of the acetyl residues results in new binding sites for Sir3 and Sir4 of additional *SIR* complex (Sir2, Sir3, and Sir4) to propagate silencing and heterochromatin formation in a directional manner. (B) Updated model of silencing. Hi-C studies have indicated *HML* and *HMR* are in spatial proximity to one another in *MATa* cells. Cohesin prevents *SIR* spreading beyond $tRNA^{Thr}$ at *HMR*, but may also help create the *SIR* mediated 3-D interaction. Condensin appears to be required for *HMR* and *HML* interaction through a currently undefined process (Li *et al.* 2019). (Adapted from Jeffrey S. Smith unpublished slides).

the 5s rRNA transcribed by RNA polymerase III in the rDNA accounts for roughly 60% of total transcriptional activity in a cell and 80% of total RNA (WARNER 1999). Therefore, it may not be surprising that RNA Pol I is also responsible for spreading a significant portion of transcriptional silencing within the rDNA (BUCK *et al.* 2002, BUCK *et al.* 2016).

While each of these loci have unique aspects unto themselves, they all require a universal protein to form transcriptionally silent heterochromatin known as Sir2. Sir2 is an NAD⁺ dependent protein deacetylase and the founding member of the highly conserved sirtuin family (LAUNDRY *et al.* 2000; IMAI *et al.* 2002). Sir2 was originally identified as recessive mutation, *mar1-1*, required for transcriptional silencing of the yeast silent mating-type loci, *HMR* and *HML*, along with its fellow Silent Information Regulators, Sir1, Sir3, and Sir4 (KLAR *et al.* 1979; RINE AND HERSKOWITZ 1987). *HMR* and *HML* are flanked by cis-acting DNA elements, the E and I silencers, containing DNA sequences recognized by up to three DNA binding proteins known as Rap1, Abf1, and the origin recognition complex (ORC1) (BRAND *et al.* 1985; MCNALLY AND RINE 1991). These proteins in turn nucleate the Sir proteins through direct physical interactions to promote heterochromatin formation despite having other non-heterochromatic roles such as Rap1 activation of ribosome protein genes (TRIOLO AND STERNGLANZ 1996; LOO *et al.* 1995; SONG AND JOHNSON 2018). Sir2 then primarily catalyzes the removal and transfer of acetyl moieties from lysine 16 on the tail of histone H4 and to a smaller extent the tail of histone H3 to the ADP-ribose ring of NAD⁺ (JOHNSON *et al.* 1990; THOMPSON *et al.* 1994; TANNY AND MOAZED 2001). This process results in the cleavage of one molecule of NAD⁺ into the pan-sirtuin inhibitor nicotinamide (NAM) and a molecule of 2'-O-acetyl-ADP-ribose (AAR) (TANNER *et al.* 2000; AVALOS *et al.* 2005). The *SIR* complex composed of Sir2, Sir3, and Sir4 then “spreads” across the cryptic mating loci via sequential

histone deacetylation by Sir2 followed by additional Sir3 and Sir4 binding to the hypoacetylated histone tails (HECHT *et al.* 1995; RUSCHE *et al.* 2002).

Unlike the other Sir proteins, Sir1 only plays a role in the establishment phase of heterochromatin, specifically at the silent mating-type loci. Sir1 primarily functions as a physical link between the Orc1 subunit of the origin recognition complex and Sir4 (TRIOLO AND STERNGLANZ 1996; BOSE *et al.* 2004). This is why it has only a minor silencing defect when mutated compared to the other Sir proteins (RINE *et al.* 1979). However, the lack of full blown derepression in *sir1-1* mutants revealed another key insight into the mysterious nature of heterochromatin, namely epigenetic heritability. In the case of the transcriptionally silenced state of the silent mating-type loci, it was shown that two distinct populations of *sir1-1* mutants existed. The first was cells with a derepressed *HML α* that would undergo mitosis to produce offspring of the same phenotype, and the second was cells whose lineage maintained silencing of *HML α* , despite the two populations being genetically identical (PILLUS AND RINE 1989). This suggested that heterochromatic heritability required something beyond the genetic code. This idea, now known as epigenetics, has become an entire field on its own, extending its influence to encompass euchromatin, yet clues of its existence started with dissection of heterochromatin in budding yeast.

Similar to Sir1, Sir4 primarily serves as a scaffold protein. Sir4 is thought to form a heterodimer with Sir2 outside of heterochromatin through interaction with a conserved N-terminal subdomain of Sir2 (MOAZED *et al.* 1997). Sir3 was originally thought to independently associate with the Sir2-Sir4 dimer at chromatin to form the complete SIR complex in an AAR-dependent fashion (HOPPE *et al.* 2002). The requirement for AAR however has been challenged with clear evidence that a Sir3-Hos3 deacetylase chimera is capable of forming heterochromatin

with Sir4 even in the absence of all 5 AAR producing yeast sirtuins, (CHOU *et al.* 2008). This suggests that histone deacetylation by Sir2 is the only requirement for *SIR* complex formation, which appears to be true, since H4K16ac promotes Sir2-Sir4 binding, but represses Sir3 binding (OPPIKOFER *et al.* 2011).

The *SIR* complex is also involved in defining a second major form of heterochromatin in yeast, known as telomeric silencing, via recruitment by Rap1 at telomeric T-G₁₋₃ repeats through physical interaction with Sir3 and Sir4 (APARICIO *et al.* 1991; MORETTI *et al.* 1994; STRAHL-BOLSINGER *et al.* 1997). This form of silencing in yeast is classically called “the telomere position effect” (TPE) since Pol II genes inserted near the left arm of chromosome VIII or right arm of chromosome V were transcriptionally silenced in a manner similar to the position effect variegation of the *white* gene in fruit flies (GOTTSCHLING *et al.* 1990). Flies possessing the *white* gene near pericentric heterochromatin exhibit a variable amount of *white* gene expression resulting in a mosaic red and white pigmentation of eye color (WALLRATH AND ELGIN 1995). Therefore, unlike the silent mating-type loci, telomeric heterochromatin is positionally less well defined, with each telomere possessing varying degrees of repressive chromatin that can often be discontinuous (PRYDE AND LOUIS 1999). The *SIR* complex was thought to be essential for this form of transcriptional silencing because it continuously spreads from Rap1 initiation sites over a wide array of distances spanning several kb (APARICIO *et al.* 1991; STRAHL-BOLSINGER *et al.* 1997). However, the exact role of the *SIR* complex has been called into question since as few as 6% of subtelomeric genes appear to be transcriptionally dysregulated when deleting any of the *SIR* genes (ELLAHI *et al.* 2015). One alternative view is that the *SIR* complex may repress telomere recombination similar to rDNA recombination (described below), but this hypothesis has not been clearly tested (ELLAHI *et al.* 2015).

The third and final major heterochromatin locus in budding yeast is the rDNA, which forms the basis of the nucleolus. It is readily apparent that the rDNA array represents unique challenges to a cell that are completely foreign to the other two heterochromatic loci. First, it is harbored on chromosome XII and composed of 150-200 repeats of a 9.1kb unique segment of DNA representing roughly 10% of the entire yeast genome (PETES 1979). In addition to sheer size, it is the only locus in which all three RNA polymerases naturally produce transcriptional output, though Pol II is responsible for producing non-coding RNAs only in the absence of Sir2, which simultaneously attempts to maintain a hypoacetylated and silent chromatin state. Indeed, Sir2 was originally shown to mediate silencing of the rDNA through experimental insertion of Pol II transcribed genes and Ty1 retrotransposable elements (SMITH AND BOEKE 1997; BRYK *et al.* 1997), but has since been shown to be responsible for repressing endogenous Pol II-transcribed non-coding RNA genes within the rDNA array (LI *et al.* 2006).

In contrast to the *HM* loci and telomeres, Sir2 localizes to the rDNA array via direct interaction with the essential gene, Net1, as part of the nucleolar RENT complex composed of Sir2, Net1, and Cdc14 (SHOU *et al.* 1999; STRAIGHT *et al.* 1999). The RENT complex is sub-localized to non-transcribed spacer 1 (NTS1, also known as IGS1) and the Pol I promoter region which defines the edge of NTS2 via Net1 interactions with Fob1 (discussed in detail later) and Pol I, respectively (SHOU *et al.* 2001; HUANG *et al.* 2003). The third component of RENT, Cdc14, is an essential phosphatase that inactivates mitotic cyclin dependent kinases (CDKs) through upregulation of APC/C mediated proteolysis of mitotic cyclins and the CDK inhibitor, Sic1, enabling cells to exit from mitosis (VISINTIN *et al.* 1998; BARDIN AND AMON 2002). Throughout the rest of the cell cycle, Cdc14 activity is inhibited by Net1 sequestering it in the nucleolus. Intriguingly enough, both Cdc14 and Sir2 are released from the rDNA during the

anaphase/telophase transition (STRAIGHT *et al.* 1999). While it is clear that Cdc14 is required for mitotic exit during this time, it is not known what function (if any) Sir2 release facilitates.

Due to direct interaction with Pol I, RENT mediated-silencing in the rDNA spreads ~2.8 kb beyond the last repeat of the tandem array in the same direction as RNA Pol I transcription (BUCK *et al.* 2002), until a boundary element (tRNA^{Gln}) gene is approached (BIWAS *et al.* 2009). Another silencing boundary consisting of tRNA^{Thr} is located between *HMR* and the telomere of chromosome III (DONZE *et al.* 1999; DONZE AND KAMAKAKA 2001; Figure 1.1B). The cohesin complex is required for the boundary function, as are the transcription factors TFIIB and TFIIC (DONZE *et al.* 1999; VALENZUELA *et al.* 2009). The mechanism of TFIIC and TFIIB is not fully understood, but artificial targeting of TFIIC alone by an array of B-box motifs (that only TFIIC can bind) is sufficient to induce insulator/boundary function without Pol III transcription (VALENZUELA *et al.* 2009). The key step appears to be maintenance of a nucleosome free region by recruiting chromatin remodelers like the RSC and ISW2 complexes to evict nucleosomes, which would simultaneously promote TFIIC binding and inhibit the Sir proteins from creating a highly ordered nucleosome array as part of the heterochromatin process (DHILLON *et al.* 2009). Importantly, tDNAs have been shown to act as silencing insulators in human cells by preventing repression of transgenes inserted near heterochromatin suggesting the barrier activity is conserved and worth further investigation (RAAB *et al.* 2012).

An alternative anti-spreading/anti-heterochromatin mechanism exists in the form of the acetyltransferase, Sas2, which acetylates H4K16 to directly counteract the biochemical activity of Sir2 (SUKA *et al.* 2002). Sas2 is special because it is not limited to acetylating a particular region of the genome and has even been proposed to counteract Sir2 deacetylation at the budding yeast point centromere, which is euchromatic, unlike the regional centromeric regions in *S.*

pombe (KIMURA *et al.* 2002, CHOY *et al.* 2011). Both of these physical and biochemical anti-heterochromatin mechanisms serve at least two purposes. The first is the obvious prevention of heterochromatin formation over such vast distances that it impinges upon transcriptional expression of essential genes in euchromatin. The second is that the Sir proteins, especially Sir2 and Sir3, have been shown to be severely limiting with a genetic manipulation as simple as deleting Sir4 resulting in increased rDNA expression or overexpression of *SIR3* restoring the telomere position effect in *Rap1 Δ BBp* expressing cells (SMITH *et al.* 1998; WILEY AND ZAKIAN 1995). Thus, preventing the *SIR* complex from spreading beyond target loci allows proper silencing to be established and maintained (KIMURA *et al.* 2002).

Initial analysis of telomeres by fluorescent microscopy revealed that heterochromatin had the ability to spatially self-organize away from euchromatin at the edge of the nuclear envelope (BYSTRICKY *et al.* 2005; SCHOBER *et al.* 2008). Furthermore, this process was reliant upon the heterochromatic *SIR* complex as well as telomere specific Ku proteins (BYSTRICKY *et al.* 2005). More recently, a new technological breakthrough in three-dimensional visualization of chromatin at the sequence level has given even greater insight. The family of techniques, dubbed chromosome conformation capture (3C), were first developed in budding yeast to reveal interactions between the point centromeres of chromosomes in *trans* (DEKKER *et al.* 2002; Figure 1.2). The techniques involve locking-in spatial chromatin interactions by extensive crosslinking of proteins and DNA with formaldehyde. DNA is then digested with a frequent cutting restriction enzyme such as *HindIII*. For Hi-C, DNA ends are then filled in with biotinylated nucleotides and blunt end ligated to form chimeric junctions between two different regions of DNA (LIBERMAN-AIDEN *et al.* 2009). The chromatin is then sheared into smaller fragments and

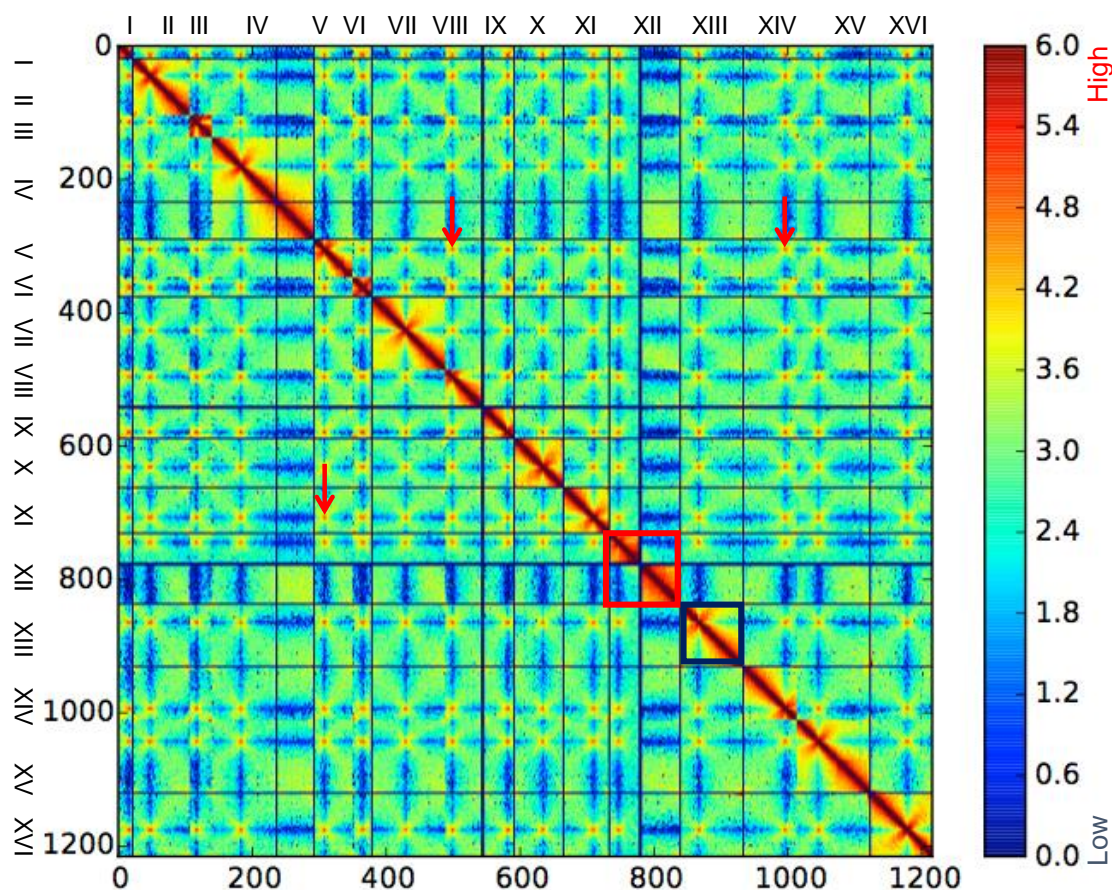


Figure 1.2. Hi-C reveals spatial features of budding yeast genome organization. From left to right, top to bottom, the entire yeast genome composed of 16 linear chromosomes can be visualized in a two-dimensional matrix where intersecting points correspond to three-dimensional interaction between two genomic regions. All 16 yeast centromeres spatially cluster *in trans* with the appearance of dots (red arrows) revealing their three-dimensional interaction. However, chromosomes clearly prefer to act *in cis* with a black diagonal line running down the center of the plot from which “square” domains of interaction outlining each chromosome emanate (e.g. chromosome XIII; black square). Unlike the other chromosomes, the left and right arms of chromosome XII (red square) show no interaction due to the rDNA array physically separating them. Furthermore, the rDNA is currently unmapped (black line in middle of chromosome XII) because the sequence underlying the 150-200 repeats is indistinguishable. Scale represents the natural log of iteratively corrected paired-end reads from a Hi-C experiment. Genome was binned at 10kb resolution. (R. D. FINE; unpublished data).

chimeric junctions are enriched by streptavidin pull down. Finally, paired-end sequencing from both ends allows reads to be mapped in a 2D matrix to create spatial information (Figure 1.2).

After a matrix has been created, data must be normalized to account for sequencing bias, GC-content, and library size. Iterative correction is one of the preferred methods since it takes an unbiased approach and treats the Hi-C matrix as a purely mathematical matrix. The sum of raw read counts across all binned rows is iteratively driven towards the mean of all row sums by computationally solving the matrix system of equations (IMAKEV *et al.* 2012). This effectively eliminates the sequencing coverage biases of bins and not only reveals three-dimensional clustering between the centromeres, but also *cis* and *trans* interactions between the telomeres of each chromosome as previously seen by microscopy (Figures 1.2 and 1.3).

While Hi-C is great for gathering genome-wide information, targeted interactions by PCR-based 3C has revealed sub-locus interaction between the E and I silencers of the *HMR* locus (VALENZUELA *et al.* 2008). Alternative restriction enzyme digestions, which limit the resolution of 3C, resolved a further layer of complexity by showing the E and I silencers of *HML* spatially interacting in *trans* with their opposite counterparts at the *HMR* locus to reveal a previously unappreciated heterochromatic superstructure (MIELE *et al.* 2009; Figure 1.1B). Presumably these interactions are mediated by protein-protein interactions of *SIR* complex family members and the cohesin and condensin complexes (Chapter II; DONZE *et al.* 1999; MIELE *et al.* 2009). Alas, the complete model is lacking evidence in terms of protein stoichiometry, geometry, and timing. Future studies will hopefully address these questions as they could all be critical in understanding more complex domains of human heterochromatin.

With this insight, one may be tempted to ask about the three-dimensional structure of the rDNA array. A number of studies have generally characterized its position in the genome as

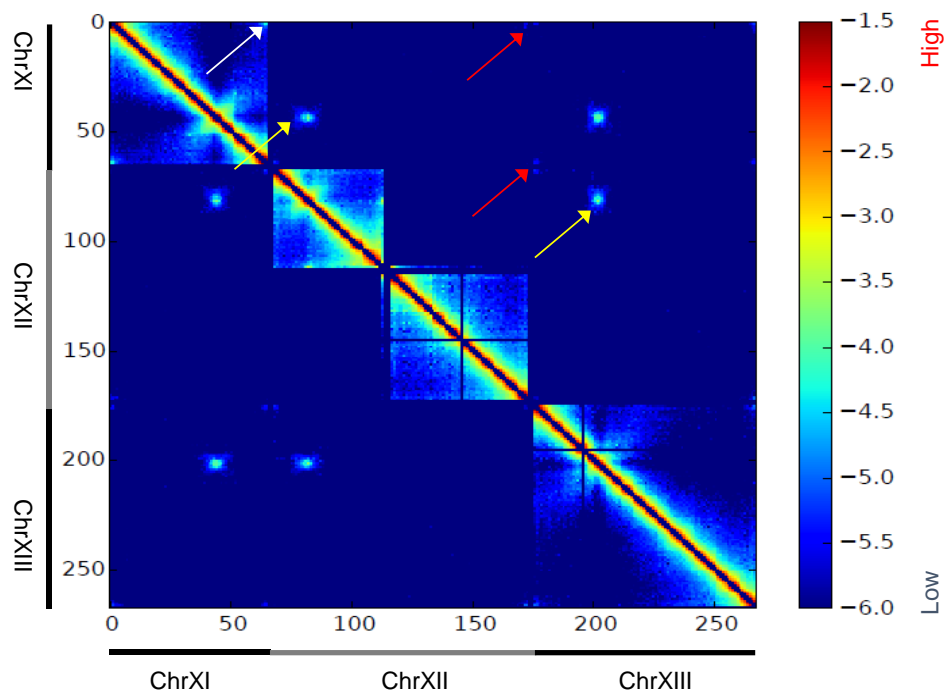


Figure 1.3. Hi-C reveals *cis* and *trans* telomeric interactions. Subset of chromosomes from genome-wide Hi-C data reveals *cis* interactions of chromosome XI telomeres *TELXIL* and *TELXIR* (white arrow) in addition to *trans* interactions between *TELXIL*, *TELXIIR* (top red arrow), and *TELXIII* (bottom red arrow). This plot also recapitulates centromeric clustering (yellow arrows) and separation of the left and right arms of chromosome XII by the rDNA array as seen in Figure 1.2.

always being separate from the other chromosomes (DUAN *et al.* 2010; TEDDEI AND GASSER 2012). Recent 3C work however, has gone on to show the leftmost unique sequence flanking the array, where the aforementioned Pol I transcriptional silencing boundary ends, does come into contact with centromere XII at least during anaphase (LAZAR-STEFANITA *et al.* 2017; FINE *et al.* 2019). Additionally, nucleolar isolation and deep sequencing has revealed multiple nucleolar associated domains (NADs) on all 22 autosomes in human cells suggesting this interaction in yeast may be the norm rather than the exception (DILLINGER *et al.* 2017). Hence, there is a currently uncharacterized process that brings the heterochromatic rDNA into contact with the euchromatic genome at least once per cell cycle in yeast and potentially throughout the cell cycle

in humans undoubtedly presenting a taxing challenge to cells. Unfortunately, the rest of the rDNA remains unmappable with our current sequencing technology due to its high copy number of repeats, but advances in sequencing will surely push our understanding of heterochromatin domains further into the spatial dimension.

Fission Yeast and Beyond

The process of cellular life requires that DNA be replicated and equally passed on to the next generation of cells. The task of equal partitioning of chromosomes falls under the realm of mitosis and requires the SMC family of proteins which will be discussed later on. The physical separation of chromosomes requires a specialized region of DNA known as the centromere, which in budding yeast are called point centromeres, since their sequence is defined by no more than 120bp amounting to a single nucleosome (CLARK AND CARBON 1980). Centromeres, in turn, direct the binding of kinetochore proteins, which are responsible for transmitting the physical motor forces provided by microtubules to pull apart sister chromatids (reviewed in (VERDAASDONK AND BLOOM 2011)). This is where the fourth general domain of heterochromatin, known as pericentric heterochromatin, is found in most eukaryotes including the fission yeast. Pericentric heterochromatin surrounds sequences of DNA called regional centromeres, defined by the replacement of histone H3 with a variant called CENP-A in the canonical histone octamer (SULLIVAN AND KARPEN 2004).

Heterochromatin formation in *S. pombe* and higher eukaryotes is not completely foreign to the mechanisms of silencing already discussed. The histone deacetylation activity of the Sir2 homolog in *S. pombe*, SpSir2, is still essential for heterochromatin silencing at all four major domains (SHANKARANARAYANA *et al.* 2003). Where formation in *S. pombe* begins to differ is

what comes afterwards. Many eukaryotic centromeres are defined by repetitive DNA such as alpha satellites in humans, minor satellites in mice, and the inner (*imr*) and outer (*otr*) centromere repeats in *S. pombe* (PIDOUX AND ALLSHIRE 2004; MCKINLEY AND CHEESEMAN 2016). Within the *otr* repeat of *S. pombe* are two smaller defined repeats termed *dh* and *dg* (NAKASEKO 1987). These elements can be transcribed in the absence of silencing, with the RNAs being further processed by a conserved protein pathway generally responsible for suppressing foreign RNAs known as the RNA interference (RNAi) pathway (VOLPE et al. 2002). After processing the repetitive RNAs, a protein complex known as RITS is capable of targeted binding to the pericentromere through complementary sequence recognition of the RNA produced by RNAi, and in doing so, physically brings along the methyl transferase, Clr4 (VERDEL et al. 2004; SAKSOUK et al. 2015). Additionally, Clr4-methylated H3K9 is bound by the mammalian HP1 homolog of *S. pombe*, Swi6, which enables the nucleated heterochromatin complex to then spread (BANNISTER et al. 2001; HALL et al. 2002).

The remaining conserved heterochromatic loci in *S. pombe* are all silenced in a similar manner requiring the RITS complex and SpSir2 (NOMA et al. 2004). Thus, once again, heterochromatin is formed by an initial nucleation step followed by processive spreading of heterochromatic factors. After recruitment, RITS is capable of interacting with Dicer to locally process aberrant RNAs from the heterochromatic loci that it is bound to *in cis* (NOMA et al. 2004). This reinforcement of silencing is different from *S. cerevisiae* perhaps due to a need to create larger domains of heterochromatin on the order of 10-100kb not observed outside the rDNA in budding yeast. *S. cerevisiae* likely lost the RNAi systems at some point in evolution recently, as it lacks the machinery, but can successfully silence genes when exogenous RNAi machinery is expressed (DRINNENBERG et al. 2013).

The Sirtuin Family of NAD⁺ Deacetylases

While the heterochromatin in each and every organism deserves recognition, the underlying principles of formation and maintenance learned from the budding and fission yeast, by and large, do not change. Thus, the final frontier of heterochromatin that will be discussed lies within the human genome. However, I will first discuss what is known of the highly conserved sirtuin family of NAD⁺ histone deacetylases responsible for the entirety of budding yeast heterochromatin and the initial steps of mammalian heterochromatin formation.

Sir2 is the most characterized yeast sirtuin having a major role in all three major domains of budding yeast heterochromatin, but four more sirtuins known as the Homologs of Sir Two or Hst1-4 were found to exist in budding yeast from cloning of Hst1 as well as homology analysis (BRACHMANN *et al.* 1995; DERBYSHIRE *et al.* 1996; Figure 1.4). The closest homolog of Sir2, Hst1, is a paralog that arose from an ancient genome duplication event and shares 71% amino acid sequence identity to Sir2 (DERBYSHIRE *et al.* 1996; HICKMAN *et al.* 2007). Unsurprisingly, Hst1 exhibits significant functional redundancy with Sir2, such that overexpression results in a partial silencing of *HMR* in the absence of Sir2 (BRACHMANN *et al.* 1995). Just like Sir2, Hst1 is unable to directly bind chromatin and requires the Sum1 DNA binding protein, which was originally discovered in the form of a dominant allele, *SUM1-1*, that could suppress loss of silencing at *HMR* when Sir2 was defective (LAURENSEN AND RINE 1991). Through Sum1 binding, both Hst1 and Sir2 have the ability to regulate thiamine biosynthesis genes and meiotic middle sporulation genes in the absence of one another (HICKMAN *et al.* 2007; LI *et al.* 2010). They also appear to play overlapping roles in chromosome segregation stability (Figure 3.1) and regulation of the *RDT1* gene on chromosome III (Figure S2.3). The former is in agreement

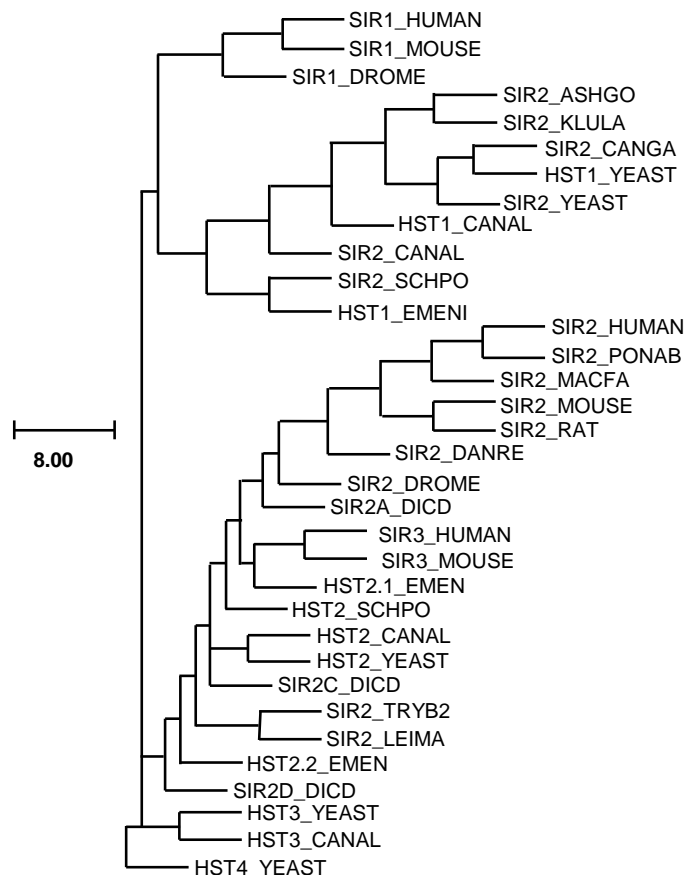


Figure 1.4. Phylogenetic distance tree of sirtuin deacetylases. Tree constructed with protdist (FELSENSTEIN 2005) using results obtained from a blast search against the UniProt database of proteins. The budding yeast Sir2 NAD⁺ catalytic core corresponding to residues 240-400 as annotated in SGD was used as the query. Gene nomenclature is derived from the UniProt database. (R. D. FINE; unpublished data).

with work showing the *SUM1-1* allele increases silencing at the *HM* loci and telomeres while also causing an increase in chromosome loss (CHI AND SHORE 1996). This essentially links a disruption in natural Sir2 distribution between the heterochromatic loci to genome wide instability, which will be explored further in the text. While Hst1 and Sir2 overlap in many pathways, Hst1 alone is responsible for regulation of the *de novo* NAD⁺ synthesis pathway, further entwining this protein with sirtuin regulation (BEDALOV *et al.* 2003).

There is a dearth of knowledge on the remaining yeast sirtuins when compared to the family founder and its paralog. Hst2 is unusual in that it localizes to the cytoplasm for the majority of the cell cycle (PERROD *et al.* 2001), but has been shown to regulate gene expression at the telomeres along with Hst1 (HALME *et al.* 2004). Hst2 may be restricted from the nucleus during interphase in an attempt to spatially regulate its extremely high deacetylase activity as compared to the other sirtuins (SMITH *et al.* 2000). During mitosis, however, its histone deacetylation activity is required to propagate the mitotic event of chromosome condensation from the centromeres (KRUITWAGEN *et al.* 2018). It is not clear if there is a shift in its distribution during this time or if the basal amount of Hst2 is sufficient. Hst2 shares close homology with human SIRT2, so a further understanding of these mitotic roles may prove useful.

The last two sirtuins, Hst3 and Hst4, are responsible for the bulk of histone H3K56 deacetylation, which has a role in DNA damage response during S-phase (PAN *et al.* 2006; YANG *et al.* 2008). These two deacetylases exhibit functional redundancy, with the most severe phenotypes occurring in double mutants. They are separated in a temporal manner, with Hst3 active from late S-phase through G2/M-phase, and Hst4 active from G2/M to G1 (CELIC *et al.* 2006). H3K56 hypoacetylation appears to have a role in maintenance of silencing as well, with *hst3Δ hst4Δ* double mutants exhibiting loss of silencing at the *HM* loci and telomeres, despite presence of the *SIR* complex (YANG *et al.* 2008). Unsurprisingly, deletion of both enzymes drastically increases CIN and decreases RLS similar to phenotypes of Sir2, providing another example of sirtuin maintenance of genome-wide chromosome stability (HACHINOHE *et al.* 2011).

Going much further up the sirtuin family tree, seven sirtuins have been found to exist in humans, numerically named SIRT1-7, with SIRT1 showing the closest homology to Sir2 (Figure

1.4; GOMES *et al.* 2015). While each of them requires NAD⁺ to perform their enzymatic activities, only SIRT1, SIRT2, SIRT6 and SIRT7 appear to reside in the nucleus at any given time (TANNO *et al.* 2006; VAQUERO *et al.* 2006; MOSTOSLAVSKY *et al.* 2006; FORD *et al.* 2006). The other sirtuins, SIRT3, SIRT4, and SIRT5, currently appear to function outside the nucleus to regulate mitochondrial function and will not be discussed further (reviewed in (VERDIN *et al.* 2010).

Of the four sirtuins in the nucleus, SIRT1 is the most well characterized, having numerous non-histone protein substrates, including cancer tumor suppressors such as NF- κ B and p53 (YUENG *et al.* 2004; LI *et al.* 2012). From a heterochromatic perspective, SIRT1 can deacetylate both major heterochromatic histone tail acetylation marks seen in the yeasts, H4K16ac and H3K9ac, which is followed by an increase in monomethylation of H4K20 and trimethylation of H3K9 when targeted to a gene promoter (VAQUERO *et al.* 2004). SIRT1 recruitment appears to also indirectly deplete dimethylation of H3K79, a histone mark associated with silencing boundary function in budding yeast by preventing Sir3 binding (LACOSTE *et al.* 2002; VAQUERO *et al.* 2004). Although a detailed understanding of heterochromatin mechanisms is still lacking in humans, one report has shown SIRT1 can bind to telomeric TTAGGG repeats and is required for maintaining telomere length (PALACIOS *et al.* 2010). In addition, SIRT1 can directly recruit the histone methyltransferase suppressor of variegation 3–9 homolog 1, SUV39H1, when targeted to a gene promoter, thereby modifying both histone acetylation and methylation (VAQUERO *et al.* 2007). SUV39H1 is the human homolog of *S. pombe* Clr4, and just like Clr4, primarily methylates H3K9 to induce heterochromatin formation. Moreover, the catalytic domain of SUV39H1 can be deacetylated by SIRT1 to increase its endogenous methylation activity in a positive feedback loop (VAQUERO *et al.* 2007). Consistent with this

idea, deletion of SIRT1 inhibits levels of H3K9me3 and recruitment of HP1, the human homolog of *S. pombe* Swi6 (VAQUERO *et al.* 2007). Lastly, SIRT1 is required for gene regulation of known targets of the polycomb repressive complexes (WAKELING *et al.* 2015). These complexes preferentially create (PRC2) and bind (PRC1) to the predominant metazoan heterochromatic histone mark H3K27me3, and can cooperatively induce heterochromatin formation with HP1 (BOROS *et al.* 2014). Collectively, this evidence once again points to the sirtuins as the major initiators of gene silencing and heterochromatin formation.

SIRT2 spends a large portion of its time in the cytoplasm, much like its closest homolog in budding yeast, Hst2 (PERROD *et al.* 2001). Outside the cytoplasm, SIRT2 is capable of deacetylating tubulin subunits (NORTH *et al.* 2003). Hst2 possesses no such function owing to a lack of tubulin acetylation in yeast, but there is some evidence that Hst2, along with Sir2 and Hst1, may deacetylate Dam1 complex subunits responsible for translating force between the microtubules and kinetochores (DOWNEY *et al.* 2015). During G2/M in humans, SIRT2 is allowed to enter the nucleus upon nuclear envelope breakdown and is responsible for bulk H4K16 deacetylation (VAQUERO *et al.* 2006). This process was proposed to aid in the chromosome condensation process required for proper chromosome segregation, and as previously stated, there is clear evidence that Hst2 is required for condensation in budding yeast (KRUITWAGEN *et al.* 2018). However, neither Hst2 nor SIRT2 are essential genes, leaving questions about their exact functions *in vivo*.

Initially, SIRT6 was classified as an ADP-ribosyl transferase more than a histone deacetylase like the other sirtuins, with reconstituted mouse SIRT6 showing no deacetylation activity of histones *in vitro* (LISZT *et al.* 2005). It turns out that SIRT6 is simply less promiscuous than its cousins and is quite capable of deacetylating the histone tails of both

histone H3 and histone H4 when in the presence of a completely reconstituted nucleosome as opposed to free floating monomers (GIL *et al.* 2013). More importantly, SIRT6 has been shown to deacetylate H3K9 and H3K56 *in vivo*, with the former being required for telomeric heterochromatin maintenance and the latter for general genome stability akin to Hst3 and Hst4 in budding yeast (MICHISHITA *et al.* 2008; YANG *et al.* 2009). SIRT6 also plays a role in cancer among other diseases, and is directly activated by p53 (ZHANG *et al.* 2014). This would appear to place SIRT6 in direct opposition to SIRT1, and as a matter of fact, the two sirtuins have been shown to directly oppose one another in control of PGC-1 α mediated gluconeogenesis in insulin resistance models (DOMINY *et al.* 2012). In this pathway, SIRT1 directly deacetylates PGC-1 α , while SIRT6 deacetylates the acetyl transferase, Gcn5, to increase its activity and directly oppose SIRT1. Clearly, future therapies must take such opposing roles into consideration when thinking about activating or repressing all SIRTs as if they were the same.

SIRT7 currently appears to be the family member that has retained Sir2's role within the rDNA since it is the only sirtuin reported to sublocalize to the nucleolus in humans thus far (FORD *et al.* 2006). Unlike its yeast brethren, depletion of SIRT7 levels alone can decrease Pol I transcriptional activity, while this function is only modified by Sir2's binding partner Net1 in yeast (SHOU *et al.* 2001). This is mediated in mammalian cells by direct deacetylation of the Pol I subunit, PAF53, enabling Pol I to interact with DNA and by deacetylation of the Fibrillarin protein (Nop1 in budding yeast) which monomethylates H2AQ104 to promote rRNA synthesis (CHEN *et al.* 2013; IYER-BIERHOFF *et al.* 2018). It is not currently understood how H2AQ104me affects Pol I transcription, but this mark must play an essential role, as it is absent during mitosis when rRNA synthesis is repressed. This is further consistent with mitotic CDK1-cyclin B cell-cycle regulation of several Pol I subunits, along with CDK1-cyclin B spatial regulation of

nucleolar SIRT7 by phosphorylation of its C-terminus (GROB *et al.* 2008). It is not known how Sir2 is released from the yeast cell nucleolus during anaphase, so this may be the rare instance where knowledge from mammals can be used to infer yeast heterochromatin biology. What remains clear is the sirtuins will collectively remain at the center of formation, assembly, and maintenance of the unique heterochromatin structures that cells have to deal with every division.

The SMC Super Family

While the core of heterochromatin is clearly shaped and molded by the sirtuins, there is a family of protein complexes which have suspiciously shown whispers, if not glaring evidence, of influence across numerous heterochromatin studies in yeast. The complexes in question are cohesin, condensin, and the Smc5/6 complex (Figure 1.5). These complexes were originally characterized by their highly conserved Structural Maintenance of Chromosome (SMC) subunits that share N- and C-terminal ATPase globular domains, a central globular “hinge” domain responsible for heterodimerization between two SMCs, and two intermediate regions that facilitate an intramolecular coiled coil allowing the N and C termini to contact one another (SCHLIEFFER *et al.* 2003; Figure 1.5). In the past, they have been studied for their roles in mitosis and DNA damage (reviewed in (HAGSTROM AND MEYER 2003; KEGEL AND SJORGREN 2010). More recently, they have attracted the attention of the rest of the chromatin community for newly defined roles in creating interphase compartments known as topological association domains (TADs) (DIXON *et al.* 2012; ZUIN *et al.* 2013). TADs are defined by Hi-C experiments, and are generally split into A and B compartments often reflecting euchromatin and heterochromatin, respectively (LIEBERMAN-AIDEN *et al.* 2009) Thus, this section will further explore the SMC ties to heterochromatin formation with special emphasis on yeast and Sir2.

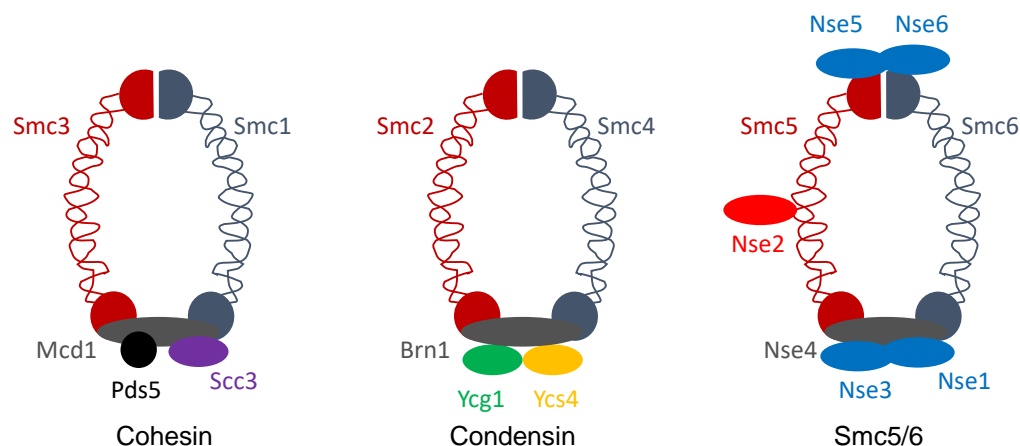


Figure 1.5. The SMC super family of complexes in budding yeast. Each member is defined by conservation of a heterodimer of SMC proteins containing ATPase head, coiled coil, and hinge domains. The ATPase heads contact a kleisin subunit (Mcd1, Brn1, and Nse4) to enclose the complexes. The hinge domains facilitate interaction between the SMC subunits. Each complex has accessory subunits proposed to perform a wide-array of functions such as DNA binding (Scc3, Brn1, Ycg1) and sumoylation (Nse2).

The Cohesin Complex

After the DNA of every chromosome has been replicated into two copies during S-phase, the pair of copies, otherwise known as sister chromatids, must be kept bound together until anaphase in mitosis. During anaphase, the sister chromatids are then sorted equally into two newly forming daughter cells by physical force provided by microtubules generated from spindle poles at opposite ends of the cell. The complex responsible for maintaining the pairing of sisters until anaphase is the cohesin complex made up of four subunits that are thought to form a ring-like structures based on electron microscope images (ANDERSON *et al.* 2002; Figure 1.5). Both budding yeast and human cohesin share the Smc1 and Smc3 monomers whose ATPase activity is essential (LADURNER *et al.* 2014). The two Smc monomers then form a heterodimer through their hinge domain while a kleisin subunit Mcd1/Scc1, RAD21 in humans, physically interacts with each of the monomer's head domains to form an enclosed ring (Figure 1.5). It is this kleisin

subunit that gets catalytically cleaved by Esp1 during anaphase, allowing sister chromatids to exit the complex and be pulled to opposite sides of the cell (CROSK *et al.* 1998). The final member Scc3/Irr1 is less understood, but is absolutely essential for sister chromatid cohesion (TOTH *et al.* 1999). However, recent work on this subunit has proposed that Scc3 and Mcd1 form a positively charged interaction surface initially required to bind DNA (LI *et al.* 2018). The Scc2-Scc4 cohesin loading complex then acts upon cohesin to entrap DNA within the Smc1/Smc3/Mcd1 ring. This is consistent with the idea that Scc3 gives some DNA binding preference to cohesin with data for the Scc3 human homologs, SA1 and SA2, demonstrating responsibility for telomeric and centromeric cohesion respectively (CANUDAS AND SMITH 2009).

At budding yeast telomeres, there does not appear to be much cohesin association, with ChIP-Chip studies revealing higher binding around the point centromeres and even intergenic regions (GLYNN *et al.* 2004). Despite this finding in budding yeast, telomeric heterochromatin in other eukaryotes generally overlaps with cohesin function. Depletion of *S. pombe* cohesin modified gene regulation within subtelomeric heterochromatin and decreased both H3K9me and Swi6 (HP1) binding (DHEUR *et al.* 2011). Conversely, Swi6 and HP1 function is required for cohesin enrichment at pericentric DNA as well as the silent mating-type locus (NONAKA *et al.* 2002). It also appears as though cohesin promotes localization of the CPC complex at centromeric heterochromatin through localization of the Haspin1 kinase (TRIVEDI AND STUKENBERG 2016). This is intriguing because Aurora B (Ipl1 in budding yeast) phosphorylates histone H3S10, which can reduce HP1 and SUV39H1 binding, and even cause transcription within pericentric heterochromatin (PHILLIP-MALLM *et al.* 2015). The resulting centromeric transcripts have the ability to increase the telomeric extension activity of telomerase, once again revealing crosstalk between heterochromatic loci.

The *HMR* locus in budding yeast has proved to be an excellent model of cohesin-heterochromatin interplay with the earliest screens implicating cohesin in silencing boundary function (DONZE *et al.* 1999). It was later shown that cohesin associated with *HMR* in a Sir2-dependent manner (WU *et al.* 2011). Surprisingly, cohesin binding and sister chromatid cohesion did not require Sir2's deacetylase activity or silent chromatin in general. Instead, a small motif dubbed EKDK in Sir2's extreme C-terminus was both necessary and sufficient for cohesion of the locus (CHEN *et al.* 2016). Hst1 shares this C-terminal domain with Sir2, further implicating sirtuin involvement in cohesion across the genome (WU *et al.* 2011). Sir2 also increases cohesin association within NTS1 of the rDNA array by repressing transcription of the non-coding RNA, E-pro (KOBAYASHI AND GANLEY 2005). This helps cohesin to maintain proper alignment of repeats between sister chromatids after S-phase to prevent unequal sister chromatid recombination during homologous recombination repair (GANLEY *et al.* 2009).

In mammals, cohesin along with the insulator protein CTCF has primarily been linked to formation of large domains of interacting chromatin known as TADs (reviewed in (DEKKER AND HEARD 2015). Large TADs have not been reported in the yeasts, perhaps due to their relatively small and compact genomes, but it has been reported that loss of cohesin function causes decompaction of sub-100kb chromatin 'globules' in *S. pombe* (MIZUGUCHI *et al.* 2014). The apparent lack of conservation of Mb TADs may simply be due to lack of CTCF in the yeasts, representing a new level of regulation in mammals. Importantly, there is a lack of insight into how these domains are clearly separated into states of euchromatin and heterochromatin. Cohesin's ATPase activity has been implicated as a DNA pump responsible for forming loops with CTCF and cohesin at the base (FUDENBERG *et al.* 2016). It has also been shown that Wapl, a negative regulator of cohesin entrapment of DNA, and the Scc2-Scc4 cohesin loading complex,

are required for maintaining a distinct separation between the domain boundaries (HAARHUIS *et al.* 2017) To date, no one has explored the relationships between cohesin/CTCF and the countless heterochromatin inducing proteins. This is in part because of the highly repetitive nature of heterochromatin, once again preventing easy sequencing analysis. Future studies should aim to take advantage of the genetic tractability of the yeast systems to yield our first insights into cohesin's impact on the yeast rDNA array three-dimensional structure as a paradigm for investigating other repetitive heterochromatin domains.

The Condensin Complex

Like cohesin, the condensins have been extensively characterized for their roles during mitosis and are responsible for condensing mammalian interphase chromosomes as much as 10-fold and yeast chromosomes as much as 2-fold (KOSHLAND AND STRUNNIKOV 1996). The difference in fold change may be attributed to two complexes existing in mammals, condensin I and II, with yeast only possessing the former, though this has not been tested. Condensin I and II each contain a set of three specific subunits CAPD2/CAPG/CAPH in condensin I and CAPD3/CAPG2/CAPH2 in condensin II, with each complex sharing the Smc2/Smc4 heterodimer (HIRANO 2016). In mammals, condensin II is localized in the nucleus throughout the cell cycle, whereas condensin I is restricted to the cytoplasm until nuclear envelope breakdown in prometaphase. Both complexes then work together in mitosis with condensin I laterally compacting chromosomes while condensin II creates loops that drive axial shortening (ONO *et al.*, 2003).

Interestingly, budding yeast condensin, which is structurally homologous to human condensin I, localizes to the nucleus throughout the cell cycle (THADANI *et al.* 2012). The

mechanism preventing its condensation activity throughout interphase was initially not fully understood. Recent work has implicated Ipl1/Aurora B kinase activity as the culprit, since it is required for condensin-mediated chromosome condensation and is cell cycle controlled (VAS *et al.* 2007; VAN DER WAAL *et al.* 2012). Additionally, condensation appears to initiate from the centromeres, where Ipl1 is primarily localized in mitosis and then spread outward along chromosome arms in a shugoshin and Hst2 dependent manner (KRUITWAGEN *et al.* 2015; KRUITWAGEN *et al.* 2018). Ipl1 activity is also required for condensation of the rDNA array, which exhibits the highest localization of fluorescent condensin subunits and the largest change in condensation among all the chromosomes in condensin temperature sensitive strains (FREEMAN *et al.* 2000; LAVOIE *et al.* 2003). It is not entirely understood how the predominantly centromeric localized Ipl1 induces condensation of the rDNA, but Hi-C analysis by our group and others has suggested that the nucleolus is pulled towards centromeres during anaphase in a condensin-mediated fashion giving a timeframe to further explore cross talk between these two loci (LAZAR-STEFANITA *et al.* 2017; FINE *et al.* 2019).

Unlike cohesin, there is little evidence that Sir2 regulates condensin binding within the rDNA, though other sirtuins may be involved, since depletion of NAD⁺ decreases condensin binding in the rDNA (LI *et al.* 2013). The best model available to explain this result is that depleted Hst3/Hst4 deacetylation activity will increase H3K56ac within the rDNA. H3K56 has been shown to stimulate Pol I transcription, which in turn has been shown to prevent condensin binding on repeats undergoing active transcription (JOHZUKA *et al.* 2007; CHEN *et al.* 2012).

There is better evidence for a sirtuin-independent recruitment mechanism of condensin to the rDNA via Fob1/Tof2 and the cohibin complex composed of the structural proteins Lrs4 and Csm1 (JOHZUKA *et al.* 2009). Fob1 is responsible for unidirectional replication of the rDNA

since it binds replication fork blocking DNA sequences in an asymmetric manner and physically prevents passage of the replication machinery (KOBAYASHI AND HORIUCHI 1996). Fob1 is also primarily responsible for localizing cohibin to the rDNA through physical interaction similar to the RENT complex (HUANG *et al.* 2006). Tof2 is a paralog of Net1 that physically interacts with Fob1 and cohibin (HUANG *et al.* 2006). Lrs4 was originally isolated from an rDNA silencing reporter assay for increased Loss of rDNA Silencing (SMITH *et al.* 1999), with Csm1 implicated more recently (MEKHAIL *et al.* 2008).

The cohibin complex itself is composed of two Csm1 homodimers with each dimer interacting with one subunit of a Lrs4 dimer to form a V-shaped complex (CORBETT *et al.* 2010). Cohibin was originally proposed to maintain rDNA stability by localizing cohesin to the array through physical interaction (HUANG *et al.* 2006). However, further analysis has shown that it can influence condensin binding through Fob1/Tof2 as well (JOHZUKA *et al.* 2009). Cohibin also performs a third function by physically interacting with the CLIP complex (Heh1 and Nur1), binding portions of the rDNA array to the nuclear membrane (MEKHAIL *et al.* 2008). CLIP mutants retain Sir2-dependent silencing, but still exhibit increased rDNA instability, once again revealing the complexity of this locus, which is explored further in this thesis.

The Smc5/6 Complex

The cohesin and condensin complexes are essential tools for a cell's ability to deal with the challenges of heterochromatin, and the final member of the family, the Smc5/6 complex, is no exception. Extensive work has been done to examine Smc5/6's role in homologous recombination DNA repair and DNA replication through the resolution of complex intermediate structures (KEGEL AND SJORGREN 2010). In hindsight, initial indications that the Smc5/6 complex

was connected to gene silencing came from classic *HMR* silencing screens in which ectopic overexpression of Esc2 was found to restore silencing in strains that had diminished Sir function (DHILLON AND KAMAKAKA 2000; CUPERUS AND SHORE 2002). Esc2 directly interacts with Sir2 and was later shown to physically associate with Smc5/6 in *S. pombe* (CUPERUS AND SHORE 2002; BODDY *et al.* 2003). Esc2 is not the only means of Smc5/6 localization to heterochromatin, with the recent finding that the Nse3 accessory subunit also physically interacts with Sir4 (MORADI-FARD *et al.* 2016; Figure 1.5).

While it is clear that Esc2 and Smc5/6 have some function in silencing, the exact mechanism(s) are not. Temperature sensitive alleles of different Smc5/6 subunits have given generally mixed results. For example, the *nse3-1* mutant decreases telomeric foci clustering, Sir4 binding, and increases loss of the TPE (MORADI-FARD *et al.* 2016). A *smc6-9* mutant, on the other hand, only reduces clustering (MORADI-FARD *et al.* 2016). An answer may come from Smc5/6's other role in the process of sumoylation, which it does not share with cohesin or condensin. The Nse2 subunit of Smc5/6 is an E3 sumo-ligase more commonly known as Mms21 (SOLLIER *et al.* 2009). Mms21-sumoylation of the Sgs1 helicase increases its ability to inhibit the HR machinery. Smc5/6 and Esc2 appear to help prevention and/or the resolving of replication "X-molecule" intermediates arising from stalled replication forks and HR (CHOI *et al.* 2010). A general issue of heterochromatin arises from a cell simply trying to replicate these highly repetitive and silenced domains. Smc5/6 depletion preferentially causes defects in rDNA replication due to an excess of recombination intermediates from stalled forks (PENG *et al.* 2018). Thus, a general mechanism is that Smc5/6 and Esc2 help resolve various forms of stalled replication forks and DNA damage intermediates in and around heterochromatic regions, allowing cells to finish replication and restore silencing in a timely manner.

Dysregulation of Sirtuins and SMCs during Aging: A Heterochromatin

Malfunction?

Aging is perhaps one of the most fundamental aspects of life, invoking philosophical questions such as whether or not it should even be considered a disease. An argument can be made that it is, in fact, the basis of chronic disease, since the number one risk factor for chronic disease is a patient's age (NICCOLI AND PARTRIDGE 2012). Fortunately, the gerontology field has greatly expanded over the past several decades, with geneticists in particular finding clues that relatively minor genetic alterations in DNA can result in large gains of lifespan and health span (LONGO *et al.* 2012). Many of these genetic alterations modify different aspects of heterochromatin, suggesting that potential failure to regulate these highly specialized domains may ultimately be a driver of aging pathologies. Indeed, one theory of aging is the rDNA theory directly implicating stability of the locus, or rather its instability with age (GANLEY AND KOBAYASHI 2014). Moreover, the major protein families discussed thus far, the sirtuins, the cohesin complex, the condensin complex, and the Smc5/6 complex, all suspiciously play a role maintaining the rDNA locus and more importantly, heterochromatin in general. This final section will attempt to reconcile observations of these complexes in terms of heterochromatin maintenance with aging pathologies observed in yeast and humans in hopes of provoking further research going forward.

There are two models of budding yeast lifespan, chronological and replicative. Chronological lifespan (CLS) asks the question of how long can a yeast cell remain viable in stationary phase cultures before losing viability. It will not be discussed extensively here, since its regulation by Sir2 is quite unclear (FABRIZIO *et al.* 2007; MCCLEARY AND RINE 2017). Budding yeast replicative life span (RLS) assays the number of times a single yeast cell divides

before senescence (MORTIMER AND JOHNSTON 1959). Sir2 is a dose-dependent longevity factor that depletes naturally with yeast replicative age, giving rise to the generally accepted mechanism for overexpression induced longevity (KAEBERLEIN *et al.* 1999; DANG *et al.* 2009; FINE *et al.* 2019). The question then becomes which of the major heterochromatic loci is responsible for this lifespan extension since Sir2 regulates all of them?

The initial breakthrough for a conserved mechanism came from the *SIR4-42* dominant allele, which siphons the *SIR* complex away from the telomeres and *HM* loci to the rDNA array (KENNEDY *et al.* 1995; KENNEDY *et al.* 1997). Since then, several studies have supported the notion that Sir2 redistribution to the rDNA from the other heterochromatic loci is vital for maximum lifespan extension (AUSTRIACO AND GUARENTE 1997; SALVI *et al.* 2013; LIU *et al.* 2016). While it is tempting to say the rDNA deserves all of the attention, additional mechanisms have been proposed including a role for Sir2 in mother cell asymmetric retention of Hydrogen peroxide, which is one of many reactive oxygen species (ROS) thought to induce aging (ERJAVEC AND NYSTROM 2007). However, the link between ROS and lifespan is not clear, with another group showing that *sir2Δ* mutant cells exhibit low levels of the superoxide (O_2^-) ROS, when detected by dihydroethidium (LAM *et al.* 2011). Furthermore, this study showed that the asymmetric retention of this ROS species was not dependent on Sir2, calling into question the idea that this is primary role of Sir2 in aging. Alternatively, it is quite clear that eventual telomere shortening arising from the end replication problem is also a limiting factor in lifespan. A general concept for this physical limit was originally termed as the Hayflick limit and arises from lack of telomerase expression in post-mitotic human cells (SHAY AND WRIGHT 2000). Among the worst aging pathologies in humans are dyskeratosis congenita and Werner syndrome both of which result in increased cancer risk, osteoporosis, diabetes and general physical signs of

old age in people as young as 20 (SONG AND JOHNSON 2018). The telomerase protein TERC, is usually mutated in dyskeratosis congenita patients, while the WRN protein responsible for Werner syndrome physically interacts with the heterochromatin proteins, HP1 and SUV39H1, directly implicating failed heterochromatin maintenance in these extreme progeroid syndromes (ZHANG *et al.* 2015).

Budding yeast should not suffer from telomere aging pathologies since they are unicellular and have the ability to express telomerase. However, Sir2 naturally depletes from telomeres in aging yeast resulting in an increase in H4K16ac (DANG *et al.* 2009). Critically, inhibition of the acetyltransferase Sas2 decreases telomeric H4K16ac and rescues lifespan in the aforementioned model of yeast aging as well as the lifespan of telomerase defective mutants (*tlc1Δ*), which model human senescence (KOZAK *et al.* 2010). In this model, the DNA binding protein Rap1 also delocalizes from the telomeres and can cause downregulation of the histone coding genes (PLATT *et al.* 2013). In agreement with this finding, several studies have suggested histone loss and uncontrolled gene expression are general hallmarks of aging and senescence (FESER *et al.* 2010; HU *et al.* 2014).

While all of the above is true, the current most widely accepted mechanism for Sir2-dependent replicative lifespan extension is the maintenance of rDNA array stability by repression of a Pol II transcribed NTS1 non-coding promoter, E-Pro, to promote cohesin loading (KOBAYASHI *et al.* 2004; GANLEY *et al.* 2009). Cohesin represses unequal homologous recombination between sister chromatids and formation of extrachromosomal rDNA circles (ERCs) upon fork collapse induced by Fob1 ((KOBAYASHI AND GANLEY 2005). Fob1 is thought to block the DNA replication fork initiated at the origin in NTS2 to prevent interference with the Pol I transcriptional machinery moving in the opposite direction (TAKEUCHI *et al.* 2003).

However, this potentially beneficial process is superseded by general rDNA instability. Indeed, a *fob1* Δ strain is long lived, and a double mutant (*fob1* Δ *sir2* Δ) rescues the short lifespan of a *sir2* Δ mutant (KAEBERLEIN 1999). Interestingly, *fob1* Δ *sir2* Δ double mutants have a shorter lifespan than *fob1* Δ single mutants. Deletion of Sir2 should not decrease the lifespan of a *fob1* Δ mutant if Sir2 only extends lifespan by suppressing ERCs, so this suggests alternative mechanisms for lifespan extension including the aforementioned role in telomere maintenance, among others (DANG *et al.* 2009).

In the context of human aging, the role of sirtuins has been controversial, with whole-body overexpression of SIRT1 resulting in no gain of mouse lifespan (HERRANZ *et al.* 2010). As previously mentioned, such shotgun approaches do not take into account the complexity of SIRT family regulation, including tissue specific regulation. Indeed, brain-specific overexpression of SIRT1 has shown to increase median mouse lifespan (SATO *et al.* 2013). Additionally, SIRT2 overexpression has been shown to increase the lifespan of BubR1 hypomorphic mice by regulating its kinase activity (NORTH *et al.* 2014). BubR1 is a mitotic checkpoint protein that regulates mouse lifespan in a dose-dependent manner and is naturally depleted in many tissues of old mice (NORTH *et al.* 2014). Finally, whole-body overexpression of SIRT6 increases the lifespan of male mice (KANFI *et al.* 2012). Combined with the mountains of evidence of Sir2 regulation in yeast lifespan, these findings suggest the sirtuin family will remain as key components of future aging studies.

Going beyond Sir2, human “cohesinopathy” mutations have been introduced into the yeast Scc2 subunit of the cohesin loading complex and the Eco1 acetyltransferase, which can cause Cornelia de Lange syndrome and Robert’s syndrome, respectively. These mutations caused severe loss of condensation along chromosome XII, in addition to fragmentation and

enlargement of the rDNA (GARD *et al.* 2009). Surprisingly, they did not induce severe sister chromatid cohesion defects. This is in complete agreement with the data in another study that artificially depleted Mcd1 protein to <30% of wild-type levels (HEIDINGER-PAULI *et al.* 2010), as well as our own data suggesting rDNA stability is the key with respect to cohesin deficiencies in yeast lifespan (FINE *et al.* 2019).

In the case of condensin, “condensinopathy” mutations found in patients have been studied in mice leading to severe neurological defects from aneuploid events due to chromosome “bridges” between sister chromatids during chromosome segregation in anaphase (MARTIN *et al.* 2016). While this study did not examine chromosome specificity for bridge formation, another has shown that knockout of condensin II subunits specifically increased bridge formation and aneuploidy of rDNA-containing chromosomes (DANILOSKI *et al.* 2019). Smc5/6 may also contribute to disease in a similar manner since siRNA mediated knockdown displaces condensin from mitotic chromosomes (GALEGO-PAEZ *et al.* 2013).

On the other hand, condensin is required for calorie restriction (CR) and mTOR inhibition mediated remodeling of the rDNA array in yeast (TSANG *et al.* 2007). Both CR and mTOR inhibition-mediated extension of lifespan are heavily conserved across organisms, and are arguably the most generally applicable anti-aging interventions to date (LONGO *et al.* 2012). Many of the processes that CR mediates occur through mTOR downregulation to affect Pol I activity, nucleolar stability, and ribosome biogenesis. For example, mTOR activity has been shown to directly reduce H3K56ac within the rDNA, leading to decreased Pol I activity (CHEN *et al.* 2012). Conversely, excess H3K56ac in *hst3Δ hst4Δ* mutants leads to shortened lifespan (HACHINOEHE *et al.* 2011). CR also counteracts rDNA instability through increased activity of RNaseH, which depletes destabilizing RNA-DNA intermediates known as R-loops (SALVI *et al.*

2014). Lastly, CR can induce silencing of the rDNA in humans through histone deacetylation and H3K9me2 by the energy dependent nucleolar silencing complex (eNoSC) composed of SIRT1, SUV39H1, and NML, an H3K9me2 reader (GRUMMT 2013). SIRT1 is once again limiting with overexpression causing enhanced silencing.

All of these CR-mediated processes converge to reduce ribosome biogenesis and promote rDNA stability. Artificial reduction of ribosome biogenesis, by deleting subunits of the large 60S ribosome subunit in yeast, increases lifespan (STEFFEN *et al.* 2008). As one might expect, reduced ribosome biogenesis decreases total protein translation and also promotes an increase in expression of Gcn4. Gcn4 is a transcription factor that activates general amino acid biosynthesis genes and has recently been shown to repress ribosome biosynthesis genes with Rap1 binding sites in their promoters (MITTAL *et al.* 2017). Overexpressing Gcn4 alone is sufficient to induce lifespan extension in yeast and appears to greatly inhibit CR and mTOR inhibition lifespan extension when deleted. To date, no one has tested whether Gcn4 overexpression increases stability of the rDNA itself, but why is this important in the first place?

Upon a double stranded break in the rDNA, there are two major routes of repair that a haploid yeast cell can take to fix the damage, homologous recombination and non-homologous end joining, because unlike euchromatin regions, there are 150-200 repeats of the rDNA sequence to utilize for homologous recombination repair, which is often considered better since it is error free. Thus, it is surprising that the homologous recombination machinery is generally inhibited from the array by condensin (TSANG AND ZHENG 2009). This process may have evolved to prevent an excessive amount of homologous recombination intermediates within the array, which could create extremely complex “X-molecule” structures between repeats. As mentioned previously, the Smc5/6 complex and Esc2 appear to help resolve such structures that

do form (CHOI *et al.* 2010). Furthermore, unequal recombination repair between sister chromatids results in ERCs, which have been suggested to be both a cause and consequence of aging (SINCLAIR AND GUARANTE 1997). It is imperative, then, to understand how HR works within the rDNA to prevent this generally beneficial process from doing more harm than good. Fortunately, the programmed DSB at the *MAT* locus on chromosome III by HO endonuclease during mating-type switching, and the subsequent HR-repair utilizing the heterochromatic loci, *HML* and *HMR*, can be used as a simplified model to dissect this process.

Chapter II

Sir2 and Condensin Regulation of the *RDT1* Locus Control Region

The NAD⁺-dependent histone deacetylase Sir2 was originally identified in *Saccharomyces cerevisiae* as a silencing factor for *HML* and *HMR*, the heterochromatic cassettes utilized as donor templates during mating-type switching. *MATa* cells preferentially switch to *MATα* using *HML* as the donor, which is driven by an adjacent cis-acting element called the recombination enhancer (RE). In this study we demonstrate that Sir2 and the condensin complex are recruited to the RE exclusively in *MATa* cells, specifically to the promoter of a small gene within the right half of the RE known as *RDT1*. We go on to demonstrate that the *RDT1* promoter functions as a locus control region (LCR) that regulates both transcription and long-range chromatin interactions. Sir2 represses the transcription of *RDT1* until it is redistributed to a dsDNA break at the MAT locus induced by the HO endonuclease during mating-type switching. Condensin is also recruited to the *RDT1* promoter and is displaced upon HO induction, but does not significantly repress *RDT1* transcription. Instead condensin appears to promote mating-type switching efficiency and donor preference by maintaining proper chromosome III architecture, which is defined by the interaction of *HML* with the right arm of chromosome III, including *MATa* and *HMR*. Remarkably, eliminating Sir2 and condensin recruitment to the *RDT1* promoter disrupts this structure and reveals an aberrant interaction between *MATa* and *HMR*, consistent with the partially defective donor preference for this mutant. Global condensin subunit depletion also impairs mating type switching efficiency and donor preference, suggesting that modulation of chromosome architecture plays a significant role in controlling mating type switching, thus providing a novel model for dissecting condensin function *in vivo*.

Introduction

Since the first descriptions of mating-type switching in budding yeast approximately 40 years ago, characterization of this process has led to numerous advances in understanding mechanisms of gene silencing (heterochromatin), cell-fate determination (mating-type), and homologous recombination (reviewed in (HABER 2012)). For example, the NAD⁺-dependent histone deacetylase, Sir2, and other Silent Information Regulator (SIR) proteins, were genetically identified due to their roles in silencing the heterochromatic *HML* and *HMR* loci, which are maintained as silenced copies of the active *MAT α* and *MATa* loci, respectively (HABER AND GEORGE 1979; KLAR *et al.* 1979; RINE 1979). The SIR silencing complex (Sir2-Sir3-Sir4) is recruited to cis-acting E and I silencer elements flanking *HML* and *HMR* through physical interactions with silencer binding factors Rap1, ORC, and Abf1, as well as histones H3 and H4 (reviewed in (GARTENBERG AND SMITH 2016)).

HML and *HMR* play a critical role in mating-type switching. Haploid cells of the same mating-type cannot mate to form diploids, the preferred cell type in the wild. Therefore, in order to facilitate mating and diploid formation, haploid mother cells switch their mating type by expressing HO endonuclease, which introduces a programmed DNA double-strand break (DSB) at the *MAT* locus (STRATHERN *et al.* 1982). The break is then repaired by homologous recombination using either *HML* or *HMR* as a donor template for gene conversion (HABER *et al.* 1980; STRATHERN *et al.* 1982). This change in mating type enables immediate diploid formation between mother and daughter. *HO* is deleted from most standard lab strains in order to maintain them as haploids, so expression of *HO* from an inducible promoter such as *P_{GALI}* is commonly used to switch mating types during strain construction (NASMYTH 1987).

There is a “donor preference” directionality to mating-type switching such that ~90% of the time, the HO-induced DSB is repaired to the opposite mating type (KLAR *et al.* 1982). For example, *MAT α* cells preferentially switch to *MATa* using *HMR* as the donor. However, while both silent mating loci can be utilized as a donor template, usage of *HML* by *MATa* cells requires a 2.5 kb intergenic region located ~17 kb from *HML* called the recombination enhancer (RE) (WU AND HABER 1996). Donor preference activity within the RE has been further narrowed down to a 700 bp segment containing an Mcm1/ α 2 binding site (DPS1) and multiple Fkh1 binding sites (WU AND HABER 1996). The RE is active in *MATa* cells, requiring Mcm1 and Fkh1 activity at their respective binding sites (WU AND HABER 1996; WU *et al.* 1998; SUN *et al.* 2002). The RE is inactivated in *MAT α* cells due to expression of transcription factor α 2 from *MAT α* (SZETO *et al.* 1997), which forms a repressive heterodimer with Mcm1 (Mcm1/ α 2) to repress *MATa*-specific genes (HABER 2012). Current models for donor preference posit that Fkh1 at the RE helps position *HML* in close proximity with *MATa* by interacting with threonine-phosphorylated H2A (γ -H2AX) and Mph1 DNA helicase at the HO-induced DNA DSB (LI *et al.* 2012; DUMMER *et al.* 2016).

Sir2-dependent silencing of *HML* and *HMR* has two known functions related to mating-type switching. First, *HML* and *HMR* must be silenced in haploids to prevent formation of the α 1/ α 2 heterodimer, which would otherwise inactivate haploid-specific genes such as *HO* (JENSEN *et al.* 1983). Second, heterochromatin structure at *HML* and *HMR* blocks cleavage by HO, thus restricting its activity to the fully accessible *MAT* locus (KLAR *et al.* 1981; NASMYTH 1982). Here we describe new roles for Sir2 and the condensin complex within the RE during mating-type switching. ChIP-seq analysis revealed strong overlapping binding sites for Sir2 and condensin at the promoter of a small gene within the RE known as *RDT1*. Sir2 was found to

repress the *MATa*-specific transcription of *RDT1*, which is also translated into a small 28 amino acid peptide. *RDT1* expression is also dramatically upregulated during mating-type switching when Sir2 redistributes to the HO-induced DNA DSB at *MATa*. Furthermore, eliminating Sir2/condensin recruitment to the *RDT1* promoter disrupts chromosome III architecture such that mating-type switching efficiency and donor preference are partially impaired. The *RDT1* promoter region therefore functions like a classic locus control region (LCR) in *MATa* yeast cells, regulating localized transcription as well as long-range chromosome interactions similar to the beta goblin locus in humans (TOLHUIS *et al.* 2002).

Methods

Yeast strains, plasmids, and media

Yeast strains were grown at 30°C in YPD or synthetic complete (SC) medium where indicated. The *SIR2*, or *HST1* open reading frames (ORFs) were deleted with *kanMX4* using one-step PCR-mediated gene replacement. *HML* was deleted and replaced with *LEU2*. A 100bp deletion within the *RDT1* promoter (chrIII coordinates 30701-30800) or *DPS2* deletion (chrIII coordinates 30557-30626) was generated using the *delitto perfetto* method (STORICI *et al.* 2001). Endogenous *SIR2*, *BRN1*, or *SMC4* genes were C-terminally tagged with the 13xMyc epitope (13-EQKLISEEDL). Deletion and tagged genes combinations were generated through genetic crosses and tetrad dissection, including Brn1 tagged with a V5-AID tag (template plasmids kindly provided by Vincent Guacci). All genetic manipulations were confirmed by PCR, and expression of tagged proteins confirmed by western blotting. The pGAL-HO-URA3 expression plasmid was kindly provided by Jessica Tyler (TAMBURINI AND TYLER 2005).

ChIP-Seq analysis

Sir2 ChIP-seq was previously described (LI *et al.* 2013). For other ChIP-seq datasets, log-phase YPD cultures were cross-linked with 1% formaldehyde for 20 min, pelleted, washed with Tris-buffered saline (TBS), and then lysed in 600 μ l FA140 lysis buffer with glass beads using a mini-beadbeater (BioSpec Products). Lysates were removed from the beads and sonicated for 60 cycles (30s “on” and 30s “off” per cycle) in a Diagenode Bioruptor. Sonicated lysates were pelleted for 5 min at 14000 rpm in a microcentrifuge and the entire supernatant was transferred to a new microfuge tube and incubated overnight at 4°C with 5 μ g of anti-Myc antibody (9E10) and 20 μ l of protein G magnetic beads (Millipore). Following IP, the beads were washed once with FA140 buffer, twice with FA500 buffer, and twice with LiCl wash buffer. DNA was eluted

from the beads in 1% SDS/TE buffer and cross-links were reversed overnight at 65°C. The chromatin was then purified using a Qiagen PCR purification kit. Libraries were constructed using the Illumina TruSeq ChIP Sample Prep kit and TrueSeq standard protocol with 10ng of initial ChIP or Input DNA. Libraries that passed QC on a Bioanalyzer High Sensitivity DNA Chip (Agilent Technologies) were sequenced on an Illumina Miseq (UVA DNA Sciences Core).

ChIP-seq computational analysis

Biological duplicate fastq files were concatenated together and reads mapped to the *sacCer3* genome using Bowtie with the following options: `---best`, `--stratum`, `--nomaqground`, and `--m10` (LANGMEAD *et al.* 2009). The resulting bam files were then converted into bigwig files using BEDTools (QUINLAN AND HALL 2010). As part of the pipeline, chromosome names were changed from the *sacCer3* NCBI values to values readable by genomics viewers e.g. "ref|NC_001133|" to "chrI". The raw and processed datasets used in this study have been deposited in NCBI's GEO and are accessible through the GEO series accession number GSE92717. Downstream GO analysis was performed as follows. MACS2 was used to call peaks with the following options: `--broad`, `--keep-dup`, `-tz 150`, and `-m 3, 1000` (LIU 2014). GFP peaks in the WT or *sir2Δ* backgrounds were subtracted from the WT *SMC4-13xMyc* and *sir2Δ SMC4-13xMyc* peaks, respectively, using BEDTools "intersect" with the `-v` option. The resulting normalized peaks were annotated using BEDTools "closest" with the `-t all` option specified, and in combination with a yeast gene list produced from USCS genome tables. The annotated peaks were then analyzed for GO terms using YeastMine (yeastmine.yeastgenome.org).

Hi-C analysis

Log-phase cultures were cross-linked with 3% formaldehyde for 20 min and quenched with a 2x volume of 2.5M Glycine. Cell pellets were washed with dH₂O and stored at -80°C. Thawed cells were resuspended in 5 ml of 1X NEB2 restriction enzyme buffer (New England Biolabs) and poured into a pre-chilled mortar containing liquid N₂. Nitrogen grinding was performed twice as previously described (BELTON AND DEKKER 2015), and the lysates were then diluted to an OD₆₀₀ of 12 in 1x NEB2 buffer. 500 µl of cell lysate was used for each Hi-C library as follows. Lysates were solubilized by the addition of 50 µl 1% SDS and incubation at 65°C for 10 min. 55 µl of 10% TritonX-100 was added to quench the SDS, followed by 10 µl of 10X NEB2 buffer and 15 µl of *Hind*III (New England Biolabs, 20 U/µl) to digest at 37°C for 2 hr. An additional 10 µl of *Hind*III was added for digestion overnight. The remainder of the protocol was based on previously published work with minor exceptions (BURTON *et al.* 2014). In short, digested chromatin ends were filled-in with Klenow fragment (New England Biolabs) and biotinylated dCTP at 37°C for 1 hr, then heat inactivated at 70°C for 10 min. Ligation reactions with T4 DNA ligase were performed at 16°C for a minimum of 6 hr using the entire Hi-C sample diluted into a total volume of 4 ml. Proteinase K was added and cross-links were reversed overnight at 70°C. The ligated chromatin was phenol:chloroform extracted, ethanol precipitated, then resuspended in 500µl dH₂O and treated with RNase A for 45 min. Following treatment with T4 DNA polymerase to remove biotinylated DNA ends that were unligated, the samples were concentrated with a Clean and Concentrator spin column (Zymogen, D4013) and sheared to approximately 300bp with a Diagenode Bioruptor. Biotinylated fragments were captured with 30 µl pre-washed Streptavidin Dynabeads (Invitrogen), then used for library preparation. Hi-C sequencing libraries were prepared with reagents from an Illumina Nextera Mate Pair Kit (FC-

132-1001) using the standard Illumina protocol of End Repair, A-tailing, Adapter Ligation, and 12 cycles of PCR. PCR products were size selected and purified with AMPure XP beads before sequencing with an Illumina Miseq or Hiseq. Raw and mapped reads deposited at GEO (GSE92717).

Hi-C computational analysis

Iteratively corrected heatmaps were produced using python scripts from the Mirny lab hiclib library, <http://mirnylab.bitbucket.org/hiclib/index.html>. Briefly, reads were mapped using the iterative mapping program, which uses Bowtie2 to map reads and iteratively trims unmapped reads to increase the total number of mapped reads. Mapped reads were then parsed into an hdf5 python data dictionary for storage and further analysis. Mapped reads of the same strains were concatenated using the hiclib library's "Merge" function. Both individual and concatenated mapped reads have been deposited in GEO. Mapped reads were then run through the fragment filtering program using the default parameters as follows: filterRsiteStart(offset=5), filterDuplicates, filterLarge, filterExtreme (cutH=0.005, cutL=0). Raw heat maps were further filtered to remove diagonal reads and iteratively corrected using the 03 heat map processing program. Finally, the iteratively corrected heatmaps were normalized for read count differences by dividing the sum of each row by the sum of the max row for a given plot, which drives all values towards 1 to make individual heatmaps comparable.

Observed/Expected heatmaps were created using HOMER Hi-C analysis software on the BAM file outputs from the iterativemapping program of the hiclib library python package (HEINZ *et al.* 2010). Tag directories were created using all experimental replicates of a given biological sample and the `tbp -1` and `illuminaPE` options. Homer was also used to score

differential chromosome interactions between the WT and mutant Hi-C heatmaps. The resulting list of differential interactions was uploaded into R where the given p-value was adjusted to a qvalue with p.adjust. An FDR cutoff of 0.05 was used to create a histogram of significantly different chromosome interactions in the mutants compared to WT. The histogram was further normalized by dividing the total number of significant differential interactions for a chromosome by total number of interactions called in the WT sample for that chromosome to account for size differences in the chromosomes. Thus, frequency represents the number of interactions that changed out of all possible interactions that could have changed.

RNA-seq data analysis

RNA-Seq data was acquired from GEO accessions GSE73274 (PORTER *et al.* 2015) and GSE58319 (SWAMY *et al.* 2014) for the BY4742 (*MAT α*) and BY4741 (*MATa*) backgrounds, respectively. Reads were then mapped to the *sacCer3* genome using Bowtie2 with no further processing of the resulting BAM files visualized in this paper.

3C assays

Chromosome Conformation Capture (3C) was performed in a similar manner to Hi-C with a few exceptions due to assay-specific quantification via quantitative real-time PCR rather than sequencing. Most notably, digested DNA ends were not filled in with dCTP-biotin before ligation and an un-crosslinked control library was created for each 3C library. Furthermore, all PCR reactions were normalized for starting DNA concentration using a *PDC1* intergenic region that is not recognized by *HindIII*, in addition to PCR of the un-crosslinked control for all tested looping interaction primer pairs.

Quantitative reverse transcriptase (RT) PCR assay

Total RNA (1 μ g) was used for cDNA synthesis with oligo(dT) and Superscript II reverse transcriptase as previously described (LI *et al.* 2010).

Western blot

Proteins were blotted using standard TCA extraction followed by SDS-PAGE as previously described (LI *et al.* 2013). Myc-tagged proteins were incubated with an anti-Myc primary antibody 9E10 (Millipore) at a 1:2000 dilution while tubulin was incubated with anti-Tubulin antibody B-5-1-2 (Sigma-Aldrich) at a 1:1500 dilution. The V5-AID tagged Brn1 was detected with anti-V5 antibody (Invitrogen, R96025) at a 1:4000 dilution. Primary antibodies were detected with an anti-mouse secondary antibody conjugated to HRP (Promega) at 1:5000 dilution in 5% fat-free milk. Bands were then visualized with HyGlo (Denville Scientific) capture on autoradiography film (Denville Scientific).

Mating-type switching assays

For tracking the efficiency of switching, strains were transformed with pGAL-HO-*URA3*, pre-cultured in SC-ura + raffinose (2%) medium overnight, re-inoculated into the same medium ($OD_{600}=0.05$) and then grown into log phase. Galactose (2%) was added to induce HO expression for 45 min. Glucose (2%) was then added and aliquots of the cultures were harvested at indicated time points. Genomic DNA was isolated and 10 ng used for PCR amplification. *MAT α* was detected using primers JS301 and JS302. The *SCR1* gene on chromosome V was used as a loading control (primers JS2665 and JS2666). PCR products were separated on a 1% agarose gel stained with ethidium bromide and then quantified using ImageJ. Donor preference

with strains containing *HMR* α -B was performed as previously described (LI *et al.* 2012). Briefly, MATa was amplified with primers Yalpha105F and MATdist-4R from genomic DNA 90 after switching was completed (90 min), and then digested with BamHI. Ethidium stained bands were quantified using ImageJ. For the conditional V5-AID degron strains, degradation of V5-AID-fused Brn1 protein was induced by addition of 0.5 mM indole-3-acetic acid (Auxin, Sigma # 13750).

Results

Sir2 and condensin associate with the recombination enhancer (RE)

We previously characterized global sirtuin distribution using ChIP-Seq to identify novel loci regulated by Sir2 and its homologs (LI *et al.* 2013). Significant overlap was observed between binding sites for Sir2, Hst1, or Sum1 with previously described condensin binding sites (D'AMBROSIO *et al.* 2008; LI *et al.* 2013), suggesting a possible functional connection. ChIP-Seq was therefore performed on WT and *sir2* Δ strains in which the condensin subunit Smc4 was C-terminally tagged (13xMyc) (Figure 2.1A). To avoid “hyper-ChIPable” loci that can appear in yeast ChIP-seq experiments, we also ran nuclear localized GFP controls (TEYTELMAN *et al.* 2013). GO terms of genes closest to Sir2-dependent condensin peaks after subtraction of GFP are listed in Table S2.1. One of the strongest peaks overlapped with a Sir2-myc binding site on chromosome III between *KAR4* and *SPB1* that was not enriched for GFP (Figure 2.1A). The specificity of Sir2 enrichment at this peak, as opposed to the adjacent *SPB1* gene, was independently confirmed by quantitative ChIP using an α -Sir2 antibody (Figure 2.1B), with enrichment comparable to levels observed at the *HML-I* silencer (Figure 2.1A and 2.1B). Sir2-dependent condensin binding was also confirmed for Myc-tagged Smc4 and Brn1 subunits (Figure 2.1C). The ~2.5 kb intergenic region between *KAR4* and *SPB1* was previously defined as a cis-acting recombination enhancer (RE) that specifies donor preference of mating-type switching in *MATa* cells (WU AND HABER 1996; SZETO *et al.* 1997). Quantitative ChIP assays revealed that Sir2 and Brn1-myc enrichment at the RE was also *MATa*-specific (Figure 2.1D and 2.1E), which was notable because the ChIP-seq datasets in Figure 2.1A happened to be generated from *MATa* strains. We next considered whether condensin binding in the *MATa sir2* Δ mutant

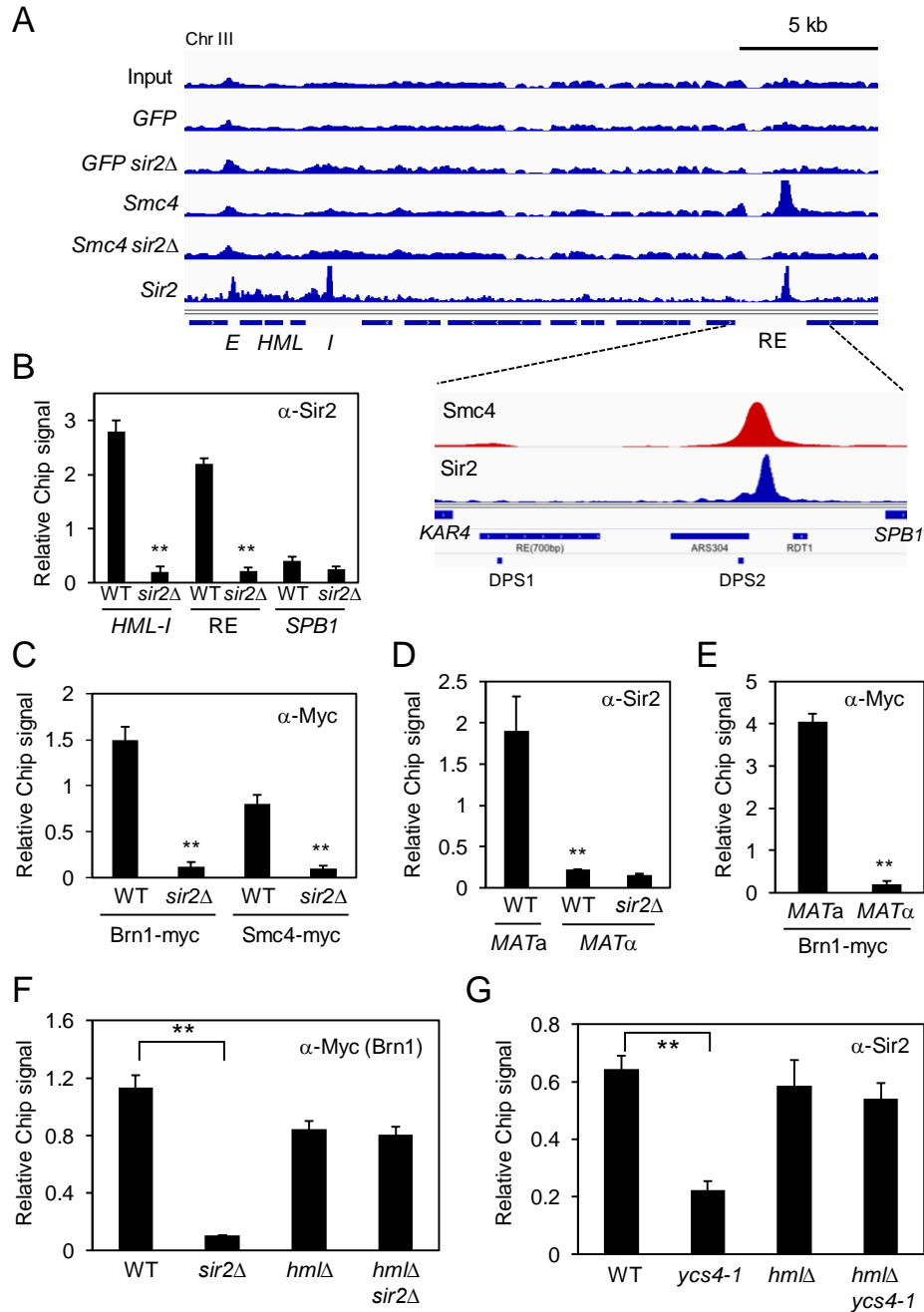


Figure 2.1. *MATa*-specific binding of Sir2 and condensin to the recombination enhancer (RE). (A) Chip-seq of Smc4-myc, Sir2-myc, and nuclear localized GFP in WT and *sir2* Δ backgrounds. The left arm of chromosome III is depicted from *HML* to *SPB1*. RE indicates the recombination enhancer region. Inset: The minimal 700bp RE element required for donor preference is indicated, as are the two Mcm1/ α 2 binding sites (DPS1 and DPS2) and *RDT1*. (B) Sir2 ChIP at the RE, *HML-I* silencer, and *SPB1*. (C) α -Myc ChIP of Brn1-myc and Smc4-myc at the RE. (D) ChIP showing *MATa*-specific binding of Sir2 to the RE. (E) ChIP showing *MATa*-specific binding of Brn1-myc to the RE. (F) Brn1-Myc ChIP at RE is not Sir2 dependent. (G) Native Sir2 ChIP at RE is not condensin dependent. ChIP signal relative to input is plotted as the mean of three replicates. Error bars = standard deviation. (***p*<0.005).

was due to *HMLALPHA2* expression caused by defective *HML* silencing. To test this idea, we retested Brn1-myc ChIP at the RE in strains lacking *HML*, and found that deleting *SIR2* no longer affected condensin recruitment (Figure 2.1F). Similarly, a *MATa* condensin mutant (*ycs4-1*) known to have an *HML* silencing defect (BHALLA *et al.* 2002) reduced Sir2 recruitment to the RE, but had no effect when *HML* was deleted (Figure 2.1G). Sir2 and condensin are therefore independently recruited to the RE specifically in *MATa* cells.

Sir2 regulates a small gene (*RDT1*) within the RE

Donor preference activity ascribed to the RE was previously narrowed down to a *KAR4* (*YCL055W*)-proximal 700 bp domain defined by an Mcm1/ α 2 binding site (Figure 2.2A, *DPS1*) (WU AND HABER 1996; SZETO *et al.* 1997; SUN *et al.* 2002). The Sir2 and condensin ChIP-seq peaks we identified were located outside this region, between a second Mcm1/ α 2 binding site (*DPS2*) and a small gene of unknown function called *RDT1* (WILSON AND MASEL 2011) (Figure 2.1A and 2.2A). We noticed the location of *RDT1* coincided with the smallest of several putative non-coding RNAs (ncRNA) previously reported as being transcribed from the RE, but not annotated in SGD (SZETO AND BROACH 1997, Figure 2.2A). Quantitative RT-PCR and analysis of publicly available RNA-seq data from BY4741 (*MATa*) and BY4742 (*MAT α*) revealed that *RDT1* expression was indeed *MATa* specific (Figure 2.2B and 2.3A).

We next asked whether Sir2 and/or condensin regulate histone acetylation and *RDT1* expression when recruited to the RE. Sir2 normally represses transcription at *HML*, *HMR*, and telomeres as a catalytic subunit of the SIR complex where it preferentially deacetylates H4K16 (reviewed in (GARTENBERG AND SMITH 2016)). Accordingly, deleting *SIR2*, *SIR3*, or *SIR4* from

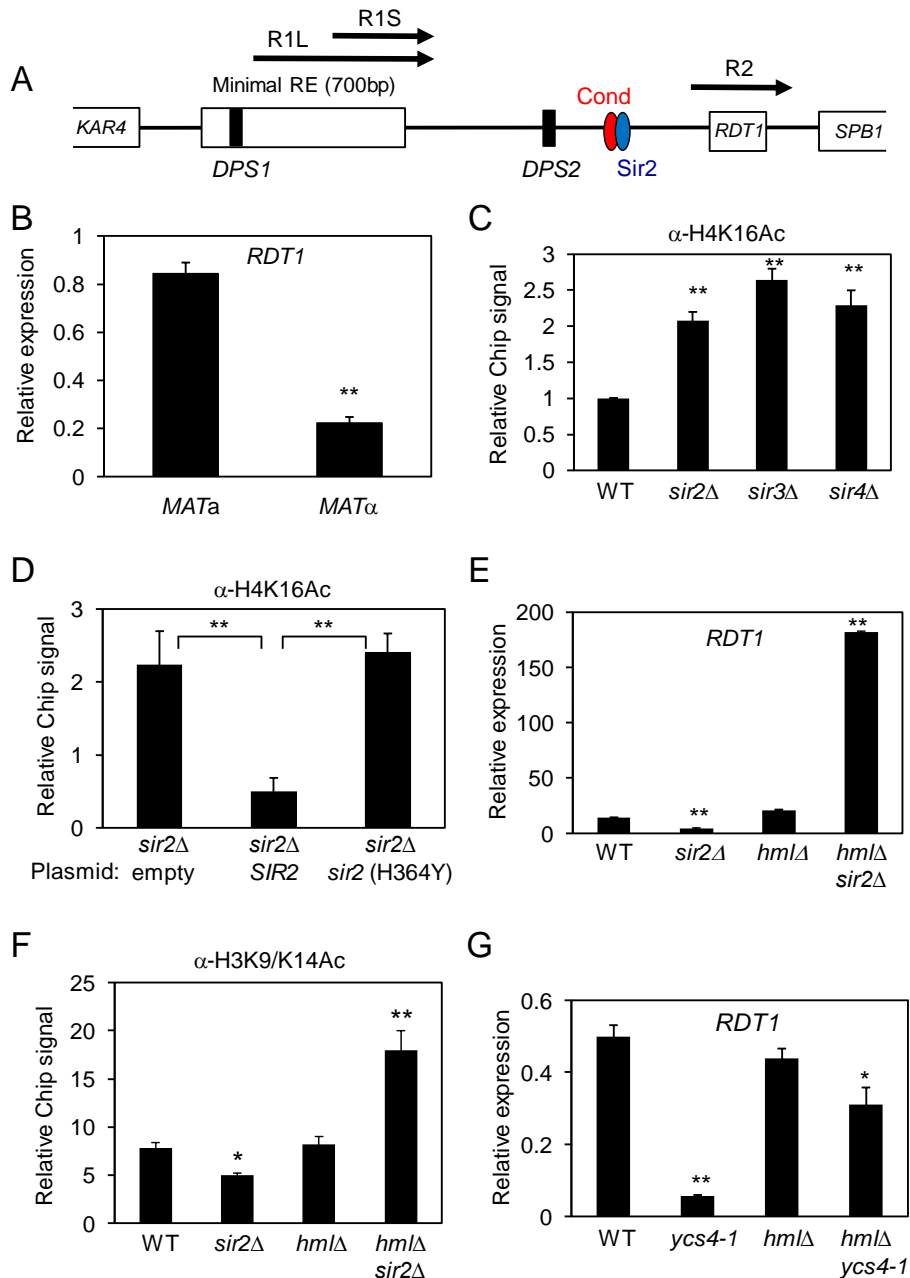


Figure 2.2. *RDT1* is a novel Sir2 regulated gene. (A) Schematic of RE locus depicting Sir2/Condensin peak location relative to previously reported R1L/S and R2 RNA (*RDT1*). (B) *RDT1* mRNA expression is *MATa* specific. (C) H4K16ac ChIP at RE in SIR complex null strains. (D) H4K16ac deacetylation is dependent on Sir2 catalytic activity. A *sir2Δ* strain was transformed with the indicated plasmids and ChIP assays performed. (E) Differential *RDT1* transcriptional regulation by *SIR2* is dependent on *HML* status. (F) Effect of *sir2Δ* on H3K9/K14ac ChIP at the *RDT1* promoter in *HML* and *hmlΔ* backgrounds. (G) effects of the temperature sensitive *ycs4-1* mutation on *RDT1* expression in *HML* and *hmlΔ* backgrounds. (* $p < 0.05$; ** $p < 0.005$).

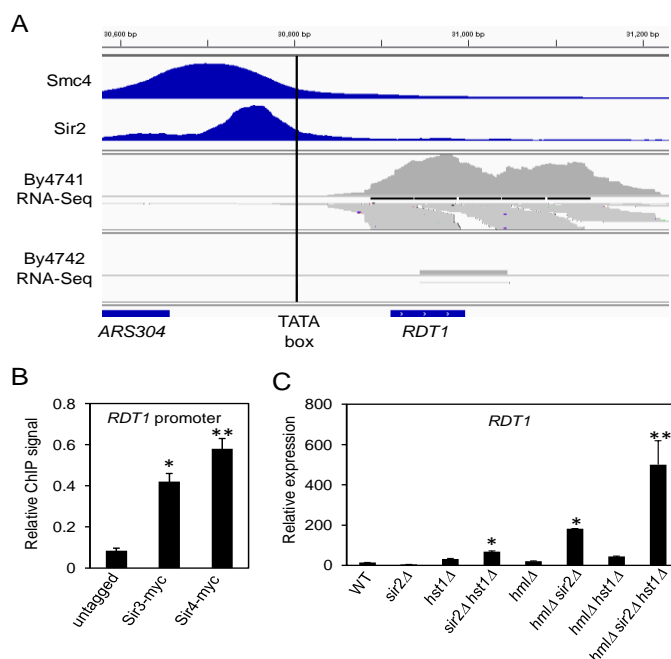


Figure 2.3. *MATa*-specific transcription of *RDT1* is repressed by Sir2 and Hst1.

(A) IGV screenshot of compiled raw RNA-seq read data from BY4741 (*MATa*) and BY4742 (*MATα*) strains. The top two blue peaks represent Smc4-myc and Sir2-myc ChIP-seq reads. (B) Quantitative ChIP assay showing additional SIR complex subunit enrichment at the *RDT1* promoter. (C) RT-qPCR showing effects of deleting *SIR2* and/or *HST1* on *RDT1* expression when HML is present or deleted (* $p < 0.05$, ** $p < .005$).

MATa cells increased H4K16 acetylation at the *RDT1* promoter (Figure 2.1C), consistent with the observed enrichment of Sir3-myc and Sir4-myc at this site (Figure 2.3B). Furthermore, reintroducing active *SIR2* into the *sir2Δ* mutant restored H4K16 to the hypoacetylated state, whereas catalytically inactive *sir2-H364Y* did not (Figure 2.2D).

Deleting *SIR2* initially appeared to repress *RDT1* expression in *MATa* cells (Figure 2.2E), but we hypothesized this was due to *HMLALPHA2* derepression and formation of the Mcm1/ α 2 repressor, which could locally repress *RDT1* through the adjacent Mcm1/ α 2 binding sites. Indeed, simultaneously deleting *SIR2* and *HML* resulted in very high *RDT1* expression (Figure 2.2E), which was increased even further when the paralogous *HST1* gene was also deleted (Figure 2.3C), indicating some redundancy. By eliminating *HML* we also observed elevated histone H3 acetylation in the absence of *SIR2* (Figure 2.2F), providing strong evidence that the SIR complex establishes a generally hypoacetylated chromatin environment at the *RDT1* promoter that requires effective silencing at *HML*. On the other hand, *RDT1* was not upregulated

in an *hml* Δ *ycs4-1* condensin mutant (Figure 2.2G), suggesting that condensin has a different functional role at this locus.

We next attempted to block Sir2 and condensin recruitment to the *RDT1* promoter by precisely deleting a 100bp DNA sequence underlying the shared enrichment region (coordinates 30701-30800), while not disturbing the adjacent Mcm1/ α 2 site (Figure 2.4A). Sir2 and Brn1-myc binding to the RE as measured by ChIP was greatly diminished in this mutant (Figure 2.4B and 2.4C), despite unaltered Sir2, Brn1-myc, or Smc4-myc expression levels (Figure 2.5A-C). Furthermore, *RDT1* transcriptional expression was significantly increased by the 100bp deletion exclusively in *MATa* cells (Figure 2.4D), consistent with the loss of Sir2-mediated repression.

Because Sir2 and condensin were not present at the *RDT1* promoter in *MATa* cells, we reasoned that their binding should require a *MATa* specific transcription factor. This made the 2nd Mcm1/ α 2 binding site (DPS2) upstream of the Sir2/condensin ChIP-seq peaks an ideal candidate because it has not been ascribed a function other than redundancy with DPS1. Deleting *MCM1* is lethal, so alternatively, we deleted the 2nd Mcm1/ α 2 binding site (ChrIII coordinates 30595 to 30626, Figure 2.6A) and then retested for Sir2 and Brn1-myc enrichment. As shown in Figure 2.6B and 2.6C, respectively, Sir2 and Brn1-myc enrichment at both the Mcm1/ α 2 binding site (DPS2) and the *RDT1* promoter (defined as the Sir2/condensin peaks) was significantly reduced in the binding site mutant. These results suggest that Mcm1 may nucleate a complex that recruits the SIR and condensin complexes to the *RDT1* promoter in *MATa* cells, and also provides a possible mechanism of blocking the recruitment in *MATa* cells due to the interaction of Mcm1 with α 2.

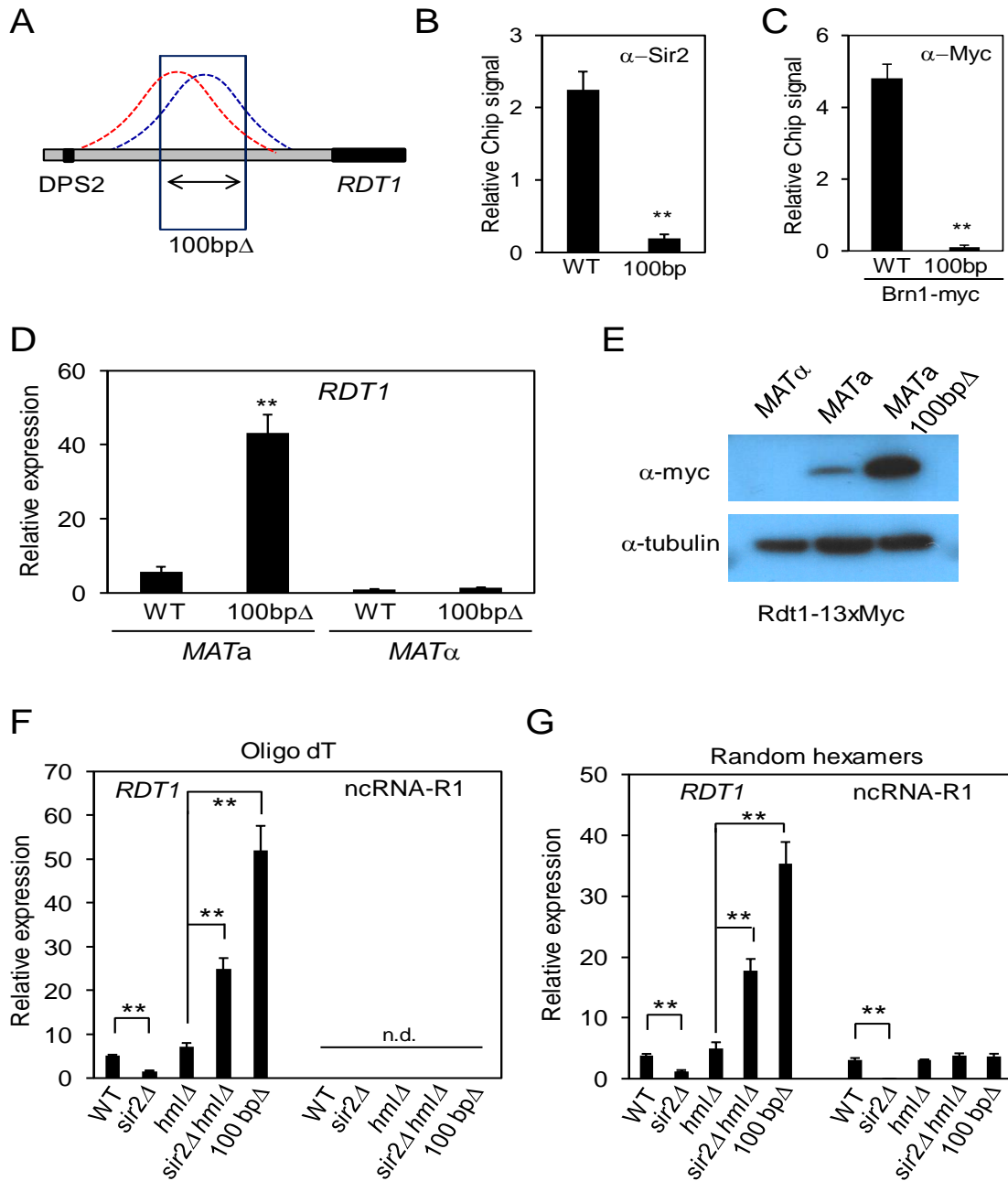


Figure 2.4. Identification of a 100bp sequence that recruits Sir2/condensin and represses *RDT1* expression. (A) Schematic indicating a 100bp deletion that covers the condensin (red) and Sir2 (blue) peaks. (B) ChIP of Sir2 in the 100bp Δ mutant (ML275). (C) ChIP of Brn1-Myc in the 100bp Δ mutant. (D) *RDT1* transcription in *MATa* cells is derepressed in the 100bp Δ mutant. (E) Western blot of Rdt1-13xMyc in WT *MATa* and *MATa* cells, as well as the *MATa* 100bp Δ mutant. (F) *RDT1* and R1 expression when using oligo dT priming for the reverse transcription step. (G) *RDT1* and R1 expression when using random hexamer priming for reverse transcription. (** $p < 0.005$).

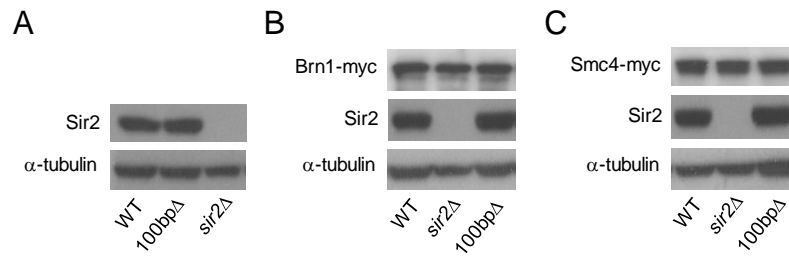


Figure 2.5. Deletion of Sir2 or the *RDT1* promoter Sir2/condensin binding site does not affect protein levels of Sir2 or Myc-tagged condensin subunits. (A) Western blot showing steady state Sir2 protein levels in WT (ML1), *sir2* Δ (ML25), and 100bp Δ (ML275) strains. (B) Western blot with anti-Myc detection of Brn1-13xMyc or Sir2 in WT (ML149), *sir2* Δ (ML161), and 100bp Δ (ML322) strains. (C) Western blot with anti-Myc detection of Smc4-13xMyc or Sir2 in WT (ML152), *sir2* Δ (ML160), and 100bp Δ version.

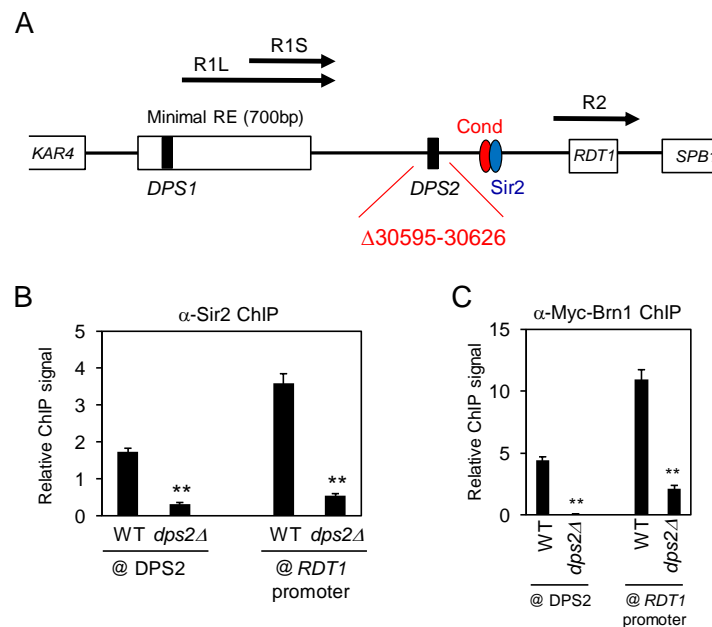


Figure 2.6. The *RDT1*-proximal Mcm1/a2 binding site (DPS2) is important for Sir2 and condensin recruitment. (A) Schematic diagram depicting the location of the DPS2 sequence deletion relative to other elements with the RE, with the deleted chromosome III coordinates indicated in red. (B) Quantitative ChIP of native Sir2 in WT and *dps2* Δ strains. (C) Quantitative ChIP of Brn1-Myc in WT and *dps2* Δ strains. @*RDT1* promoter indicates enrichment at the Sir2/condensin peak (**p < 0.005).

***RDT1* encodes a translated mRNA**

Ribosome Detected Transcript-1 (*RDT1*) was originally annotated as a newly evolved gene whose transcript was associated with ribosomes and predicted to have a small open reading frame of 28 amino acids (WILSON AND MASEL 2011). Our work suggested that *RDT1* and the putative non-coding R2 transcript were the same (Figure 2.2A). To determine if *RDT1*/R2 codes for a small protein, the ORF was C-terminally fused with a 13x-Myc epitope in *MATa* and *MATα* cells. As shown in Figure 2.4E, a fusion protein was detectable in exponentially growing *MATa* WT cells and also highly expressed in the 100bpΔ background, correlating with the increased RNA level observed for that mutant in Figure 2.4D.

Additional *MATa*-specific RNAs are derived from the minimal 700bp RE domain (Figure 2.2A; R1L and R1S) (SZETO *et al.* 1997; ERCAN *et al.* 2005), so we next tested whether Sir2 controls their expression from a distance. As shown in Figure 2.4F, qRT-PCR using standard oligo(dT) primers for cDNA synthesis effectively measured *RDT1* expression at predicted levels for the various strains tested, but the R1 RNAs were not detectable. Many long non-coding RNAs (lncRNAs) are not polyadenylated (YANG *et al.* 2011), so the cDNA synthesis was repeated using random hexamer primers. In *MATa* WT cells (ML1), R1L/S RNAs were now detected at levels comparable to *RDT1* (Figure 2.4G). Similar to *RDT1*, R1L/S RNAs were repressed in the absence of *SIR2* due to the *HMLALPHA2* pseudodiploid derepression phenotype. But unlike *RDT1*, the R1L/S RNA expression level was not elevated in the 100bpΔ or *hmlΔ sir2Δ* mutants, indicating these RNAs are not under direct Sir2 control, but are strongly repressed in the absence of Sir2. We conclude that the R1L/S RNAs are most likely non-polyadenylated lncRNAs, whereas *RDT1* is Sir2-repressed and polyadenylated mRNA that can be translated into a small protein of unknown function.

Sir2 and condensin are displaced from the *RDT1* promoter during mating-type switching

We next asked if Sir2 played any role in regulating *RDT1* during mating-type switching. Sir2 was previously shown to associate with a HO-induced DSB at the *MAT* locus during mating-type switching, presumably to effect repair through histone deacetylation (TAMBURINI AND TYLER 2005). Transient Sir2 recruitment to the DSB could potentially occur at expense of the *RDT1* promoter, thus resulting in *RDT1* derepression. To test this idea, HO was induced at time 0 with galactose and then turned off 2 hours later by glucose addition to allow for repair/switching to occur (Figure 2.7A and 2.7B). By the 3 hr time point (1hr after glucose addition), ChIP analysis indicated Sir2 was maximally enriched at the *MAT* locus (Figure 2.7C), corresponding to the time of peak mating-type switching (TAMBURINI AND TYLER 2005 and Figure 2.7B). Interestingly, Sir2 was significantly depleted from the *RDT1* promoter within 1 hr after HO induction, and by 3 hr there was actually stronger enrichment of Sir2 at *MAT* than *RDT1* (Figure 2.7C). Critically, this apparent Sir2 redistribution coincided with maximal induction of *RDT1* mRNA and the Myc-tagged Rdt1 protein (Figure 2.7D and 2.7E, 3 hr). Once switching was completed by 4 hr (2hr after glucose addition), *RDT1* transcription was permanently inactivated and Sir2 binding never returned because most cells were now *MAT α* . The Myc-tagged Rdt1 protein, however, remained elevated for the rest of the time course (Figure 2.7E), suggesting that it is relatively stable, at least when epitope tagged. A parallel ChIP time course experiment was performed with condensin (Brn1-myc), resulting in significant depletion from the *RDT1* promoter within 1 hr (Figure 2.7F), similar to the timing of Sir2 loss. However, rather than redistributing to the DSB, Brn1-myc enrichment was actually reduced at the break

site, suggesting that condensin normally associates with *MATa* in non-switching cells, but becomes displaced in response to the HO-induced DSB, perhaps to facilitate structural reorganization associated with switching.

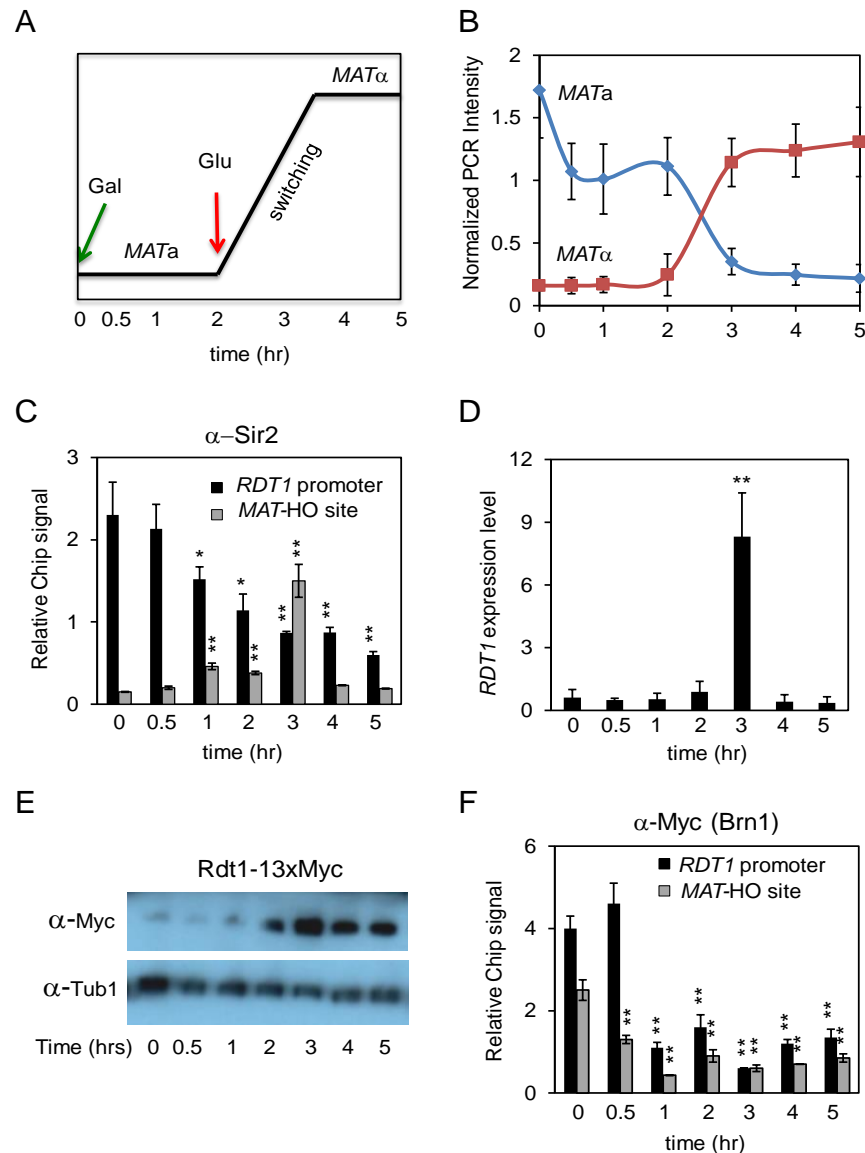


Figure 2.7. Dynamics of Sir2 and condensin binding at the *RDT1* promoter and *MATa* locus during mating-type switching. (A, B) Mating-type switching time course where HO was induced by galactose at time 0, then glucose added at 2 hr to stop HO expression and allow for break repair. Switching is maximal at 3 hr (TAMBURINI AND TYLER 2005). (C) ChIP of Sir2 at the *RDT1* promoter and the HO-induced DSB (*MAT-HO*). (D) qRT-PCR of *RDT1* expression across the mating-type switching time course. (E) Rdt1-13xMyc protein expression across the same time course. (F) ChIP of Brn1-myc at the *RDT1* promoter and *MAT-HO* break site across the same time course. (* $p < 0.05$, ** $p < 0.005$ compared to time 0).

The *RDT1* promoter region controls chromosome III architecture

The coupling of Sir2 and condensin distribution with *RDT1* transcriptional regulation during mating-type switching was reminiscent of classic locus control regions (LCR) that modulate long-range chromatin interactions. We therefore hypothesized that the *RDT1* promoter region may function as an LCR to modulate long-range chromatin interactions of chromosome III. To test this hypothesis, we performed Hi-C analysis with WT, *sir2* Δ and the 100bp Δ strains. Genomic contact differences between the mutants and WT were quantified using the HOMER Hi-C software suite (HEINZ *et al.* 2010), and the frequency of statistically significant differences for each chromosome calculated (Figure 2.8A). Chromosome III had the most significant differences in both mutants, so we focused on this chromosome and used HOMER to plot the observed/expected interaction frequency in 10kb bins for each strain as a heat map (Figure 2.8B).

In a WT strain (ML1) there was strong interaction between the left and right ends of chromosome III, mostly centered around the *HML* (bin 2) and *HMR* (bin 29) loci. Interestingly, *HML* (bin 2) also appeared to sample the entire right arm of chromosome III, with the interaction frequency increasing as a gradient from *CEN3* to a maximal observed interaction at *HMR*, thus also encompassing the *MATa* locus at bin 20. This distinct interaction pattern was completely disrupted in the *sir2* Δ mutant, whereas some telomere-telomere contact was retained in the 100bp Δ mutant (Figure 2.8B), suggesting there was still limited interaction between the left and right ends of the chromosome. We confirmed the changes in *HML-HMR* interaction for these strains using a quantitative 3C-PCR assay to rule out sequencing artifacts, and also confirmed an earlier *sir2* Δ 3C result from the Dekker lab (MIELE *et al.* 2009). Importantly, despite the loss of *HML-HMR* interaction in the 100bp Δ mutant, heterochromatin at these domains was unaffected

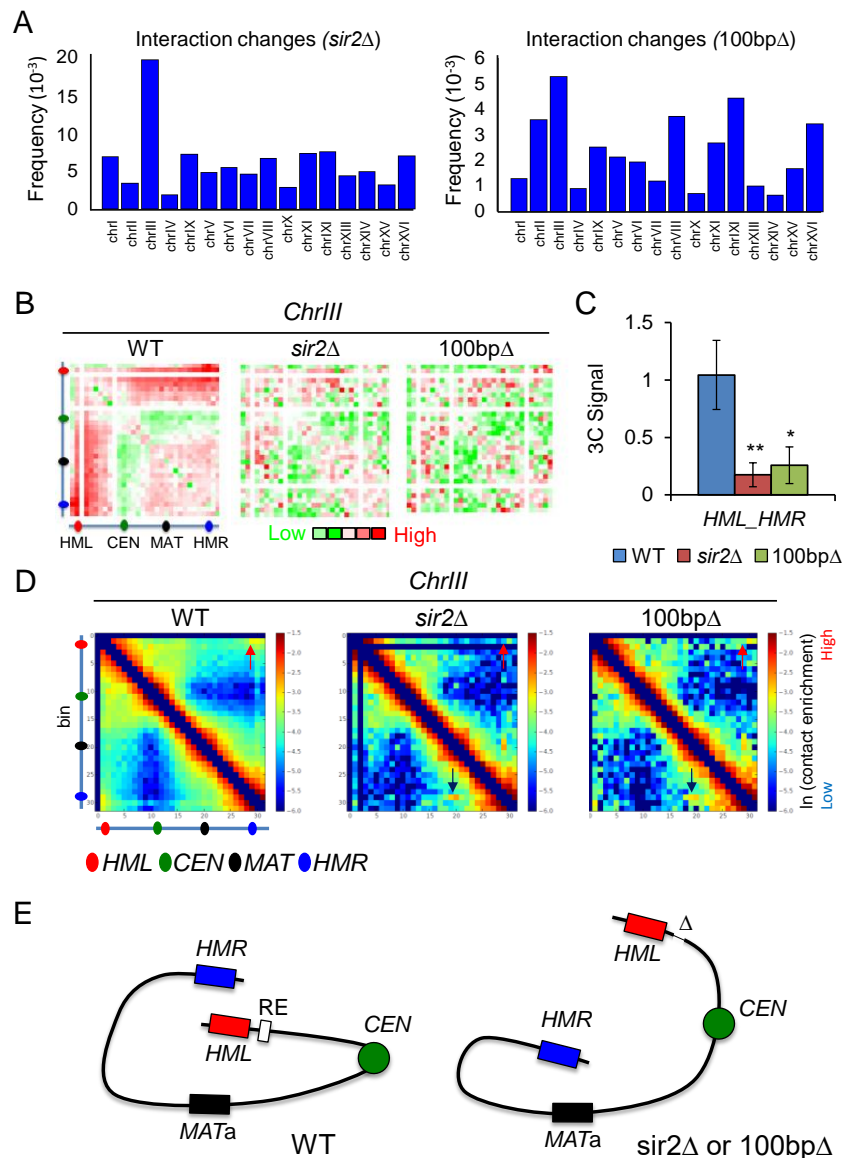


Figure 2.8. The Sir2/condensin binding site controls chromosome III architecture.

(A) Frequency of significant Hi-C interaction changes identified using HOMER for each chromosome in the *sir2Δ* (ML25) and 100bpΔ (ML275) strains compared to WT (ML1). (B) HOMER-generated observed/expected Hi-C interaction frequency heat maps (10kb bins) for chromosome III. (C) qPCR detection of *HML-HMR* interaction using 3C analysis. (* $p < 0.05$, ** $p < 0.005$). (D) Iteratively corrected and read-normalized Hi-C heat maps revealing a loss of interaction between *HMR* and *HML* (red arrows) as well as gain of interaction between *HMR* (bin 29) and *MATa* (bin 20) in the *sir2Δ* and 100bpΔ mutants (black arrows). (E) Summary of large-scale changes in chromosome III architecture. Δ indicates the 100bp deletion.

based on normal quantitative mating assays (Figure 2.9A), and unaltered Sir2 association with *HML* (Figure 2.9B).

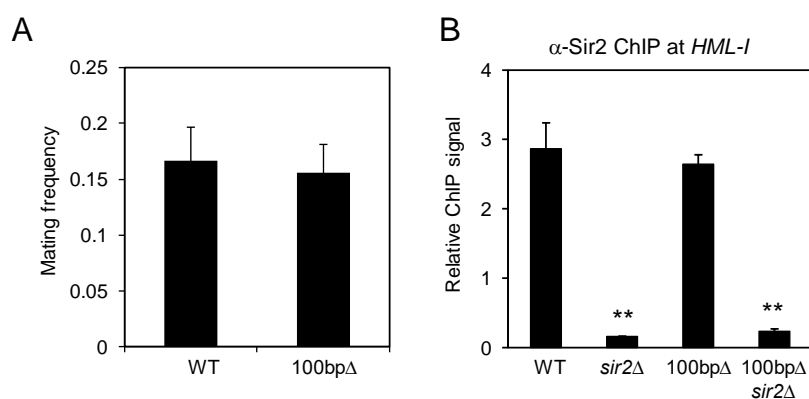


Figure 2.9. Deleting the Sir2/condensin binding site within the RE (100bpΔ) does not alter Sir2 function at *HMLa*. (A) Quantitative mating assay for WT (ML1) and 100bpΔ (ML275) strains. (B) Quantitative ChIP assay showing Sir2 enrichment at *HML-I* in WT (ML1) and 100bpΔ (ML275) strains. (**p<0.005).

We next analyzed the Hi-C data using an iterative correction method that reduces background to reveal interacting loci that potentially drive the overall chromosomal architecture, rather than passenger locus effects (IMAKAEV *et al.* 2012). *HML* (bin 2) and *HMR* (bin 29) again formed the dominant interaction pair off the diagonal in WT, which was lost in the *sir2Δ* or 100bpΔ mutants (Figure 2.8D). Importantly, a prominent new interaction between *HMR* (bin 29) and *MATa* (bin 20) appeared in both mutants (Figure 2.8D and 2.8E), as would be predicted if normal donor preference of *MATa* cells was altered. We conclude that the *RDT1* promoter does function like an LCR in *MATa* yeast cells, regulating localized transcription as well as long-range chromatin interactions relevant to mating-type switching (Figure 2.8E).

Sir2 and condensin regulate mating-type switching

Sir2/condensin binding was observed in the right half of the RE (Figure 1A), but this region was previously reported as being dispensable for donor preference activity (WU AND HABER 1996). Considering that *HMR* was aberrantly associated with the *MAT α* locus in *sir2 Δ* and 100bp Δ mutants (Figure 2.8), we proceeded to test whether these mutants had any alterations in donor preference. A reporter strain was used in which *HMR α* on the right arm of chromosome III was replaced with an *HMR α* allele containing a *Bam*HI site (*HMR α -B*) (Figure 2.10A). After inducing switching to *MAT α* following HO induction with galactose, the proportion of *HML α* or *HMR α -B* utilization for switching was determined by *Bam*HI digestion of a *MAT α* -specific PCR product (Figure 2.10B) (LI *et al.* 2012). As expected for normal donor preference, *HMR α -B* on the right arm was only utilized ~9% of the time in the WT strain, as compared to 91% for *HML α* (Figure 2.6C). Strikingly, donor preference was completely lost in the *sir2 Δ* mutant, similar to a control strain with the RE deleted (Figure 2.10C and 2.10D), and consistent with the clear interaction between *HMR* and *MAT α* observed for the *sir2 Δ* mutant in Figure 2.8D and 2.8E. This interaction was less prominent in the 100bp Δ mutant (Figure 2.8D), and the change in donor preference was also less severe (~25% *HMR α -B*), though still significantly different from WT (Figure 2.10C and 2.10D). Additionally, we measured the efficiency of switching to *MAT α* across a time course in the ML1 strain background used for ChIP and Hi-C analyses, and did not observe a significant difference between WT and the 100bp Δ mutant. However, switching to *MAT α* was severely impaired in the *sir2 Δ* mutant (Figure 2.10E). We suspect the larger effect on switching efficiency and donor preference in *sir2 Δ* cells is due to the derepression of *HMLALPHA2*, because $\alpha 2$ protein normally inactivates the RE in *MAT α* cells (SZETO *et al.* 1997). Silencing of *HML* is therefore critical for donor preference in the mating-type switching

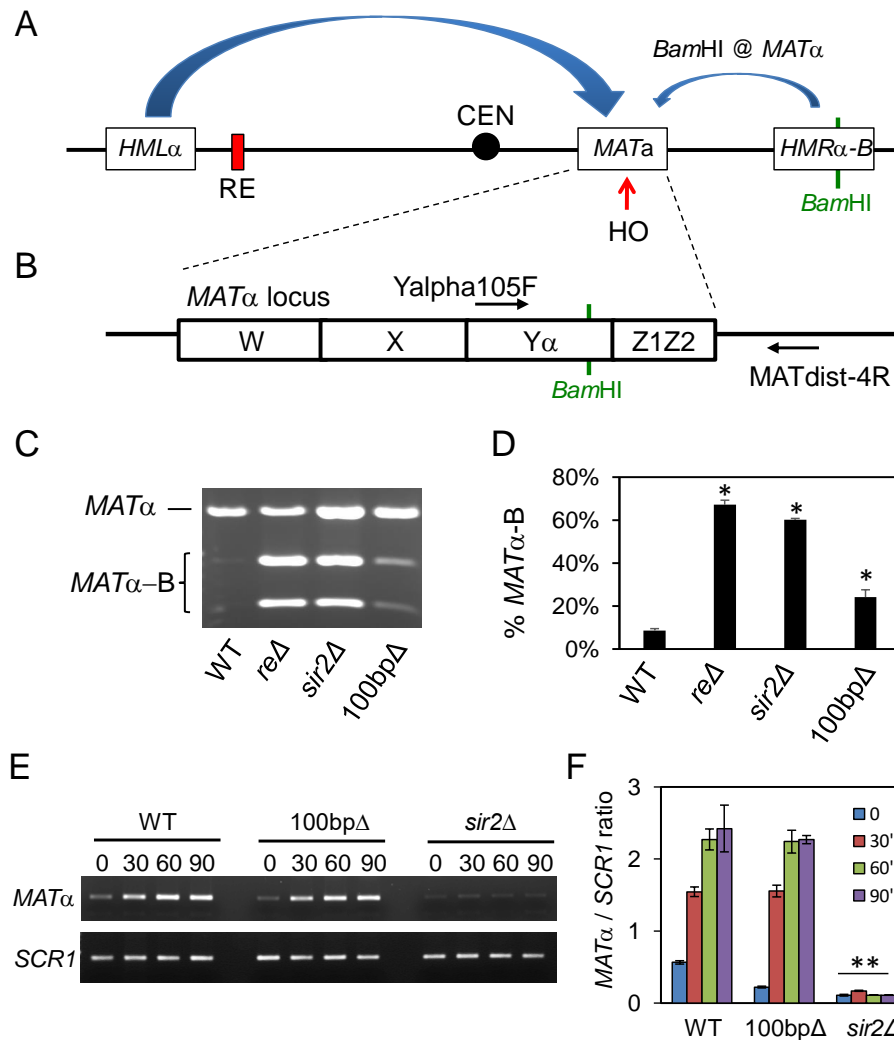


Figure 2.10. Loss of Sir2 and the Sir2/condensin binding site alters mating-type switching. (A) Schematic of a donor preference assay in which utilization of an artificial *HMR α -B* cassette as the donor for switching introduces a unique *Bam*HI site to the *MAT* locus. (B) Locations of primers flanking the *Bam*HI site used for PCR detection of *MAT α* . (C) Representative ethidium bromide stained agarose gel of *Bam*HI-digested *MAT α* PCR products after mating-type switching in WT (XW652), *re Δ* (XW676), *sir2 Δ* (ML557), and 100bp Δ (SY742) strains. The *MAT α -B* product is digested into 2 smaller bands. (D) Quantifying the percentage of *MAT α* PCR product digested by *Bam*HI, from three biological replicates. ImageJ was used for the quantitation. (* $p < 0.05$). (E) Time course of switching from *MAT a* to *MAT α* in WT (ML447), 100bp Δ (ML460), and *sir2 Δ* (ML458) strains after HO was induced for 45 min and then shut down with glucose. Aliquots were harvested at 30 min intervals. *SCR1* is a control for input genomic DNA. (F) ImageJ quantification of *MAT α -B* PCR relative to *SCR1* for each time point (** $p < 0.005$).

of *MAT α* cells by preventing expression of the repressive $\alpha 2$ transcription factor.

Since condensin is also recruited to the *RDT1* promoter region, we were next interested in whether condensin activity was important for mating-type switching. Each gene for the condensin subunits is essential, so instead of using deletions, in the ML1 strain background we C-terminally tagged the Brn1 subunit with an auxin-inducible degnon (AID) fused with a V5 epitope. This system allows for rapid depletion of tagged proteins upon addition of auxin to the growth media (NISHIMURA *et al.* 2009). Indeed, Brn1-AID was effectively degraded within 15 min of adding auxin (Figure 2.11A). Importantly, even after 1 hr of auxin treatment, there were

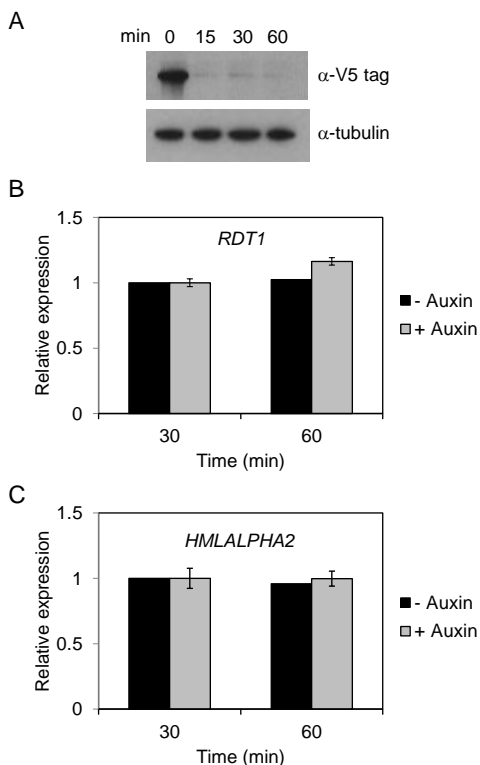


Figure 2.11. Auxin inducible degnon (AID)-mediated depletion of Brn1 does not derepress *RDT1* or *HML α* . (A) Western blot time course of auxin induced degradation of Brn1-V5-AID. Time indicates minutes after addition of auxin. (B) RT-qPCR of *RDT1* expression following 30 or 60 minutes of Brn1 depletion by auxin. (C) RT-qPCR of *HMLALPHA2* expression following 30 or 60 min of Brn1 depletion by auxin.

no changes in *RDT1* or *HMLALPHA2* gene expression indicated by qRT-PCR (Figure 2.11B and C), indicating that silencing of *HML* was unaffected, unlike the *ycs4-1* condensin mutant used in Figure 1G (BHALLA *et al.* 2002), which eliminates the possibility of pseudodiploid effects. The efficiency of ML1 switching from *MAT α* to *MAT α* was then tested across a time course with or

without auxin treatment (Figure 2.12A). As shown in Figure 2.12B and 2.12C, auxin treatment significantly slowed the pace of switching to *MAT α* , which also suggested there could be a modest effect on donor preference similar to that observed with the 100bp Δ strain. Indeed, Brn1-AID depletion produced a minor, yet significant, alteration in donor preference using the *HMR α -B* reporter strain (Figure 2.12D). Taken together, these results support a model whereby condensin recruited to the *RDT1* promoter in *MAT α* cells organizes chromosome III into a conformation that favors association of the *MAT α* locus with *HML* instead of *HMR*, thus partially contributing to donor preference regulation.

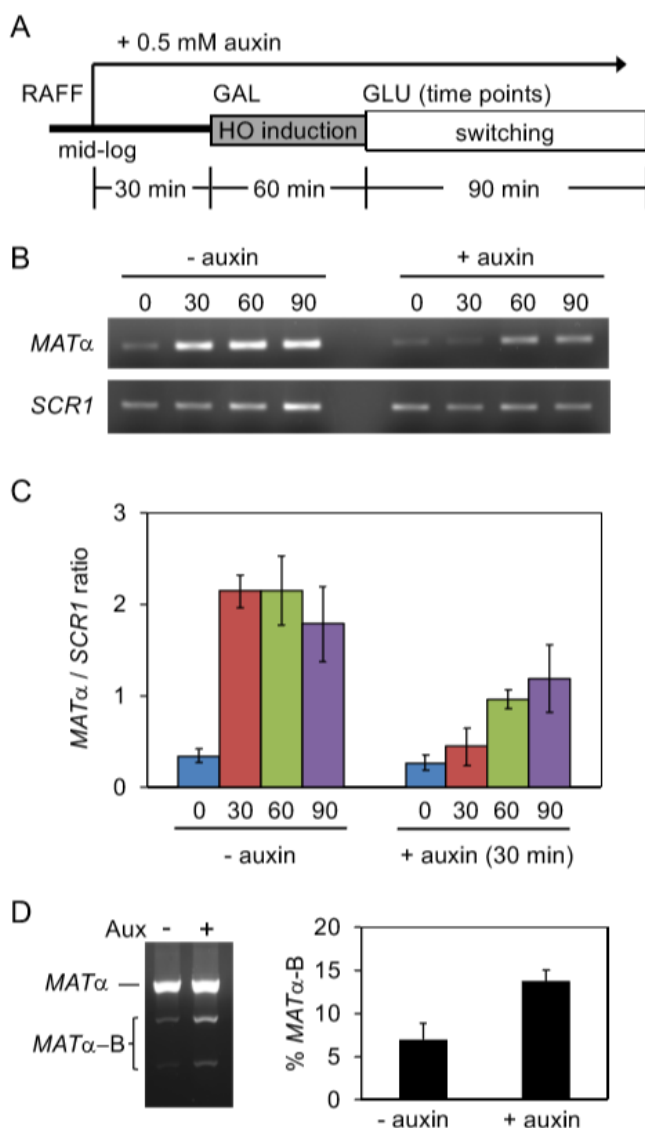


Figure 2.12. Effects of condensin depletion on mating-type switching. (A)

Schematic of the time course used to deplete Brn1-AID prior to the induction of mating-type switching in the ML1 strain background. Auxin was added 30 min prior to the induction of HO expression by galactose. (B) EtBr stained agarose gel of *MAT α* qPCR products amplified from each time point during mating-type switching. *SCR1* PCR was used as a control for input DNA. (C) Quantification of the *MAT α* /*SCR1* PCR product ratio across the time course from 3 biological replicates. (D) Effect of Brn1-AID depletion on mating-type switching donor preference. A representative biological replicate is shown, along with quantitation of switching using the *HMR α -B* cassette.

Discussion

SIR2 was identified almost 40 years ago as a recessive mutation unlinked to *HML* and *HMR* that caused their derepression (KLAR *et al.* 1979; RINE 1979), and has been extensively studied ever since as encoding a heterochromatin factor that functions not only at the *HM* loci, but also telomeres and the rDNA locus (reviewed in (GARTENBERG AND SMITH 2016)). In this study we describe a previously unidentified Sir2 binding site that overlaps with a major non-rDNA condensin binding site within the RE on chromosome III in *MATa* cells. Here, Sir2 regulates a small gene of unknown function called *RDT1*, which is transcriptionally activated during mating-type switching due to redistribution of repressive Sir2 from the *RDT1* promoter to the HO-induced DSB at *MATa*. The *RDT1* RNA transcript is also polyadenylated and translated into a small protein, but we have not yet been able to assign a function to the gene or protein because deleting the 28 amino acid ORF had no measurable effect on mating-type switching when using the *GAL-HO* based assays tested thus far (data not shown). It remains possible that deleting *RDT1* would have a significant effect on switching in the context of native HO expression, which is expressed only in mother cells during late G1, whereas the *GAL1-HO* is overexpressed in all cells throughout the cell cycle. It is also possible that *RDT1* functions as a non-coding RNA that happens to be translated into a small non-functional peptide. Alternatively, transcription of *RDT1* could directly function in chromosome III conformation by altering local chromatin accessibility at the promoter. Such a model was proposed for regulation of donor preference by transcription of the R1S/R1L non-coding RNAs (SZETO *et al.* 1997; ERCAN *et al.* 2005). Dissecting the function(s) of *RDT1* therefore remains an area of active investigation for the lab, and perhaps the key to fully understanding how its promoter functions as an LCR.

Functional complexity within the RE

While we do not yet know the molecular function of *RDT1* in mating-type regulation or other cellular processes, the promoter region of this gene clearly controls the structure of chromosome III. Three-dimensional chromatin structure has long been proposed to influence donor preference (WU AND HABER 1995; COIC *et al.* 2006). However, deleting the minimal 700bp (left half) of the RE alters donor preference without a large change in chromosome III conformation. Furthermore, deleting the right half of the RE, which includes *RDT1*, changes chromosome III conformation without a dramatic change in donor preference (WU AND HABER 1996; SZETO *et al.* 1997; BELTON *et al.* 2015). Based on these findings it was proposed that the RE is a bipartite regulatory element (BELTON *et al.* 2015), with the left half primarily responsible for donor preference activity and the right half for chromosome III structure. Our results support this view and narrow down the structural regulatory domain of the RE to a small (100bp) region of the *RDT1* promoter bound by the SIR and condensin complexes. Importantly, deleting this small region not only altered chromosome III structure, but also had a significant effect on donor preference, though not as strong as the *sir2* Δ mutation.

The coordination of *RDT1* expression with loss of Sir2/condensin binding at its promoter during mating-type switching, together with the loss of *HML-HMR* interaction in the 100bp Δ mutant, makes this site intriguingly similar to classic locus control regions (LCRs) in metazoans, which are cis-acting domains that contain a mixture of enhancers, insulators, chromatin opening elements, and tissue-specificity elements (LI *et al.* 2002). The minimal RE was previously described as an LCR in the context of donor preference (WU AND HABER 1996), and transcription of the R1S/R1L long non-coding RNAs via activation by the 1st Mcm1/ α 2 binding site (DPS1) appears to be important for this activity in *MATa* cells (ERCAN *et al.* 2005). We find

that Sir2 indirectly supports donor preference from the left half of the RE in *MATa* cells by silencing *HMLALPHA2* expression, which prevents transcriptional repression by an Mcm1/ α 2 heterodimer. Similarly, the loss of Sir2 also represses *RDT1* expression and condensin recruitment in the right half of the RE due to *HMLALPHA2* expression. However, Sir2 directly represses *RDT1* through localized histone deacetylation. How the loss of *RDT1* regulation and condensin recruitment changes chromosome III structure in the *sir2* Δ mutant remains unknown, but we propose that the *HMR-MATa* interaction is a default state, while the *HML-HMR* association has to be actively maintained by condensin and likely additional factors co-localized to this element.

Interestingly, there also appears to be a function relationship between the RE and silencing at the *HML* locus, such that deleting the left half of the RE specifically stabilizes *HML* silencing in *MATa* cells (DODSON AND RINE 2016). The mechanism involved remains unknown, but we hypothesize that eliminating this part of the RE could potentially allow the SIR and condensin complexes bound at the *RDT1* promoter to encroach and somehow enhance the heterochromatic structure at *HML*. In this scenario, the left half of the RE could be insulating *HML* from the chromosomal organizing activity that occurs at the *RDT1* promoter.

Condensin function in mating-type switching

The *RDT1* promoter was a major condensin binding site identified by ChIP-seq (Figure 2.1), and given the strong Hi-C interaction between nearby *HML* and the *HMR* locus, we initially hypothesized that condensin at the *RDT1* promoter would crosslink with another condensin site bound on the right arm of chromosome III. ChIP-seq of Smc4-myc did not reveal any strong peaks near *HMR*, but condensin was clearly enriched at *CEN3* (data not shown). Interestingly,

the *S. cerevisiae* condensin complex was recently shown to catalyze ATP-dependent unidirectional loop extrusion using an *in vitro* single molecule assay (GANJI *et al.* 2018). The mechanism involves direct binding of condensin to DNA, followed by one end of the bound DNA being pulled inward as an extruded loop. Applying this model to the strong binding site at the *RDT1* promoter, this region could act as an anchor bound by condensin, with DNA to the right being rapidly extruded as a loop until pausing at *CEN3*. Extrusion would then continue at a slower rate toward *HMR*, allowing *HML* the time to sample the entire right arm of chromosome III, until clustering with *HMR*. HOMER analysis of the Hi-C data in Figure 2.5B provides evidence for such a model because there is an ascending gradient of *HML* interaction frequency with sequences extending from the centromere region (bin 2) toward *HMR*, suggesting that *HML* “samples” the right arm of chromosome III. Once brought in contact, *HML* and *HMR* would then remain associated due to their heterochromatic states and shared retention at the nuclear envelope (BYSTRICKY *et al.* 2009) In addition to preventing *HMR* association with *MATa*, we hypothesize that the looped chromosome III structure makes the chromosome licensed for mating-type switching in response to the HO-induced DSB during G1.

***MATa* specific recruitment of Sir2 and condensin to the RE**

Condensin and Sir2 each strongly associated with the *RDT1* promoter exclusively in *MATa* cells, though it is not clear if they bind at the same time, or are differentially bound throughout the cell cycle. Since *DPS2* was required for Sir2 and condensin recruitment, and derepression of *HMLALPHA2* from *HML* also eliminated binding, we hypothesized and then demonstrated (Figure S2.3) that Mcm1 was a key DNA binding factor involved. Mcm1 is a prototypical MADS box combinatorial transcription factor that derives its regulatory specificity

through interactions with other factors, such as Ste12 in the case of *MATa* haploid-specific gene activation, or $\alpha 2$ when repressing the same target genes in *MAT α* cells (MESSENGUY AND DUBOIS 2003). This raises the question of whether Mcm1 directly recruits the SIR and condensin complexes, or perhaps additional factors that work with Mcm1 are involved. At the *RDT1* promoter, specificity for Sir2/condensin recruitment could originate from sequences underlying the condensin/Sir2 peaks. There are no traditional silencer-like sequences for SIR recruitment within the deleted 100bp (coordinates 30702 to 30801), and yeast condensin does not appear to have a consensus DNA binding sequence (WANG *et al.* 2005). Closer inspection of the *RDT1* promoter indicates an A/T rich region with consensus binding sites for the transcription factors Fkh1/2 and Ash1, each of which regulates mating-type switching (BOBOLA *et al.* 1996; SIL AND HERSKOWITZ 1996; SUN *et al.* 2002). Fkh1 and Fkh2 also physically associate with Sir2 at the mitotic cyclin *CLB2* promoter during stress (LINKE *et al.* 2013). Ash1 is intriguing because it represses HO transcription in daughter cells (SIL AND HERSKOWITZ 1996; LONG *et al.* 1997), raising the possibility of *RDT1* repression in daughter cells. Mcm1 activity in *MATa* cells could also indirectly establish a chromatin environment that is competent for Sir2/condensin recruitment, rather than direct recruitment through protein-protein interactions. In *MATa* cells, Mcm1 appears to prevent the strong nucleosome positioning across the RE that occurs in *MAT α* cells (ERCAN *et al.* 2005), and indicative of an actively remodeled chromatin environment. Perhaps condensin is attracted to such regions, which is consistent with the association of condensin with promoters of active genes in mitotic cells, where enrichment was greatest at unwound regions of DNA (SUTANI *et al.* 2015). Furthermore, nucleosome eviction by transcriptional coactivators was found to assist condensin loading in yeast (TOSELLI-MOLLEREAU *et al.* 2016), though the mechanism of loading remains poorly understood. Recruitment of

condensin to the *RDT1* promoter LCR therefore provides an outstanding opportunity for dissecting mechanisms of condensin loading and function.

Supplemental Data

Table S2.1 Go terms of genes closest to Sir2-dependent condensin peaks.

GO Term	Pvalue
cytoplasmic translation	4.42E-20
small molecule metabolic process	1.90E-11
single-organism metabolic process	3.97E-10
oxoacid metabolic process	4.90E-09
organic acid metabolic process	6.71E-09
carboxylic acid metabolic process	1.24E-08
single-organism process	1.93E-08
small molecule biosynthetic process	2.23E-08
cellular amino acid biosynthetic process	1.02E-07
single-organism biosynthetic process	1.70E-07
alpha-amino acid biosynthetic process	9.39E-07
coenzyme metabolic process	2.61524E-06
pyruvate metabolic process	8.02676E-06
pyridine nucleotide metabolic process	1.02001E-05
nicotinamide nucleotide metabolic process	1.02001E-05
external encapsulating structure organization	1.31639E-05
cell wall organization	1.31639E-05
fungal-type cell wall organization	1.76708E-05
fungal-type cell wall organization or biogenesis	4.15628E-05
pyridine-containing compound metabolic process	5.79504E-05
cofactor metabolic process	6.62449E-05

oxidoreduction coenzyme metabolic process	0.000111548
organic acid biosynthetic process	0.000129693
carboxylic acid biosynthetic process	0.000129693
nucleobase-containing small molecule metabolic process	0.000220817
cell wall organization or biogenesis	0.000307043
ADP metabolic process	0.000369256
sulfur compound metabolic process	0.000464396
single-organism cellular process	0.000472596
nucleotide metabolic process	0.000546555
alpha-amino acid metabolic process	0.000649989
nucleoside phosphate metabolic process	0.000670356
purine nucleoside diphosphate metabolic process	0.001066375
purine ribonucleoside diphosphate metabolic process	0.001066375
ribonucleoside diphosphate metabolic process	0.001066375
glycolytic process	0.001104533
ATP generation from ADP	0.001104533
monocarboxylic acid metabolic process	0.001341511
catabolic process	0.003552415
nucleoside diphosphate phosphorylation	0.003747006
nucleotide phosphorylation	0.004543228
ammonium transport	0.004768668
sulfur compound biosynthetic process	0.004860838
organic substance catabolic process	0.005122472
sulfur amino acid biosynthetic process	0.005743769
cellular amino acid metabolic process	0.008159581

serine family amino acid metabolic process	0.008405278
response to chemical	0.010077049
alcohol metabolic process	0.013615956
methionine metabolic process	0.016388097
nucleoside diphosphate metabolic process	0.016388097
organic cation transport	0.01843373
methionine biosynthetic process	0.022979633
sulfur amino acid metabolic process	0.023730723
oxidation-reduction process	0.026189219
aspartate family amino acid biosynthetic process	0.030225051

Chapter III

Sir2 and Cohesin Regulation of Genome Stability

Sir2 is a highly conserved NAD⁺-dependent histone deacetylase that functions in heterochromatin formation and promotes replicative lifespan (RLS) in the budding yeast, *Saccharomyces cerevisiae*. Within the yeast rDNA locus, Sir2 is required for efficient cohesin recruitment and maintaining stability of the tandem array. In addition to the previously reported depletion of Sir2 in replicatively aged cells, we discovered that subunits of the Sir2 containing complexes, SIR and RENT, were depleted. In addition to the RENT complex, several other rDNA structural protein complexes exhibited age-related depletion, most notably the cohesin complex. We hypothesized that mitotic chromosome instability (CIN) due to cohesin depletion could be a driver of replicative aging. ChIP assays of the residual cohesin (Mcd1-13xMyc) in aged cells showed strong depletion from the rDNA and initial redistribution to the point centromeres, which was then lost in older cells. Despite the shift in cohesin distribution, sister chromatid cohesion was partially attenuated in aged cells and the frequency of chromosome loss was increased. This age-induced CIN was exacerbated in strains lacking Sir2 and its paralog, Hst1, but suppressed in strains that stabilize the rDNA array due to deletion of *FOB1* or through caloric restriction (CR). Furthermore, ectopic expression of *MCD1* from a doxycycline-inducible promoter was sufficient to suppress rDNA instability in aged cells and to extend RLS. Taken together we conclude that age-induced depletion of cohesin and multiple other nucleolar chromatin factors destabilize the rDNA locus, which then results in general CIN and aneuploidy that shortens RLS.

Introduction

Budding yeast replicative lifespan (RLS) was originally described decades ago as the number of times a mother cell divides before losing viability (MORTIMER AND JOHNSTON 1959), and has been an effective model system for the identification and/or characterization of several conserved aging-related genes and pathways, including *SIR2*, AMPK (Snf1), and TOR signaling (WASKO AND KAEBERLEIN 2014). *SIR2* is possibly the most famous yeast gene associated with replicative aging and encodes the founding family member of the NAD⁺-dependent histone/protein deacetylases, commonly known as sirtuins (reviewed in (BUCK *et al.* 2004)). The NAD⁺ dependence of sirtuins provides a direct link between metabolism and cellular processes regulated by these enzymes. In fact, recent evidence points to depletion of cellular NAD⁺ pools as a potential mechanism for aging-associated disease, which could be mediated by impairment of sirtuins or other NAD⁺ consuming enzymes (GOMES *et al.* 2013). Therefore, understanding how sirtuins are impacted by aging and how they regulate age-altered cellular processes is of intense interest.

Eukaryotic genomes generally encode for several sirtuin homologs. The *Saccharomyces cerevisiae* genome, for example, encodes *SIR2* and four additional Homologs of Sir Two (*HST1-HST4*) (BRACHMANN *et al.* 1995). Sir2 and its fellow Silent Information Regulator proteins, Sir1, Sir3, and Sir4 were originally shown to establish and maintain silencing of the silent mating loci, *HML* and *HMR* (RINE AND HERSKOWITZ 1987). These proteins form the so-called SIR complex that is recruited to and then spreads across the *HM* loci and telomeres to form hypoacetylated heterochromatin-like domains (reviewed in (GARTENBERG AND SMITH 2016)). Sir2 is required for replicative longevity and its abundance is significantly reduced in replicatively aged yeast cells (DANG *et al.* 2009), presenting a possible mechanism for the decline of Sir2-dependent

processes during aging, including gene silencing. Indeed, the depletion of Sir2 in aged cells causes hyperacetylated H4K16 and silencing defects at subtelomeric loci (DANG *et al.* 2009). It has been reported that aged cells become sterile (mating-incompetent) due to loss of silencing at *HML* and *HMR* (SMEAL *et al.* 1996), which results in co-expression of the normally repressed $\alpha 1/\alpha 2$ and $a 1/a 2$ transcription factor genes encoded at these loci. In theory, this should induce a diploid-like or “pseudodiploid” gene expression pattern and sterility, as is observed for a silencing defective *sir2* Δ mutant (RINE AND HERSKOWITZ 1987). However, more recent experiments point toward a silencing-independent mechanism of sterility, whereby aggregation of the Whi3 protein in aged cells makes them insensitive to pheromones (SCHLISSEL *et al.* 2017).

Alternative models for Sir2 control of RLS have focused on the rDNA tandem array where Sir2 is important for cohesin recruitment (KOBAYASHI *et al.* 2004; GANLEY AND KOBAYASHI 2014). Cohesin association with the rDNA also requires Tof2 and the Lrs4/Csm1 (cohibin) complex (HUANG *et al.* 2006). Sir2 silences RNA polymerase II-dependent transcription at the rDNA locus via a nucleolar HDAC complex called RENT (BRYK *et al.* 1997; SMITH AND BOEKE 1997), consisting of Sir2, Net1, and Cdc14 subunits (SHOU *et al.* 1999; STRAIGHT *et al.* 1999). Specifically, RENT represses transcription of endogenous non-coding RNAs from the intergenic spacer (IGS) regions (LI *et al.* 2006). Derepression of the bidirectional promoter (E-pro) within IGS1 in *sir2* Δ cells displaces cohesin from the rDNA, thus destabilizing the array by making it more susceptible to unequal sister chromatid exchange (KOBAYASHI AND GANLEY 2005). Mild Sir2 overexpression, on the other hand, enhances silencing, suppresses recombination between repeats, and extends RLS (SMITH *et al.* 1998; KAEBERLEIN *et al.* 1999).

Extrachromosomal rDNA circles (ERCs) derived from these unequal recombination events specifically accumulate to high levels in mother cells (SINCLAIR AND GUARENTE 1997),

where they can interfere with G1 cyclin expression (NEUROHR *et al.* 2018). Such an ERC-centric model is supported by RLS extension of *fob1* Δ strains (DEFOSSEZ *et al.* 1999). Fob1 binds to the rDNA at IGS1 to block DNA replication forks from colliding with elongating RNA polymerase I molecules (KOBAYASHI AND HORIUCHI 1996). The blocked forks can collapse, resulting in double-stranded DNA breaks that trigger unequal sister chromatid exchange (TAKEUCHI *et al.* 2003). The frequency of rDNA recombination and ERC production is reduced in a *fob1* Δ mutant due to loss of the fork block, thus extending RLS (DEFOSSEZ *et al.* 1999). More recently, this rDNA-centric model of aging has been extended to include general rDNA instability having negative effects on genome integrity, including ERC accumulation, and is also considered a critical contributor to aging (GANLEY AND KOBAYASHI 2014).

In addition to promoting cohesin recruitment to the rDNA, Sir2 is also required for establishing sister chromatid cohesion (SCC) at *HML* and *HMR* (CHANG *et al.* 2005; WU *et al.* 2011). Moreover, we previously observed significant overlap between Sir2 and cohesin at additional binding sites throughout the genome (LI *et al.* 2013). Outside heterochromatin, the cohesin loading complex (Scc2/Scc4) deposits cohesin (Mcd1, Irr1, Smc1, Smc3) onto centromeres and other cohesion associated regions (CARs) (CIOSK *et al.* 2000; KOGUT *et al.* 2009), in order to maintain SCC until anaphase, when Mcd1 is cleaved by separase to facilitate sister chromatid separation (reviewed in (MARSTON 2014)). Cohesin defects therefore result in chromosome instability (CIN) due to improper chromosome segregation (reviewed in (WOOD *et al.* 2010)). A previous study found that cells deleted for *SIR2* have a CIN phenotype related to hyperacetylation of H4K16 (CHOY *et al.* 2011), though the functional relationship to cohesin was not considered. Given the natural depletion of Sir2 from replicatively aging yeast cells (DANG *et al.* 2009), we hypothesized the frequency of CIN should increase with age. Here, we establish

that CIN is indeed more frequent in aged cells and is associated with SCC defects. We go on to show that like Sir2, cohesin subunits are depleted from aged mother cells, providing a likely reason for problems with SCC. Interestingly, despite the overall reduction in cohesin protein levels, the chromosomal distribution of cohesin enrichment was not uniform. Enrichment at the rDNA was drastically reduced, while binding at centromeres was not, suggesting a mechanism by which SCC is preferentially maintained at centromeres to ensure cell viability. However, this comes at the expense of chronic rDNA instability that is exacerbated by additional age-induced reductions in the RENT and cohibin/monopolin complexes. The defects in rDNA stability can be suppressed by overexpressing the Mcd1 subunit of cohesion, which also extends RLS, thus making cohesin a dose dependent longevity factor. Lastly, the age associated CIN phenotype is suppressed by deleting *FOBI* or by CR growth conditions, suggesting a model whereby rDNA instability on chromosome XII caused by RENT, cohibin, and cohesin depletion drives the mitotic segregation defects of other chromosomes during replicative aging.

Methods

Yeast strains, plasmids, and media

Yeast strains were grown at 30°C in Yeast Peptone Dextrose (YPD) or Synthetic Complete (SC) medium for strains bearing plasmids (MATECIC *et al.* 2010). *SIR2*, *HST1*, or *FOB1* open reading frames were disrupted with one-step PCR-mediated gene replacement using *kanMX4*, *natMX4*, or *hphMX4* drug resistance markers, respectively. The *HMR* deletion by replacement with *hphMX4* spans *sacCer3* genome ChrIII coordinates 293170-294330. All C-terminally 13xMyc (EQKLISEEDL) tagged proteins were targeted at endogenous loci in the Mother Enrichment Program (MEP) strains UCC5181 and UCC5179 (LINDSTROM AND GOTTSCHLING 2009), followed by mating to generate homozygous diploids. All deletions and fusions were confirmed by colony PCR, western blotting, or both. pRF4 was constructed by PCR amplifying the *MCD1* open reading frame from ML1 genomic DNA and ligating into *PstI* and *NotI* sites of pCM252 (BELLI *et al.* 1998), a tetracycline inducible overexpression vector (Euroscarf). pRF10 and pRF11 were constructed by removing the expression cassette by *PvuII* blunt end digestion of pCM252 and pRF4, respectively, and ligating it between the *PvuII* sites of pRS405 bearing *LEU2*, thus replacing the *TRP1* marker with *LEU2*. pRF10 and 11 were then digested with *EcoRV* and integrated into the genome at *leu2Δ1*. pJSB186 was constructed by ligating a *XhoI* and *SpeI* fragment from pSB766 containing *SIR2* and its promoter into the MCS of pRS306 using the same enzymes (BUCK *et al.* 2002). pJSB186 was then integrated into *ura3-52* by digesting with *BstBI*.

Isolation of aged yeast cells

Aged yeast cell enrichment was based on the MEP strain background (LINDSTROM AND GOTTSCHLING 2009; LINDSTROM *et al.* 2011). For all assays, 1 μL of stationary phase culture

was inoculated into 100 mL of YPD medium and then grown into log phase. Approximately 1×10^8 cells were harvested, and centrifuged cell pellets washed 3 times with 1x phosphate buffered saline (PBS). Cells were then resuspended in 1 mL PBS and mixed with 5 mg of Sulfo-NHS-LC-Biotin (Pierce) per 1×10^8 cells for 30 min at room temperature. After biotin labeling, 5×10^7 cells were added to 1.5 L YPD cultures containing 1 μ M estradiol, and 100 μ g/mL ampicillin to prevent bacterial contamination. These cultures were allowed to grow for 24 hr to 36 hr before processing in an assay specific manner (see below). For non-MEP strain backgrounds, estradiol was not added to the cultures.

Western blotting

Two 1.5 L cultures were used for each western blot experiment, corresponding to approximately 2×10^7 total aged cells after purification for each biological replicate. Cells were pelleted using a Sorvall RC-5B Plus centrifuge with an SLA-3000 rotor at 2000 rpm, then resuspended at a density of 6×10^8 cells/mL in RNAlater (Ambion) for 45 min in two separate conical tubes. Following fixation, cells were pelleted and resuspended in 45 mL of cold PBS, 2 mM EDTA in 50 mL conical tubes. The mixture was incubated at 4°C for 30 min with 800 μ L of Streptavidin MicroBeads (Miltenyi Biotec), which were then purified through an autoMACS Pro Cell Separator using the posseld2 program (UVA Flow Cytometry Core Facility). A 20 μ L aliquot of each output was used for bud scar counting using calcofluor white staining, before combining the isolated samples into a single microfuge tube. Samples were frozen at -80°C before protein extraction. Thawed cells were vortexed twice for 1 min in 20% TCA (trichloroacetic acid) with ~100 μ L of acid washed glass beads with a brief cooling period in between vortexing. Beads were allowed to settle before transferring the supernatant to a fresh

microfuge tube. A 250 μ L wash of 5% TCA was applied twice to the beads and pooled with the initial lysis sample. Proteins were precipitated at 10,000 rpm in a microfuge for 5 min at 4°C. Pellets were then resuspended in 50 μ L of 1x SDS sample buffer (50 mM Tris-HCl pH 6.8, 2% SDS, 10% Glycerol, 3.6 M 2-mercaptoethanol) and neutralized with 30 μ L of 1M Tris-HCl, pH 8.0. Samples were run on a 9% (w/v) SDS-polyacrylamide gel and transferred to an Immobilon-P membrane (Millipore). Membranes were incubated for 1 hour at room temperature in 1xTBST + 5% non-fat milk with primary antibodies (1:2000 α -Myc 9E10, 1:5000; α -Vma2 (Life Technologies); 1:5000 α -Sir2 (Santa Cruz Biotechnology); 1:1000 α -Sir4 (Santa Cruz Biotechnology); 1:1000 α -Sir3 (Santa Cruz Biotechnology). HRP-conjugated secondary antibodies (Promega) were diluted 1:5000, and detected using chemiluminescence with HyGLO (Denville Scientific). Quantitation was performed with ImageJ by using the rectangle tool to outline protein bands and an equivalent sized box for background. After subtraction of background, the signal of the aged cell band was divided by the signal of the Vma2 loading control, and finally normalized to the quantity of the Vma2 normalized young cell band which was arbitrarily set at 1.0.

ChIP Assays with aged and young cell populations

Two 1.5 L cultures were used for each biological replicate. After centrifugation, cells were washed with 1xPBS then resuspended with 45 mL of PBS and incubated with 800 μ L of streptavidin microbeads, followed by sorting with the autoMACS Pro Cell Separator. Sorted cells were immediately crosslinked with 1% formaldehyde for 20 min at room temperature, then transferred to screw cap microcentrifuge tubes and the pellets flash frozen in liquid nitrogen. Cells were thawed and lysed in 600 μ L FA140 Lysis buffer (50 mM HEPES, 140 mM NaCl, 1%

Triton X-100, 1 mM EDTA, 0.1% SDS, 0.1 mM PMSF, 1x protease inhibitor cocktail; Sigma) by shaking with acid-washed glass beads in a Mini-Bead beater (Biospec Products). Cell lysates were recovered and sonicated for 30 cycles of 30 sec “on” and 30 sec “off” in a Diagenode Bioruptor followed by centrifugation at 16,000 x g. A 1/10th supernatant volume input was taken for each sample and crosslinking reversed by incubating overnight at 65°C in 150 µL elution buffer (TE, 1% SDS). The remaining supernatant was used for immunoprecipitation overnight at 4°C with 5 µg of primary antibody and 30 µL of protein G magnetic beads (Pierce), followed by washing 1x with FA-140 buffer, 2x with FA-500 buffer (FA-140 with 500 mM NaCl), and 2x with LiCl solution (10 mM Tris-HCl, pH 8.0, 250 mM LiCl, 0.5% NP-40, 0.5% SDS, 1 mM EDTA). DNA was eluted twice with 75 µL of elution buffer in a 65°C water bath for 15 min. The eluates were combined and crosslinking reversed. Input and ChIP DNA samples were purified by an Invitrogen PureLink™ PCR purification kit. Finally, ChIP DNA was quantified by real-time PCR and normalized to the input DNA signal. Young cells were collected flow-through from the autoMACS cell sorter and then processed as described for the aged cells.

Sister chromatid cohesion assay

From 50 mL log phase SC cultures of strains 3349-1B, 3312-7A, 3460-2A, RF258, RF278, and RF290, 5×10^7 cells were washed and biotinylated as described in the Isolation of aged yeast cells section. This population was transferred into a 1.5 L SC culture and allowed to grow for 14 hr. The original biotinylated cells were then purified by incubation with 300 µL of streptavidin micro beads followed by gravity filtration through a Miltenyi LS column. The column was washed twice with 5 ml of PBS and then processed as described below for young cells.

From the original log phase culture, 5×10^7 cells were transferred to a fresh 50 mL SC culture and arrested in mitosis with 10 $\mu\text{g}/\text{mL}$ nocodazole for 1.5 hr. For the *mcd1-1* strain 3312-7A, cells were also shifted to 37°C at this time. For bud scar staining, 5 mg of calcofluor white was dissolved in 1 mL of PBS and any remaining aggregate removed by centrifugation. The 1 mL of soluble calcofluor was then added to the 50 mL SC culture. Non-arrested cells were directly stained with calcofluor. Cells were then pelleted and washed in PBS. Following staining, 200 μL of 4% paraformaldehyde was added directly to the cell pellet and allowed to crosslink for 15 min at room temperature. The cell pellet was washed once with PBS and resuspended in ~100-200 μL of 0.1 $\text{MKPO}_4/1$ M sorbitol, pH 6.5. Images were captured with a Zeiss Axio Observer z1 widefield microscope using a 64x oil objective lens.

Replicative lifespan assays

Lifespan assays were carried out as previously described (STEFFEN *et al.* 2009). Briefly, small aliquots of log phase cultures were dripped in a straight line onto solid agar YPD with 2% glucose. From the initial populations, a minimum of 32 virgin daughter cells were picked for lifespan assays with daughter cells being selectively pulled away from mother cells using a fiberoptic dissection needle and on a Nikon Eclipse 400 microscope. All virgin daughters were required to bud at least one time to be included in the experiment and dissection was carried out over the course of several days with temporary incubation at 4°C in between dissection periods to stop division. Cells were considered dead when they stopped dividing for a minimum of 2 generation times (180 min). For p-values indicated in the text, a Wilcoxon rank-sum test was conducted for respective lifespan assays using the basic `wilcox.test` function in R.

Mini-chromosome loss (sectoring) assay

The colony sectoring assay was performed on SC plates with adenine limited to 80 μ M. Frequency of mini-chromosome loss represents the number of $\frac{1}{2}$ red/white sectored colonies divided by the sum of sectored and white colonies. Cells were plated to an approximate density of 500 cells/plate based on counts from a Brightline hemacytometer. Any plates bearing greater than 1000 cells were discarded. Three biological replicates of each strain were performed, with at least 10 plates counted per replicate. For aged cell populations, $\sim 5 \times 10^6$ biotinylated cells were aged in 1.5 L of YPD for 24 hr. Cells were incubated with 300 μ L of streptavidin magnetic beads (New England Biolabs) and manually washed 4 times with PBS on a magnetic stand, then plated onto the limiting adenine SC plates such that ~ 500 colonies appeared. Bud scars were not counted because the size of the beads prohibited visualization.

RT-qPCR measurement of *MCD1* overexpression

Doxycycline was added to log phase cultures at a concentration of 2 μ g/mL for 4 hr in order to induce expression of *MCD1*. Total RNA was extracted using a standard acid phenol extraction protocol (AUSUBEL *et al.* 2000). cDNA was created from 1 μ g of RNA using a Verso cDNA synthesis kit (Thermo Fisher). *MCD1* expression levels were quantified on an Applied Biosystems StepOne real time PCR machine with primers JS2844 and JS2949, and normalized to actin transcript levels (primers JS1146 and JS1147).

Hi-C Library Construction

Log-phase cultures were cross-linked with 3% formaldehyde for 20 min and quenched with a 2x volume of 2.5M glycine. Cell pellets were washed with dH₂O and stored at -80°C.

Thawed cells were resuspended in 5 ml of 1X NEB2 restriction enzyme buffer (New England Biolabs) and poured into a pre-chilled mortar containing liquid N₂. Nitrogen grinding was performed twice as previously described (BELTON AND DEKKER 2015), and the lysates were then diluted to an OD₆₀₀ of 12 in 1x NEB2 buffer. 500 µl of cell lysate was used for each Hi-C library as follows. Lysates were solubilized by the addition of 50 µl 1% SDS and incubation at 65°C for 10 min. 55 µl of 10% Triton X-100 was added to quench the SDS, followed by 10 µl of 10X NEB2 buffer and 15 µl of *HindIII* (New England Biolabs, 20 U/µl) to digest at 37°C for 2 hr. An additional 10 µl of *HindIII* was added for digestion overnight. The remainder of the protocol was based on previously published work with minor exceptions (BURTON *et al.* 2014). In short, ends were filled in with dNTPs and biotinylated dCTP at 0.4 mM concentration using Klenow Exo- (NEB) for 1 hr at 37°C. After a brief heat inactivation, blunt ends were ligated together in 3 mL reaction volumes with T4 DNA-ligase for 6 hr at 16°C with a minimum DNA concentration of 0.5 ng/µL. Following ligation, cross-links were reversed at 70°C O/N and DNA was purified by phenol/chloroform extraction and ethanol precipitation. Unligated-biotinylated ends were removed using T4 DNA Polymerase (NEB). DNA was purified one final time with two Zymogen DNA Clean and Concentrate-5 Kit columns per ligation reaction and eluted with 65 µL TE (130 µL total). Chromatin was quantitated with a Qubit fluorometer and then sheared using a Diagenode Bioruptor. Hi-C sequencing libraries were prepared with reagents from an Illumina Nextera Mate Pair Kit (FC-132-1001) using the standard Illumina protocol of End Repair, A-tailing, Adapter Ligation, and 12 cycles of PCR. PCR products were size selected and purified with AMPure XP beads before sequencing with an Illumina Miseq or Hiseq.

Hi-C Data Analysis

Iteratively corrected heatmaps appearing in this manuscript were produced using python scripts from the Mirny lab hiclib library, publicly available at:

<http://mirnylab.bitbucket.org/hiclib/index.html>. Briefly, reads were mapped using the iterative mapping program and then run through the fragment filtering program using the default parameters. Raw heat maps were further filtered to remove diagonal reads and iteratively corrected. Finally, the iteratively corrected heatmaps were normalized for read count differences to make them comparable. The *cdc15-2* sample data was pulled from the SRA database at SRP094582 (LAZAR-STEFANITA *et al.* 2017), and our data is available from GEO at GSE117037.

Results

Sir2 binding partners are depleted in aged yeast cells

Sir2 is a dosage dependent longevity factor such that strains provided one extra *SIR2* gene copy have an extended RLS (KAEBERLEIN *et al.* 1999). Mother cells experience a natural and progressive reduction of Sir2 protein during normal replicative aging that presumably contributes to the aging process (DANG *et al.* 2009). Sir2 does not function in isolation, so we hypothesized that protein levels of key Sir2-interacting partners could also be depleted with age. To isolate sufficient quantities of aged cells for Western blot assays we turned to Mother Enrichment Program (MEP) strains developed by the Gottschling lab (LINDSTROM AND GOTTSCHLING 2009). The aged cell purification procedure was validated by increased average bud scar counts with calcofluor white and the expected reduction of Sir2 protein (Figure 3.1A). The vacuolar protein Vma2, used as a loading control for these western blots, does not deplete with age (LINDSTROM *et al.* 2011). Since Sir2 is the catalytic subunit of both SIR and RENT (Figure 3.1B), it was important to know which complexes were impacted by age. As shown in Figure 3.1C and 3.1D, Sir4 was strongly depleted in aged cells while Sir3 was actually enriched. Sir3 enrichment in aged cells was also observed in a previous proteomics screen (JANSSENS *et al.* 2015). Such a stark difference was considered relevant because Sir2 and Sir4 interact as a heterodimer that associates with the acetylated H4 N-terminal tail (MOAZED *et al.* 1997), while Sir3 is subsequently recruited following H4K16 deacetylation to complete SIR holocomplex formation on heterochromatin (OPPIKOFER *et al.* 2011). Myc-tagged Net1 (RENT complex) was also depleted from aged cells (Figure 3.1E), indicating that Sir2/Sir4 and the nucleolar RENT complex are both depleted during aging. It should be noted that the Sir2 paralog, Hst1, which has

the capacity to compensate for loss of Sir2 (HICKMAN AND RUSCHE 2007; LI *et al.*), was also partially depleted from aged cells (Figure 3.1F).

Chromosome instability (CIN) increases during replicative aging

Considering the depletion of multiple heterochromatin factors in aged yeast cells, as well as the CIN phenotype of a *sir2Δ* mutant (CHOY *et al.* 2011), we next tested whether aged cells had a CIN phenotype that was exacerbated by loss of *SIR2* and/or *HST1*. Strains utilized for this experiment have an artificial chromosome III bearing a suppressor tRNA gene, *SUP11* (SPENCER *et al.* 1990). Loss of the chromosome prevents suppression of an ochre stop codon in *ade2-1*, resulting in the classic *ade2* red colony phenotype. The frequency of nondisjunction events was measured by counting half-sectoring red/white colonies from young and aged cell populations (Figure 3.1G). Sectoring was elevated in young populations of *sir2Δ* and *hst1Δ* mutants, and additively increased in a *sir2Δhst1Δ* double mutant (Figure 3.1H, black bars, left side of panel). Interestingly, sectoring was significantly higher for aged populations of each strain (Figure 3.1H, gray bars, left side of panel), suggesting additional age-associated factors were involved. We next tested whether the *sir2Δ* effect on sectoring was related to the pseudodiploid phenotype caused by derepression of the *HM* loci. This reporter strain background was *MATα*, so we deleted *HMR* (chrIII 293170-294330) to eliminate the a1/a2 transcription factors. Reversal of the pseudodiploid phenotype was confirmed by restoration of mating to the *sir2Δ hmrΔ* strains (data not shown). Importantly, this manipulation significantly suppressed sectoring of the young *sir2Δ* and *sir2Δ hst1Δ* mutants, but not the *hst1Δ* mutant (Figure 3.1H, middle of panel), indicating there was indeed a *sir2Δ*-induced pseudodiploid effect that contributed to mini-chromosome loss (Figure 3.1H, black bars, middle of panel). However, aging still increased sectoring in each strain even when *HMR* was deleted (Figure 1H, gray bars, middle of panel), suggesting

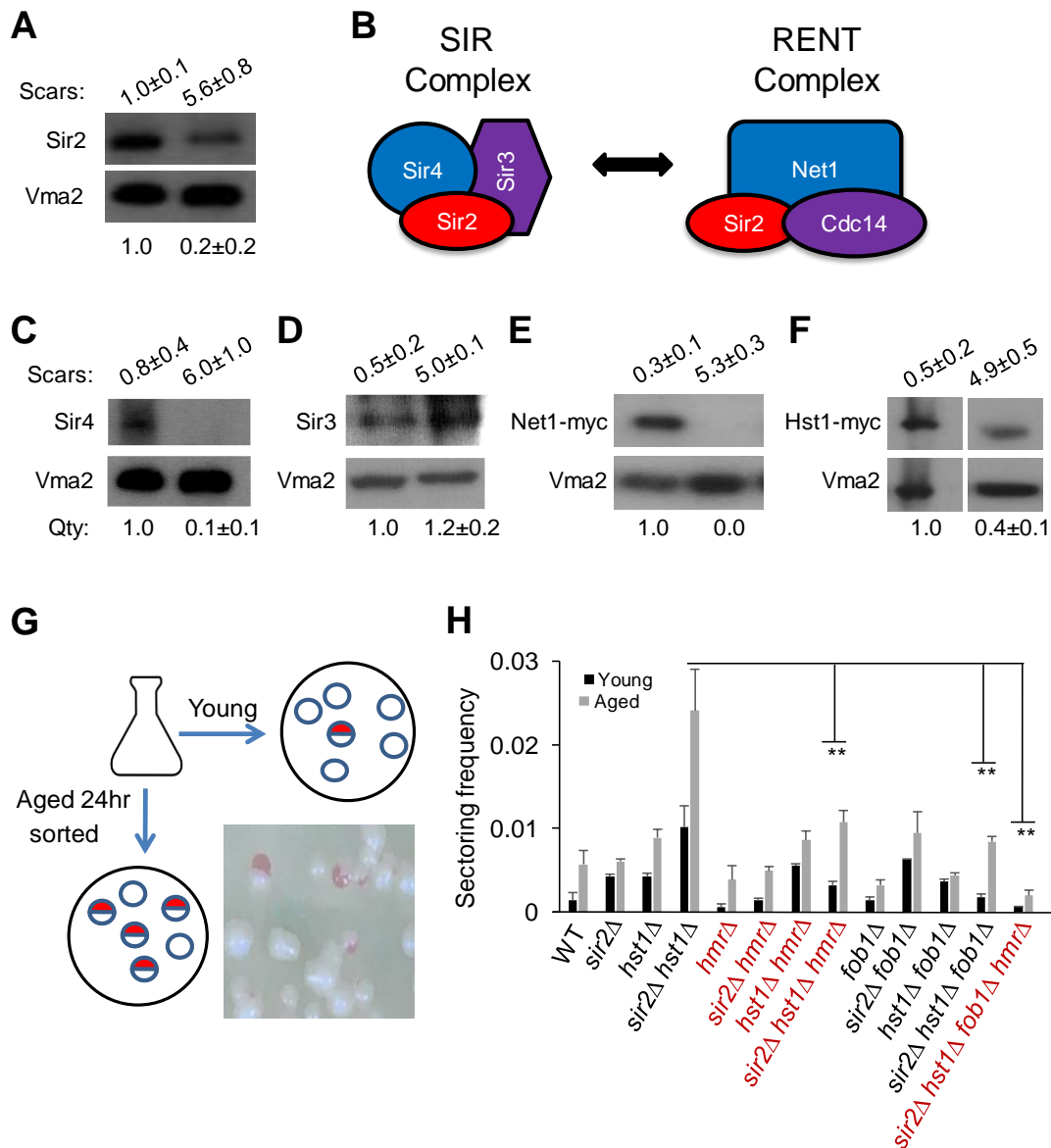


Figure 3.1. Depletion of Sir2 complexes and elevated chromosome instability in replicatively aging cells. (A) Western blot of Sir2 protein levels in young and aged cells. Vma2 serves as a loading control. (B) Depiction of the SIR and RENT complexes, which share Sir2 as a catalytic subunit. (C, D) Western blots of native Sir4 and Sir3. (E, F) Western blots of 13xMyc tagged Sir2 paralog, Hst1, and the Net1 subunit of RENT. (G) Schematic of artificial chromosome loss assay for $\frac{1}{2}$ sectored colonies. (H) Quantification of sectoring frequency for young or aged cell populations. Approximately 10,000 colonies were analyzed for each strain across several biological replicates. * $p < 0.05$, two-tailed student t-test. Bud scar counts are an average for each enriched population. Qty: indicates the mean western signal of each protein in aged cells relative to the signal in young cells, which is set at 1.0 ($n=3$ biological replicates).

that the aging-associated CIN factor was unrelated to mating type control.

Because of the observed Net1 depletion (Figure 3.1E), we hypothesized that age-induced mini-chromosome loss could be related to rDNA instability caused by loss of the RENT complex. To address this idea, *FOBI* was deleted from WT, *sir2Δ*, *hst1Δ*, and *sir2Δ hst1Δ* reporter strains to stabilize the rDNA, followed by retesting the sectoring phenotypes. As shown in Figure 3.1H (right side of panel), frequency of sectoring observed for each aged *fob1Δ* strain was generally similar to that observed with young *FOBI*⁺ versions of the strains (Figure 3.1H, black bars, left side of panel), suggesting that destabilization of the rDNA during aging does contribute to the instability of other chromosomes. The *hmrΔ* and *fob1Δ* mutations were potentially suppressing chromosome loss through independent mechanisms, thus begging the question of whether combining them would fully suppress CIN in a *sir2Δ hst1Δ hmrΔ fob1Δ* quadruple mutant. Remarkably, aged cells from this mutant combination lost the mini chromosome marker at a very low rate comparable to young WT cells, with no statistical difference (Figure 3.1H, 1-way ANOVA).

Cohesin levels are depleted in aged yeast cells

The above results raised the question of what factor(s) related to rDNA stability, chromosome segregation, and Sir2, was becoming defective in aged cells. Cohesin perfectly fit this profile and was earlier shown in mammalian oocytes to become depleted with age (reviewed in (JESSBERGER 2012)). To test whether cohesin was another Sir2-linked factor depleted during yeast aging, we C-terminally myc-tagged the Mcd1 and Smc1 subunits of cohesin (Figure 3.2A) in the MEP strain background. Western blotting demonstrated that both subunits were significantly depleted from aged cells (Figure 3.2B), implying depletion of the whole cohesin complex. We also

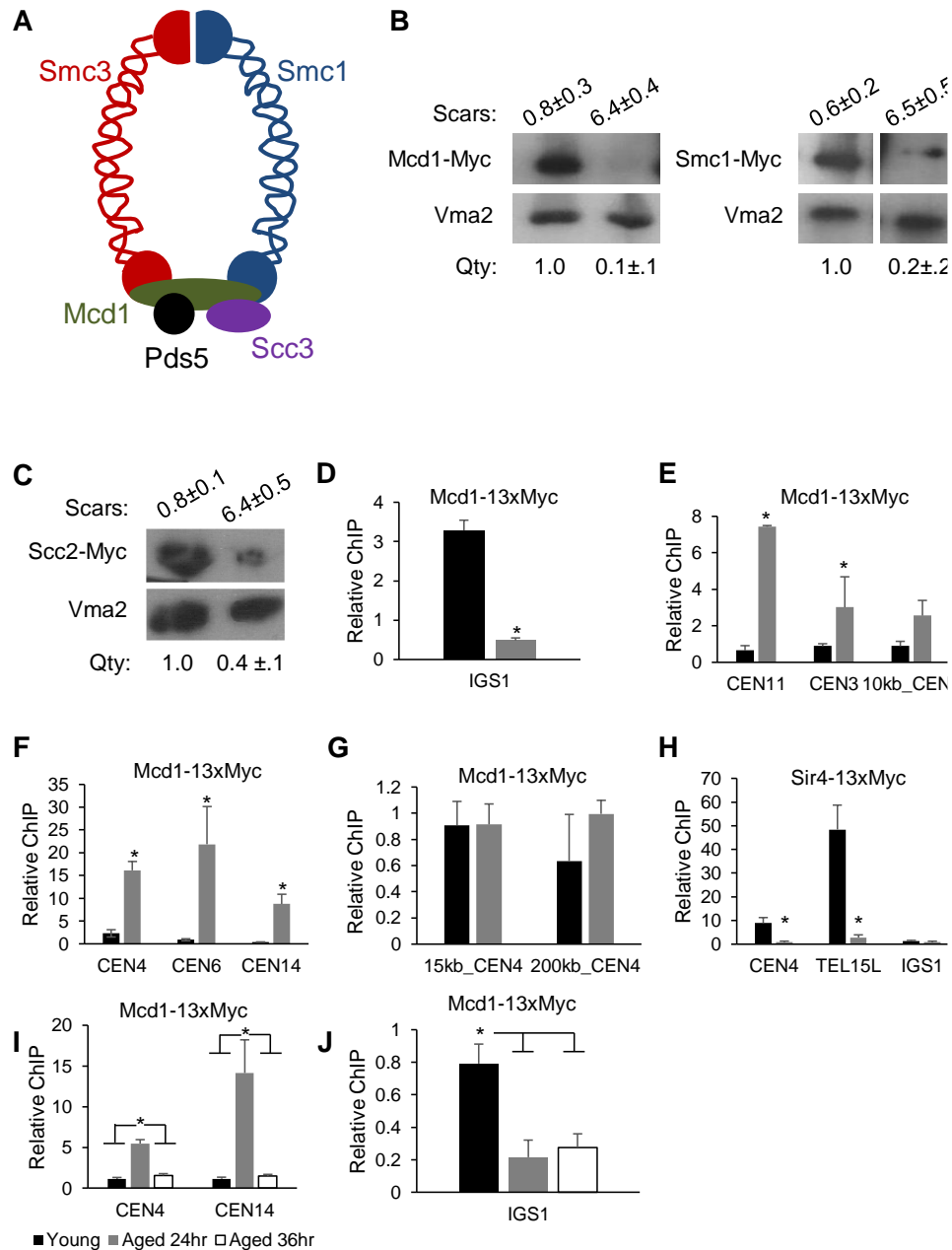


Figure 3.2. Chromosome instability is linked to rDNA stability and cohesin redistribution

(A) Schematic of the cohesin complex subunits. (B) Western blot of Mcd1-13xMyc and Smc1-13xMyc from young and aged cells. (C) Western blot of 13xMyc tagged Scc2. (D, E, F, G) ChIP-qPCR of Mcd1-13xMyc in young and aged cells at the indicated loci normalized to background signal in the *STE2* ORF. (H) ChIP-qPCR of Sir4-13xMyc in young and aged cells normalized to an intergenic *PDC1* site that shows SIR complex association (LI *et al.* 2013). (I, J) ChIP-qPCR of Mcd1-13xMyc from a time course of young, 24hr, and 36hr aged cells at indicated loci normalized to *STE2* background signal. Asterisks indicate significant differences between young and aged cells ($p < 0.05$).

observed depletion of the cohibin/monopolin subunit Lrs4 (Figure 3.3), which can function as a cohesin clamp at the rDNA (HUANG *et al.* 2006).

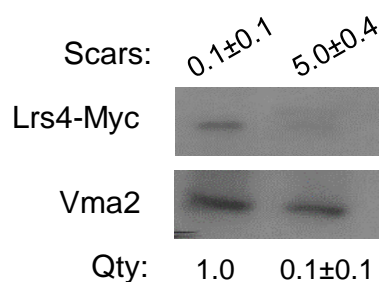


Figure 3.3. The Lrs4 subunit of cohibin/monopolin is depleted in aged yeast cells. Representative western blot of 13xMyc-tagged Lrs4. Vma2 is used as a loading control. Average bud scar counts are indicated above, and relative Lrs4-myc signal compared to the Vma2 loading control is indicated at the bottom.

Furthermore, a Myc-tagged Scc2 subunit of the Scc2/Scc4 cohesin loading complex was age-depleted (Figure 3.2C), though not as severely as the cohesin complex predicting that the remaining cohesin complex could still be loaded onto chromatin in aged cells. ChIP assays for Mcd1-myc in MEP cells aged 24 hr demonstrated strong depletion from the rDNA intergenic spacer (IGS1) (Figure 3.2D), but enrichment was surprisingly enhanced at the centromeres of chromosomes XI and III, though it did not appear to significantly extend into the pericentric region of chromosome III (Figure 3.2E). In order to rule out primer specific effects or chromosome size effects, we tested an array of centromeres from different chromosomes and found the initial trend in agreement regardless of centromere tested (Figure 3.2F). To confirm the enhanced enrichment was centromere specific, we tested two additional sites on chromosome IV that were 15kb and 200kb away from the centromere, and observed no increase in the aged samples compared to young (Figure 3.2G). To test if the enrichment of Mcd1-myc to centromeres in aged cells was specific to cohesin, we next tested the distribution of Sir4-myc, which was also depleted from aged cells (Figure 3.1C). In this case, Sir4-myc was depleted from *TELXV* in aged cells (one of its normal targets) without any apparent redistribution to centromeres (*CEN4*) or the rDNA (Figure 3.2H), indicating that not all age-depleted proteins

become enriched at centromeres. Based on these results, we hypothesize that as cohesin starts depleting during replicative aging, enrichment at the rDNA is severely affected while a significant portion of the remaining complex is retained and potentially redistributed to centromeres. This is consistent with an earlier finding that cohesin preferentially associates with pericentromeric regions instead of chromosome arms when Mcd1 expression is artificially reduced below 30% of normal (HEIDINGER-PAULI *et al.* 2010). We next wanted to ask if a further aged population of cells would exhibit depleted cohesin levels from the centromeres. To test this, we conducted an extended time course enriching for a 36 hr population of Mcd1-Myc tagged cells and found that cohesin levels reverted to the original levels seen in log phase cells (Fig 3.2I) while remaining depleted at the rDNA array (Fig 3.2H). It is important to note that in a recent report (PAL *et al.* 2018), cohesin enrichment at centromeres was actually reduced in very old yeast cells (>25 generations). Combined with our findings, a model emerges whereby cohesin enrichment at centromeres is initially enhanced during aging, but then catastrophically lost as cells approach the end of their lifespan.

Sister chromatid cohesion is compromised in aged yeast cells

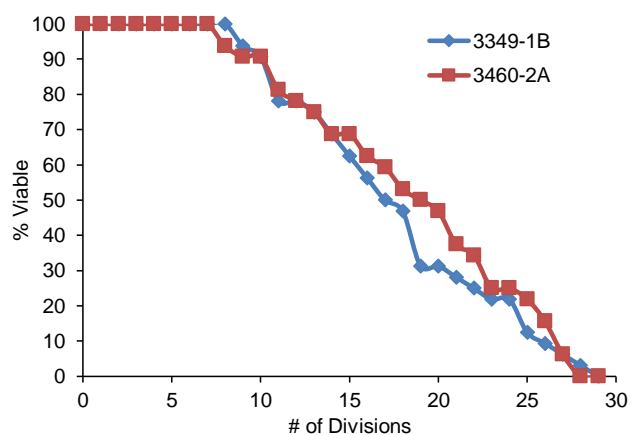


Figure 3.4. RLS of the cohesion visualization strains is normal and unaffected by position of the lacO array. Strain 3349-1B contains a lacO array at the *LYS4* locus on ChrIV and is used as a proxy for arm cohesion, while strain 3460-2A contains a lacO array on ChrIV 10 kb away from the *CEN4* locus that is used to monitor centromeric cohesion.

Previous work found that SCC was surprisingly normal despite the forced reduction (<30%) of Mcd1 protein levels (HEIDINGER-PAULI *et al.* 2010), leading us to ask whether cohesion would be maintained in our aged yeast cells that were also depleted for cohesin, yet still showed enrichment at centromeres. To this end, we utilized strains with a LacO array located approximately 10 kb away from centromere IV (*CEN4*) as a proxy for centromeric cohesion, or at the *LYS4* locus on chromosome IV, located approximately 400 kb away from the centromere, as a proxy for arm cohesion (UNAL *et al.* 2008; GUACCI AND KOSHLAND 2012). Differential positioning of the array had no significant impact on RLS (Figure 3.4). SCC was monitored by LacI-GFP appearing either as one dot in the case of cohesion maintenance or two dots in the case of cohesion loss. Using an *mcd1-1* temperature sensitive mutant as a positive control (GUACCI *et al.* 1997), we observed a significant increase in two dots when cells were synchronized in mitosis with nocodazole and shifted to 37°C (Figure 3.5A and 3.5B). WT cells for the equivalent reporter strain were next biotinylated and aged for 24 hours, followed by purification with magnetic streptavidin beads and arrest with nocodazole. Analyzing cells with >7 bud scars,

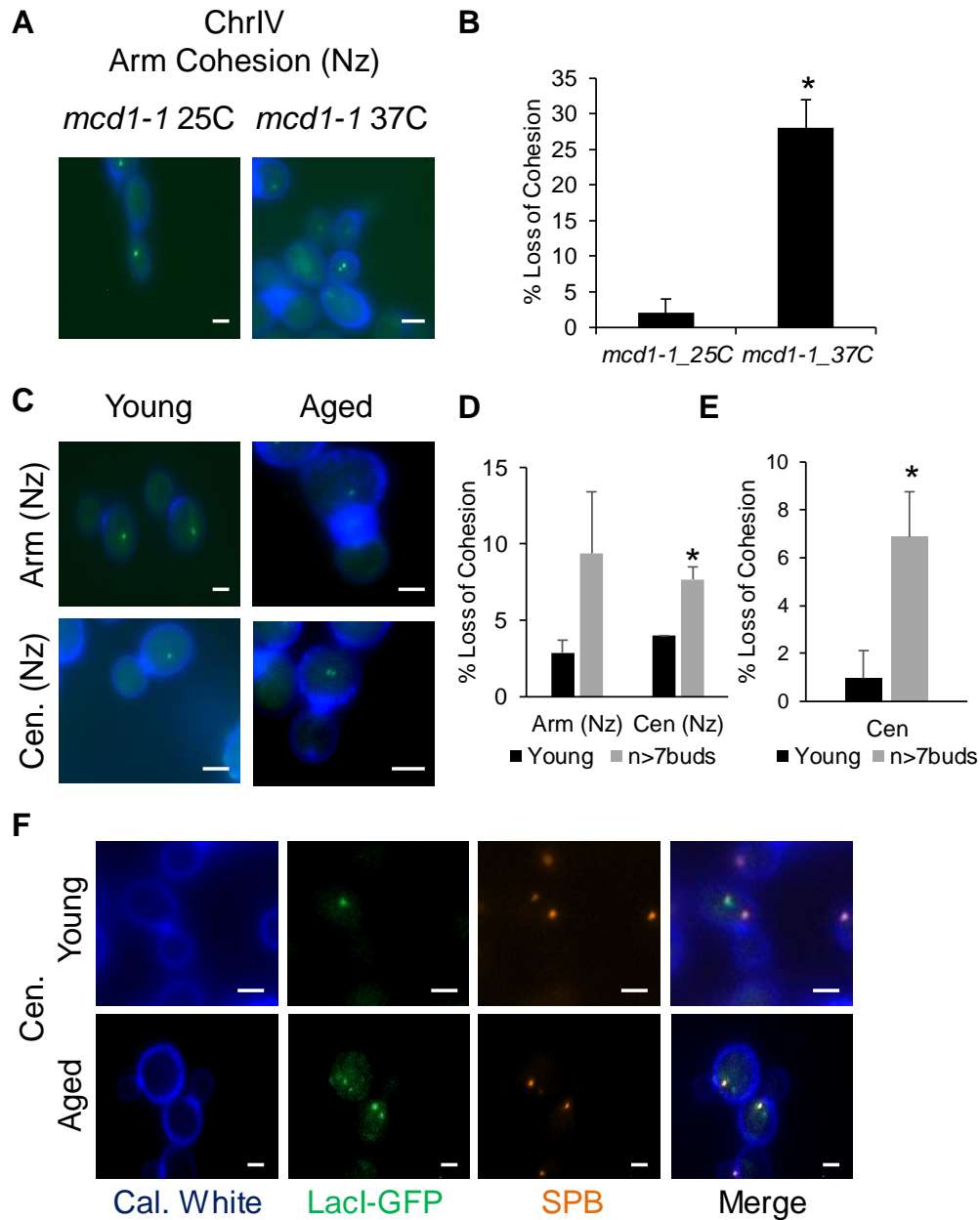
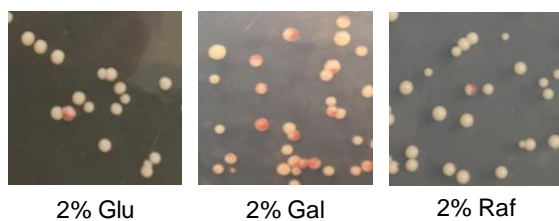


Figure 3.5. Sister chromatid cohesion is weakened in aged yeast cells. (A) Representative control images of arm cohesion in an *mcd1-1* mutant at permissive (25°C) and non-permissive (37°C) temperatures. (B) Quantification of cohesion maintenance (1-dot) or loss (2-dots) from 100 *mcd1-1* cells. (C) Representative images of young (log-phase) or aged cells arrested with nocodazole (Nz) and monitored for centromere or arm cohesion. (D) Quantifying cohesion loss (2-dots) in cells with at least 7 bud scars. * $p < 0.05$, two-tailed t-test ($n > 50$ cells). Quantification of cohesion loss for young and aged cells in the absence of nocodazole (E) Representative images of nocodazole untreated cells. White scale bar represents 2 microns.

which is older than the average bud scar count of our western blot experiments, revealed a mild loss of centromeric cohesion (Figure 3.5C and 3.5D). A similar analysis was then performed without the use of nocodazole to rule out any side-effects related to triggering the mitotic spindle checkpoint. To avoid misinterpreting anaphase events as lost SCC, we C-terminally tagged the spindle pole body subunit Spc42 with dsRED, and only counted GFP dots from large-budded cells where the spindle pole bodies had not separated between the mother and daughter cell. With this analysis, the fold-change of SCC defect between young and aged cells was more pronounced (Figure 3.5E and F), but the absolute frequency of loss was still much weaker than observed with the *mcd1-1* mutant, which was not surprising given that mean lifespan of this strain background is ~16 generations (Figure 3.4). In very old cells (>25 bud scars) of a different strain background, an independent study observed SCC loss on chromosome XII at a frequency that approached 50% (PAL *et al.* 2018) suggesting that CIN may become most severe in the oldest cells where cohesin is not only depleted from the rDNA, but also from centromeres.

RLS is modulated by Mcd1 expression levels

Since Sir2 and cohesin are both naturally depleted from replicatively aging yeast cells (Figures 3.1A and 3.2B), and mild Sir2 overexpression extends RLS (KAEBERLEIN *et al.* 1999), we hypothesized that manipulating cohesin expression levels would also impact CIN and RLS in a dose-dependent manner. We initially attempted to overexpress the Mcd1 subunit from a galactose inducible *GALI* promoter and then measure mini-chromosome loss frequency by counting $\frac{1}{2}$ sectored colonies. However, simply growing the reporter strain in galactose containing media, even with an empty expression cassette, resulted in severe mini-chromosome loss compared to glucose-containing media (Figure 3.6A and 3.6B). This effect was specific to galactose, as growth with another non-preferred carbon source (raffinose) had no effect on

A

2% Glu

2% Gal

2% Raf

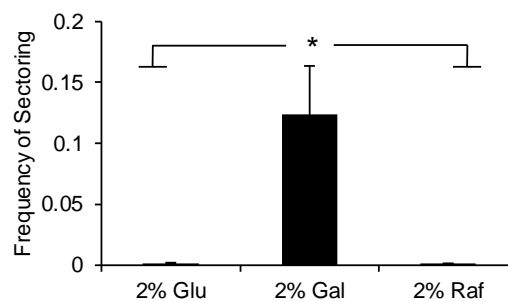
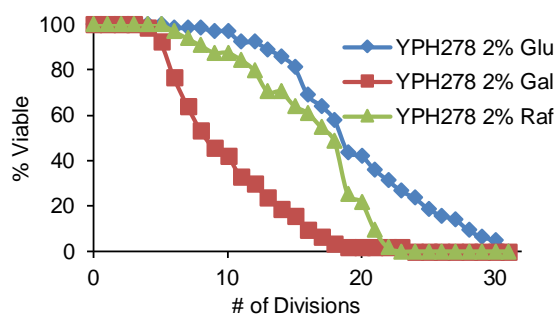
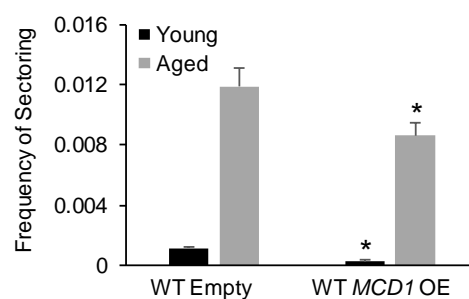
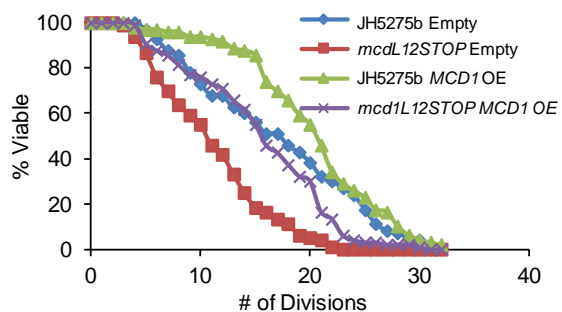
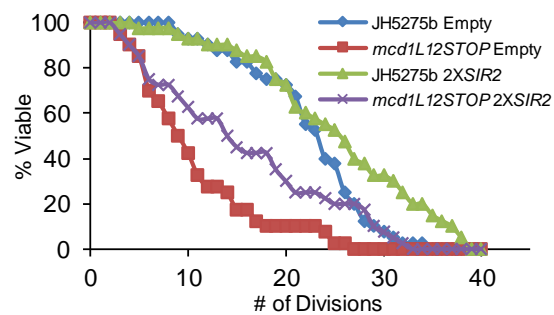
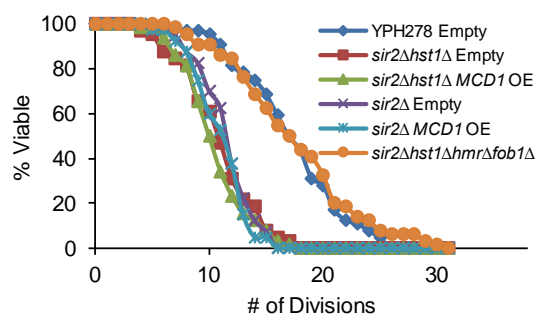
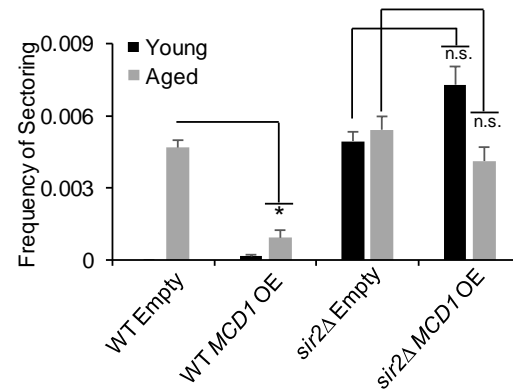
B**C****D****E****F****G****H**

Figure 3.6. Modulation of RLS and CIN by manipulating *MCD1* and *SIR2* expression levels. (A) Representative images of chromosome loss (sectoring) for WT (YPH278) cells grown continuously in 2% glucose, galactose, or raffinose. (B) Quantification of half-sector colonies shown in 4A. * $p < 0.001$, two-tailed student t-test. (C) RLS assay of YPH278 cells growing on rich YEP agar plates containing either 2% glucose, galactose, or raffinose. (n=64, each condition; mean rls = ♦ 18.9 ■ 9.2 ▲ 15.5) (D) Quantification of chromosome loss (1/2 sectors) for strains with an integrated tet^{On} empty (pRF10) or *MCD1* (pRF11) construct. RLS assays of WT (*MCD1*⁺) and *mc1L12STOP* strains with integrated pRF10 or pRF11 constructs (mean rls = ♦ 16.2 ■ 10.3 ▲ 19.2 × 15.6). (E) RLS assay of WT and *mc1L12STOP* strains with integrated empty, pRS306, or *SIR2* containing plasmid, pJSB186 (n=40 cells each; mean rls = ♦ 21.5 ■ 9.9 ▲ 30.4 × 14.8). (F) RLS assay with *MCD1* OE or *fob1Δ hmrΔ* rescue of *sir2Δ* or *sir2Δ hst1Δ* mutants (mean rls = ♦ 16.5 ■ 10.1 ▲ 9.7 × 10.7 * 10.25 ● 16.7). (G) rDNA recombination (marker loss, 1/2 sector) assay with rDNA marker loss reporter strain W303AR bearing *ADE2* within the rDNA array. (* $p < 0.05$, two-tailed t-test).

sectoring (Figure 3.6A and 3.6B). Though not useful for assaying the effects of *MCD1* overexpression, it was still possible that the unexpectedly high CIN phenotype would correlate with reduced RLS. We therefore measured RLS with the mini-chromosome reporter strain on YEP plates with 2% glucose, galactose, or raffinose. As shown in Figure 3.6C, galactose strongly decreased the mean RLS by ~50% compared to glucose (9.2 vs. 18.9 divisions, $p < 1.0 \times 10^{-15}$), while raffinose only had a marginal effect (15.5 divisions, $p < 0.01$). To confirm the galactose effect on RLS was not specific to the mini-chromosome strain, lifespan assays were repeated with the commonly used strains BY4741 (*MATa*) and BY4742 (*MAT α*). Again, a significant decrease in mean lifespan was observed for BY4741 (17.7 divisions) and BY4742 (18.9 divisions) on galactose as compared to glucose (24.3 and 24.2 divisions, respectively) (Figure 3.7, $p < 0.001$), suggesting that galactose triggers a high rate of CIN through an unknown mechanism that also shortens RLS.

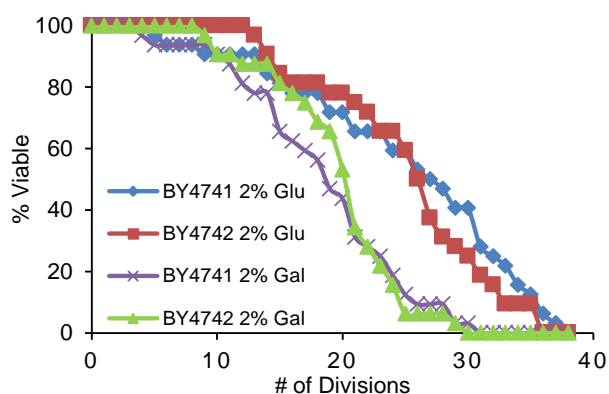


Figure 3.7. Galactose shortens yeast RLS in the common yeast BY4741/4742 strain background. (A) RLS of WT BY4741(*MATa*) and BY4742 (*MAT α*) cells ($n=32$; mean rls: \blacklozenge 24.3, \blacksquare 24.2, \blacktriangle 17.7, \times 18.9) growing on YEP agar plates containing either 2% glucose or galactose as the carbon source.

To circumvent the use of galactose for *MCD1* overexpression we turned to an inducible “Tet-On” promoter that is activated by doxycycline (BELLI *et al.* 1998). Strains harboring this integrated cassette transcriptionally overexpressed *MCD1* approximately 2- to 7-fold compared to the empty vector control (Figure 3.8A and 3.8B). In the mini-chromosome reporter strain, *MCD1* overexpression significantly reduced the frequency of $\frac{1}{2}$ sectored colonies in both young and aged populations (Figure 3.6D), in agreement with *MCD1* being isolated as a high copy

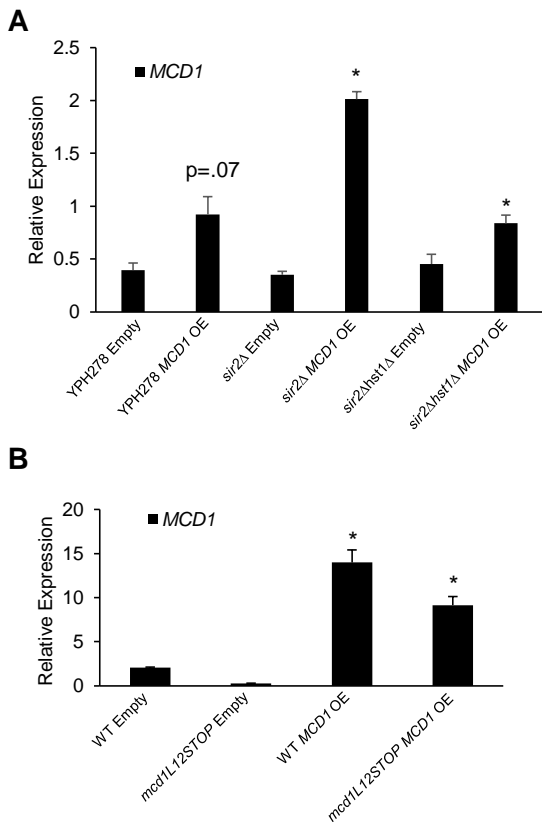


Figure 3.8. Doxycycline-induced *MCD1* overexpression in WT and *mcd1L12STOP* strains. (A) RT-qPCR of *MCD1* transcript levels relative to actin transcript levels in chromosome loss assay strains (YPH background) used to examine *SIR2* and *MCD1* epistasis in RLS. (B) RT-qPCR of *MCD1* transcript levels relative to actin transcript levels were quantified from the empty vector strains (RF146 and RF147) or the *MCD1* overexpression strains RF179 and RF180. Total RNA was isolated following 4 hours doxycycline induction during log-phase growth. (* $p < 0.05$, student's two-tailed t-test).

suppressor of CIN using a different reporter system (ZHU *et al.* 2015). Next, *MCD1* was overexpressed in a strain containing an ochre stop codon in the *MCD1* open-reading frame (*mcd1L12STOP*) that reduces Mcd1 protein to ~30% of normal (HEIDINGER-PAULI *et al.* 2010). With an empty pCM252 control CEN vector, *mcd1L12STOP* exhibited a 40% reduction in mean RLS (9.9 divisions) compared to an isogenic WT control (16.5 divisions), indicating that Mcd1 depletion shortens RLS (Figure 3.6E, $p < 0.001$). Overexpressing *MCD1* almost fully restored longevity to the mutant (14.7 divisions) and, remarkably, also extended RLS of the control WT strain to 19.6 divisions ($p < 1.0 \times 10^{-7}$), which was primarily due to improved survival during the first ~15 divisions and then followed by a steeper decline in viability (Figure 3.6E). This biphasic pattern was highly reproducible and suggested that the CEN *MCD1* OE plasmid was being lost around mid-life due to increased chromosome loss, as previously seen in aged cells of

our CIN assay (Figure 3.1H). To account for this potential variable, we also integrated the empty and *MCD1* OE vectors into a different FY834 strain background related to the long lived BY4741/42 background (WINSTON *et al.* 1995). Not only did *MCD1* OE extend the mean RLS (28.0 divisions) in this background compared to the control (21.0 divisions), but the maximum number of divisions was also increased by 25% (Figure 3.9, $p < 1.0 \times 10^{-7}$). We therefore conclude that similar to Sir2, Mcd1 is a strong dose-dependent longevity factor.

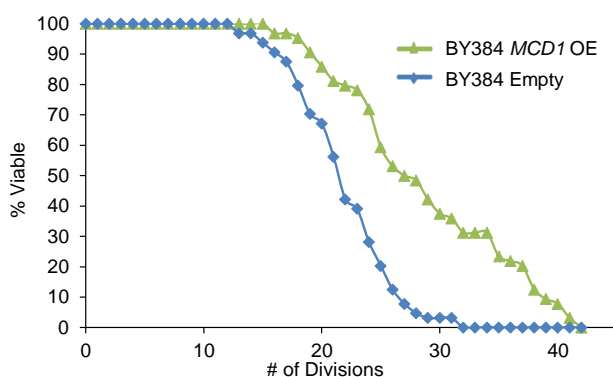


Figure 3.9. Doxycycline-induced *MCD1* overexpression in BY Background.

Replicative lifespan viability assay in which an integrated inducible tetracycline promoter over expressed either the *MCD1* gene or an empty vector (mean rls = ▲ 28.0 ◆ 21.0).

Sir2 functions upstream of cohesin for RLS (KOBAYASHI *et al.* 2004; KOBAYASHI AND GANLEY 2005), and for SCC at *HMR* (WU *et al.* 2011), implying that Sir2 is upstream of cohesin loading and function. However, this relationship could potentially be more complex since both factors are depleted with age. To explore this further, we next tested if *SIR2* overexpression could rescue the short RLS of an Mcd1-depleted *mcd112STOP* strain by integrating a second copy of *SIR2* (*2xSIR2*) at the *LEU2* locus. As shown in Figure 3.6F, *2xSIR2* partially rescued mean RLS of the *mcd112STOP* strain (14.1 versus 9.9 divisions, $p < 1.0 \times 10^{-4}$), and also increased maximum RLS of the WT strain. Reciprocally, we asked if *MCD1* overexpression would suppress the short RLS of a *sir2Δ* or *sir2Δ hst1Δ* mutant. The double mutant was included to rule out any redundancy between the two sirtuins. Mean RLS was clearly not increased by *MCD1* overexpression as compared to empty vector for either the single (10.7 versus 10.2) or double mutant (10.1 versus 9.7 divisions, Figure 3.6G), confirming that *SIR2* was required for

MCD1 in regulating RLS. Interestingly, the *sir2Δ hst1Δ fob1Δ hmrΔ* quadruple mutant combination, which suppressed CIN in aged cells (Figure 3.1H), fully restored RLS of the short lived *sir2Δ hst1Δ* combination to WT levels (Figure 3.6G, p=n.s.), suggesting that CIN is a key driver of replicative aging downstream of Sir2 and Hst1.

Considering the strong depletion of cohesin from rDNA in aged cells (Figure 3.2D), and extended RLS when *MCD1* was overexpressed (Figure 3.6E), we next tested if age-induced rDNA instability was suppressed by *MCD1* overexpression using a reporter strain harboring *ADE2* in the rDNA array (KAEBERLEIN *et al.* 1999). There was a large increase of red/white ½ sectoring (marker loss) from aged cells that was suppressed upon *MCD1* overexpression (Figure 3.6H). In the absence of *SIR2*, ½ sectoring was high from young and aged cells when the empty vector (pRF10) was integrated, and *MCD1* overexpression did not significantly reduce rDNA instability in either population (Figure 3.6H), indicating that at least some Sir2 was required for Mcd1 to impact rDNA stability. We conclude that loss of Sir2 and cohesin in aging cells causes rDNA array instability that generally exacerbates CIN.

RLS extension by CR correlates with improved chromosome stability

Reducing glucose concentration in the growth medium is effective at extending RLS and is considered a form of caloric restriction (CR) for yeast (JIANG *et al.* 2000; LIN *et al.* 2002). There have been several hypotheses put forth for the underlying mechanisms, including stabilization of the rDNA, as CR suppresses recombination within the rDNA (LAMMING *et al.* 2005; RIESEN AND MORGAN 2009; SMITH *et al.* 2009). Since *MCD1* overexpression suppressed rDNA recombination and extended RLS, we hypothesized that CR may suppress the abbreviated RLS of a cohesin-depleted *mcd112STOP* mutant strain. Indeed, CR extended RLS of both the

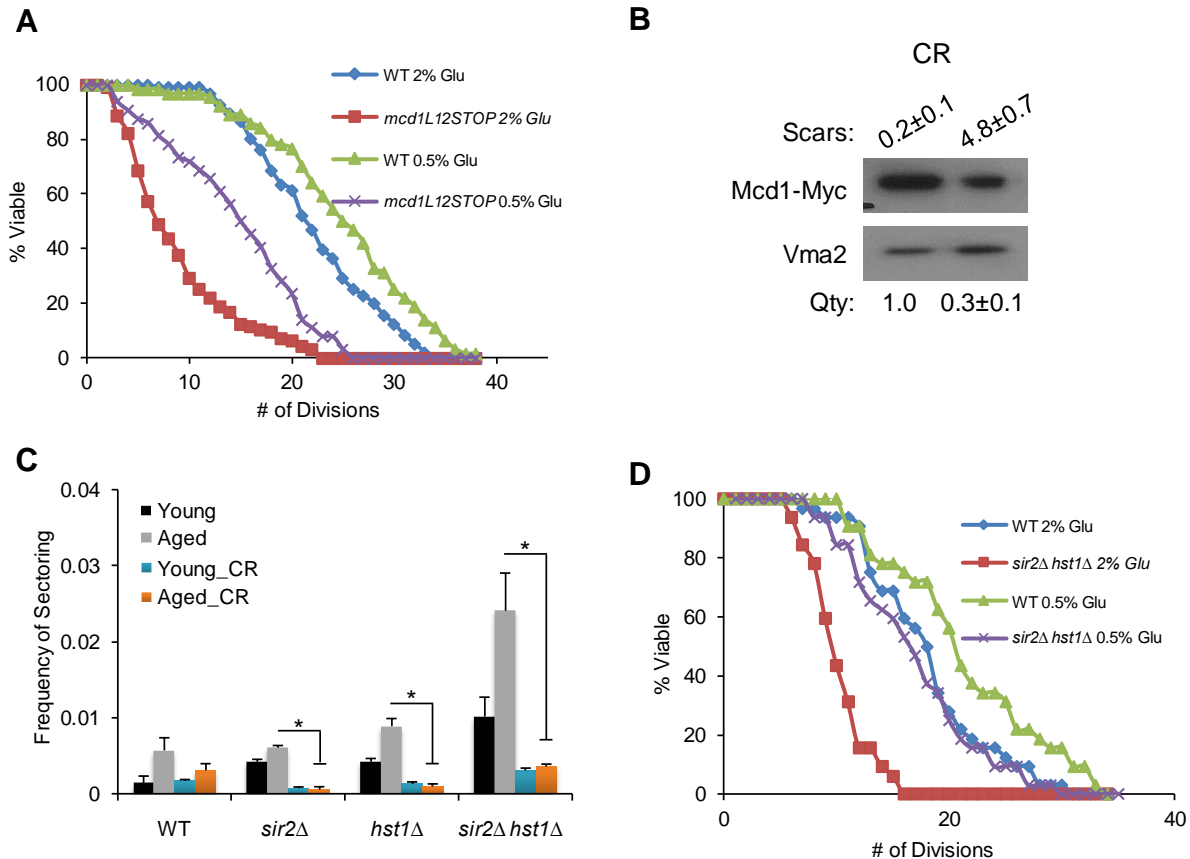


Figure 3.10. CR suppresses the CIN and RLS defects of *sir2Δ* and *mcd1* mutants. (A) RLS assay of WT (JH5275b) and *mcd1L12STOP* (JH5276b) strains under normal 2% glucose and CR (0.5% glucose) conditions (n=32 cells; mean rls = \blacklozenge 21.3 \blacksquare 8.1 \blacktriangle 24.1 \times 13.8). (B) Western blot of Mcd1-13xMyc for cultures grown in YEP media containing 0.5% glucose. (C) Chromosome loss (sectoring) assay of strains grown in media containing 0.5% glucose. Data from Figure 1H included for reference. *p<0.05, two-tailed t-test. (D) RLS assay of WT and *sir2Δ hst1Δ* mutant strains under normal and CR conditions. (n=32 cells; mean rls = 19.6 \blacksquare 9.3 \blacktriangle 23.5 \times 17.1).

WT and *mcd1L12STOP* strains (Figure 3.10A, p<0.01 and p< 1.0×10^{-7} respectively). However, the suppression was apparently not due to maintenance of global cohesin levels because steady state Mcd1-13xMyc was still depleted in glucose restricted aged cells (Figure 3.10B). CR also strongly suppressed minichromosome loss in young and aged cells, even in the *sir2Δ hst1Δ* double mutant (Figure 3.10C). Importantly, this CR effect also correlated with almost complete rescue of RLS for the *sir2Δ hst1Δ* mutant (Figure 3.10D, p=n.s.). Taken together, the results

support a mechanism for RLS extension by CR, whereby stabilization of the rDNA locus helps maintain general mitotic chromosome stability to protect against aneuploidy.

The rDNA array has an opportunity to interact with centromeres during anaphase

To conclude this study, we asked whether there is any mechanistic connection between the rDNA and centromeres that could cause CIN. If rDNA instability has a direct effect on SCC during aging, then we should observe elevated dissociation of sister chromatids in a *sir2Δ* mutant and improved SCC in a *fob1Δ* mutant. However, as shown in Figure S3.2, the frequency of 2 GFP dots in the SCC assay for these two mutants in aged populations was comparable to WT (see Figure 3.5E and 3.5F). Alternatively, the rDNA could potentially affect centromere function through direct contacts. Previous Hi-C analysis of the yeast genome and fluorescence microscopy of nucleolar proteins positioned the rDNA off to one side of the nucleus, apparently secluded from the rest of the genome (GOTTA *et al.* 1997; DUAN *et al.* 2010). The repetitive nature of rDNA precludes it from appearing in Hi-C contact maps, but closer inspection of iteratively corrected chromosome XII contact maps at 10 kb resolution indicated a clear interaction between unique sequences flanking the centromere-proximal (left) edge of the array and *CEN12* (Figure 3.11A, yellow arrow). We hypothesized that this contact was regulated by Sir2 since it is in the vicinity of a known tRNA boundary (tQ(UUG)L) for rDNA silencing (BISWAS *et al.* 2009), but deletion of *SIR2* had no effect on the contact (Figure 3.12). Interestingly, all centromeres of the yeast genome, including *CEN12*, cluster together in asynchronous cell population Hi-C data (Figure 3.11B, yellow arrows; (DUAN *et al.* 2010)), which potentially places them in proximity with the rDNA given the association of *CEN12* with sequences flanking the rDNA. During anaphase, the rDNA is thought to be separated from

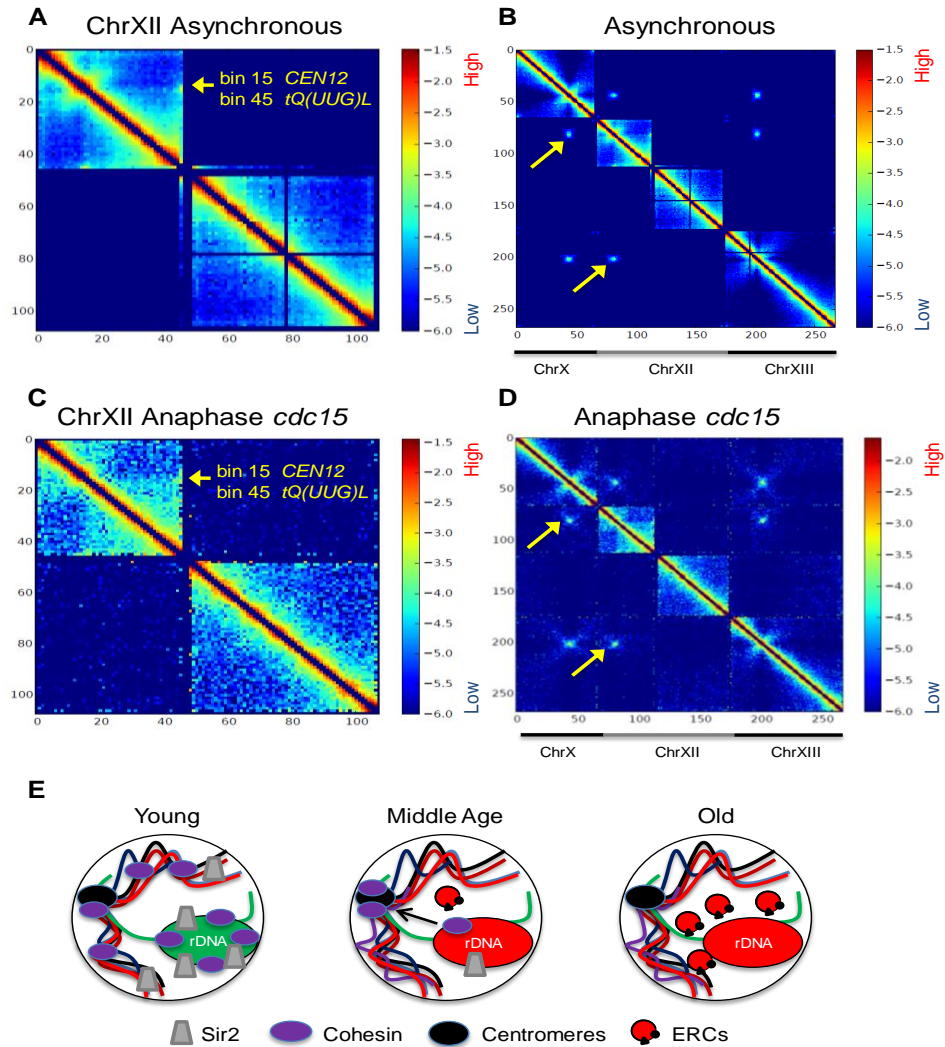


Figure 3.11. Chromosomal instability during replicative aging is linked to the rDNA.

(A) Iteratively corrected and read-normalized heatmap of ChrXII Hi-C contact data at 10 kb resolution in WT cells growing asynchronously, revealing an interaction between *CEN12* (bin 15) and unique sequence adjacent to the rDNA (bin 45), indicated by yellow arrow. (B) Contact heatmap of chromosomes XI, XII, and XIII showing centromere clustering in asynchronously growing WT cells. Yellow arrows indicate examples of centromere alignment with *CEN12* and sequence adjacent to the rDNA. (C) Iteratively corrected Chromosome XII heatmap from *cdc15* cells arrested in anaphase. Yellow arrow indicates the interaction between *CEN12* and the rDNA-adjacent bin. (D) Contact map showing interactions between centromeres in the anaphase-arrested *cdc15* mutant. (E) Model for cohesin and Sir2 depletion from the rDNA of aged mother cells. Cohesin is initially retained at centromeres (Middle Age, black arrow), and then ultimately lost in the oldest cells. ERCs begin to form during middle age and may contribute in a self-perpetuating cycle resulting in chronic destabilization of the rDNA array due to loss of cohesin, RENT, and the cohesin complex (red).

centromeres, but analysis of Hi-C data from a *cdc15-2* mutant, which arrests cells in anaphase, revealed that the rDNA-proximal/*CEN12* contact specifically occurs during anaphase (Figure 3.11C, (LAZAR-STEFANITA *et al.* 2017)), during which time the centromeres are still clustered together by the spindle pole body (Figure 3.11D). Taken together, these results suggest that the rDNA may transiently contact the centromeres during mitosis, providing a potential window of time for a destabilized rDNA array to negatively impact the integrity of general chromosome segregation during mitosis (Figure 3.11E).

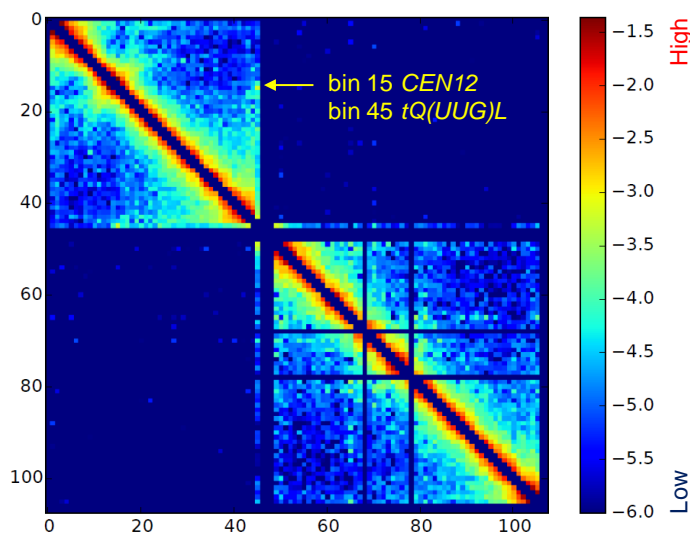


Figure 3.12. Deleting Sir2 had no effect on the left rDNA flank chromatin loop interaction with centromere XII. Heatmap of the natural log of paired end read counts from a *sir2Δ* mutant Hi-C experiment binned at 10kb resolution for chromosome XII. The *CEN12-tQ(UUG)L* interaction loop is not eliminated by the deletion of *SIR2* (yellow arrow).

Discussion

Nuclear protein depletion during replicative aging as a paradigm for aging pathologies

During this study the majority of chromatin-associated proteins that we analyzed by western blotting were depleted in replicatively aged yeast cells. The only protein unaffected by age that we tested, other than the vacuolar Vma2 control, was Sir3 (Figure 3.1D). A similar proportion of homologous recombination proteins were depleted in an independent analysis of aged cells, with Rad52 the only one tested that was not affected (PAL *et al.* 2018). These results suggest that there is at least some selectivity to the depletion of nuclear proteins in aged cells. However, the large number of depleted factors also makes it likely that targeted nuclear protein deficiency could lead to multiple age-associated phenotypes. Replicatively aging yeast cells appear especially susceptible to this phenomenon, as even total core histone levels are depleted (HU *et al.* 2014). Evidence also exists for histone depletion during aging of metazoan organisms, including mammals (reviewed in (SONG AND JOHNSON 2018)). More generally, global protein turnover is elevated in cells from prematurely aging progeria patients, which may trigger higher translation rates (BUCHWALTER AND HETZER 2017). This is significant because reducing translation is a means of extending lifespan in multiple organisms (MEHTA *et al.* 2010). The mechanism(s) driving nuclear protein depletion in aged yeast mother cells or other organisms remain unclear.

The specificity for Sir2/Sir4 depletion over Sir3 is intriguing given that Sir2 and Sir4 form a tight complex that allosterically stimulates the deacetylase activity of Sir2 (HSU *et al.* 2013), while Sir3 is a subunit of the SIR holocomplex (OPPIKOFER *et al.* 2011). Since Sir3 levels are elevated in aged cells (Figure 3.1D; (JANSSENS *et al.* 2015)), it likely has a function independent of the SIR complex during aging. The mechanism for Sir2/Sir4 depletion from aged

cells remains uncharacterized, though in non-aging cell populations the stability/turnover of Sir4, but not Sir2, is mediated by the E3 ubiquitin ligase San1 (DASGUPTA *et al.* 2004), which has also been implicated as a quality control E3 ligase for mutated/unfolded nuclear proteins (GARDNER *et al.* 2005). Whether San1 controls Sir4 stability during aging remains unknown, but since Sir4 is more severely depleted than Sir2 in aged cells (Figures 3.1A and 3.2C), Sir4 could be selectively depleted from the SIR complex, thus leaving Sir2 unprotected and subject to turnover through a different mechanism. Consistent with this idea, we note that Sir4 is depleted independently of Sir2 during extended G1 arrest (LARIN *et al.* 2015). Alternatively, Sir2/Sir4 could be equally depleted as a complex from telomeres and the *HM* loci (not necessarily via San1), leaving the nucleolar pool of Sir2/RENT as more resistant to aging. Under this scenario, protecting integrity of the rDNA array could take precedence over other heterochromatic domains. Interestingly, the *Schizosaccharomyces pombe* San1 ortholog has also been implicated in a chaperone-assisted degradation pathway that functions in quality control of kinetochores to promote chromosome stability (KRIEGENBURG *et al.* 2014).

Sir2 depletion in replicatively aged yeast cells is reminiscent of SIRT1 depletion in serially passaged mouse embryonic fibroblasts (MEFs), which correlates with declining mitotic activity (SASAKI *et al.* 2006). Sir2 and SIRT1 are both known to function in regulating DNA replication origins (HOGGARD *et al.* 2018; UTANI AND ALADJEM 2018), and the effect of deleting *SIR2* on early origin firing is thought to be mediated by competition for limiting factors with the repeated rDNA origins (YOSHIDA *et al.* 2014). Furthermore, CR has been proposed to extend RLS by reducing rDNA origin firing, which improves overall genome replication (KWAN *et al.* 2013). This may help explain why CR can extend RLS and suppress CIN even when *SIR2* and

HST1 are deleted. Conversely, depleted cohesin in old cells could potentially cause rDNA instability by impacting DNA replication and repair.

A precarious balance between rDNA and centromeric cohesion

SCC ensures chromosomes are not segregated until the Mcd1/Scc1 cohesin subunit is cleaved in response to a mitotic spindle checkpoint signal that all chromosomes are properly attached to microtubules and aligned at the metaphase plate (reviewed in (MARSTON 2014)). Cohesin is also critical during meiosis, and it is well established in mammals that SCC defects occur in the oocytes of older mothers, causing meiotic chromosome missegregation events during both anaphase I and II (JESSBERGER 2012). This phenomenon is believed to be a major mechanism for increased aneuploidy risk that usually results in embryonic lethality, or in the case of chromosome 21 trisomy, Down's syndrome. The meiotic cohesin subunit Rec8 is depleted in the oocytes of older mice, as is Shugoshin (*Sgo2*), which normally protects/maintains centromeric cohesin (LISTER *et al.* 2010). More recent experiments in *Drosophila* suggest that oxidative stress in aged oocytes contributes to the SCC defects (PERKINS *et al.* 2016). Our results in replicatively aging yeast cells reveal that aging-induced cohesin depletion and the resulting chromosome missegregation can extend to mitotic cells. Though cohesin depletion or defects have not been reported for mammalian somatic cells, the mitotic spindle checkpoint protein BubR1 is depleted in dynamic somatic tissues such as spleen in aged mice (BAKER *et al.* 2004). Deficiency of this protein results in premature aging phenotypes (BAKER *et al.* 2004), while overexpression extends lifespan (BAKER *et al.* 2013). This is similar to the effects we observe with Mcd1 depletion and overexpression on yeast RLS. Interestingly, BubR1 is also a deacetylation target of SIRT2, which appears to stabilize the protein and extend lifespan, thus

linking mitotic spindle checkpoint regulation to NAD⁺ metabolism (NORTH *et al.* 2014). It remains unclear if Sir2, Hst1, or other sirtuins regulate the yeast BubR1 ortholog, Mad3, or additional checkpoint and kinetochore proteins.

SCC is the canonical function for cohesin, though the complex also functions in establishing and regulating genome organization at the level of chromatin structure, gene regulation, and double strand break (DSB) repair (reviewed in (UHLMANN 2016)). Among these various processes, SCC at centromeres appears the most critical because artificial depletion of Mcd1 to <30% of normal levels results in preferential cohesin binding to pericentromeric regions rather than cohesin associated regions (CARs) on chromosome arms (HEIDINGER-PAULI *et al.* 2010). SCC was also well maintained in these strains at the expense of normal chromosome condensation, DNA repair, and rDNA stability (HEIDINGER-PAULI *et al.* 2010). In aged yeast cells, we observed relative enrichment of Mcd1-myc at centromeres as compared to loss at the rDNA (IGS1) locus (Figures 3.2D and 3.2E) consistent with pericentromeric cohesin retention in the artificially depleted system. Despite maintaining the cohesin complex at centromeres, SCC was still slightly impaired in the aged cells, but only if we analyzed cells >7 generations old. We suspect cohesin was reduced at centromeres in these older cells, which would be consistent with the loss of centromeric Mcd1 enrichment when cells were aged longer for 36 hr. These results are in line with an independent study that analyzed significantly older mother cells (~25 generations) and observed reduced cohesin enrichment at centromeres as well as increased loss of SCC (PAL *et al.* 2018). Another recent study using single cell microfluidics found that chromosome loss was very common just prior to the last cell division (NEUROHR *et al.* 2018). Collectively, the results suggest that centromere-associated cohesin is preferentially retained

during the initial stages of replicative aging, but then eventually breaks down below a critical threshold in the oldest cells.

Supporting this hypothesis, numerous nuclear proteins are depleted in aged yeast cells, not just cohesin subunits, so we hypothesize that defects in other nuclear processes mediated by such factors also contribute to SCC defects and chromosome instability either directly or indirectly. The depleted cohesin loading complex (Scc2/4) is an obvious candidate due to its role in loading cohesin at centromeres and CARs. Similarly, the depleted cohibin complex (Figure S3.2) is proposed to act as a cohesin clamp onto rDNA chromatin (HUANG *et al.* 2006), and also functions at centromeres to maintain mitotic integrity (BITTO *et al.* 2015). Sir2 and Hst1 are also obvious candidates given the earlier finding that H4K16 deacetylation at centromeres by Sir2 helps maintain chromosome stability (CHOY *et al.* 2011). Part of this effect is apparently due to the pseudo-diploid phenotype of a *sir2* Δ mutation, which has been previously shown to impact RLS (KAEBERLEIN *et al.* 1999). Hst1 also binds centromeric DNA *in vitro* and *in vivo* (OHKUNI AND KITAGAWA 2011), though the functional relevance of that association remains uncharacterized. The suppression of age-associated mini-chromosome loss in the absence of *FOBI* clearly points to rDNA instability as an unexpected source of general CIN. Such a relationship is reinforced by the observed depletion of nucleolar proteins Net1 and Lrs4 in aged cells (Figures 3.2E and 3.3), both of which are required for normal rDNA/nucleolar integrity and stable cohesin association with the rDNA (SMITH *et al.* 1999; STRAIGHT *et al.* 1999; HUANG *et al.* 2006).

How could destabilization of the rDNA locus result in general chromosome instability and shortened RLS? As depicted in Figure 3.11, unique sequence flanking the rDNA contacts the centromere of chromosome XII, thus placing it in proximity to other centromeres during

anaphase. Whether the actual rDNA genes contact centromeres remains unclear due to the current limitations of Hi-C analysis with repetitive DNA. However, specific regions of the rDNA were previously shown to associate with various non-rDNA chromosomal regions using an anchored 4C approach (O'SULLIVAN *et al.* 2009). Furthermore, multiple nucleolar associated domains have been identified in metazoan cells that copurify with nucleoli (MATHESON AND KAUFMAN 2016). Loss of cohesin from the rDNA could potentially disrupt long-range interactions with centromeres or non-centromeric regions of cohesin association that influence chromosome integrity. One potential mechanism could be significant disruption of overall chromosome condensation during mitosis, as cohesin appears to play a larger role in the DNA looping associated with chromosome condensation in budding yeast than previously thought (SCHALBETTER *et al.* 2017).

Interestingly, another class of nuclear factors depleted in aged yeast cells are several DNA repair proteins (PAL *et al.* 2018). Consequently, the lack of proper DNA repair while the rDNA becomes destabilized correlates with fragmentation of chromosome XII and the other chromosomes (PAL *et al.* 2018). Rad52 foci also appear in aged cells indicating persistent DNA damage (NEUROHR *et al.* 2018). It was proposed that accumulation of breaks and rearrangements ultimately causes cell death during replicative aging. Such cells were significantly older (>25 divisions) compared to the cells in our study, which exhibited a maximum of 13 divisions after 24 hr. Alternatively, it is possible that these presumably random rearrangements disrupt normal SCC, leading to CIN.

Aneuploidy as an aging mechanism

All 16 *S. cerevisiae* chromosomes harbor essential genes, so if a single chromosome is lost from a haploid yeast cell, then the affected mother or daughter cell should become inviable

and no longer divide. Given the elevated frequency of chromosome loss during replicative aging, the chances of generating an inviable mother cell during a replicative aging assay increase after each subsequent division. Therefore, at least a portion of the replicative lifespan in haploid yeast cells is controlled by the ability to maintain all 16 chromosomes. Complete loss of a chromosome would not be an immediate viability issue for diploid cells, however, due to the chances of losing both homologs in a single mitosis being exceedingly rare. On the other hand, haploid strains that are disomic for individual chromosomes are often short lived, with longer chromosomes typically having larger effects (SUNSHINE *et al.* 2016). It was hypothesized that such strains suffer from proteotoxic stress due to inappropriate protein expression levels. Therefore, a similar mechanism could shorten RLS in a diploid strain that is trisomic for an individual chromosome, though this has not yet been tested. Aneuploidy is also a hallmark of aging in the germline (NAGAOKA *et al.* 2012), and somatic tissues of mammals (LUSHNIKOVA *et al.* 2011; BAKER *et al.* 2013), making it a conserved feature of aging from yeast to humans.

Another exciting feature of this study is the suppression of CIN by CR growth conditions that extend RLS. This effect was independent of the reduced cohesin levels in aged cells, and even improved RLS of the cohesin-depleted strains. Since SCC is normal in the cohesin-depleted strain (HEIDINGER-PAULI *et al.* 2010), we hypothesize that CR reinforces other processes that are defective due to reduced cohesin or other depleted factors that promote rDNA stability. Indeed, CR is known to suppress rDNA instability in yeast cells (RIESEN AND MORGAN 2009; SMITH *et al.* 2009), and improve overall genome replication efficiency (KWAN *et al.* 2013).

Hi-C analysis also suggests there could be direct effects of rDNA structure on centromere function, which will be a focus of future investigation.

Supplemental Data

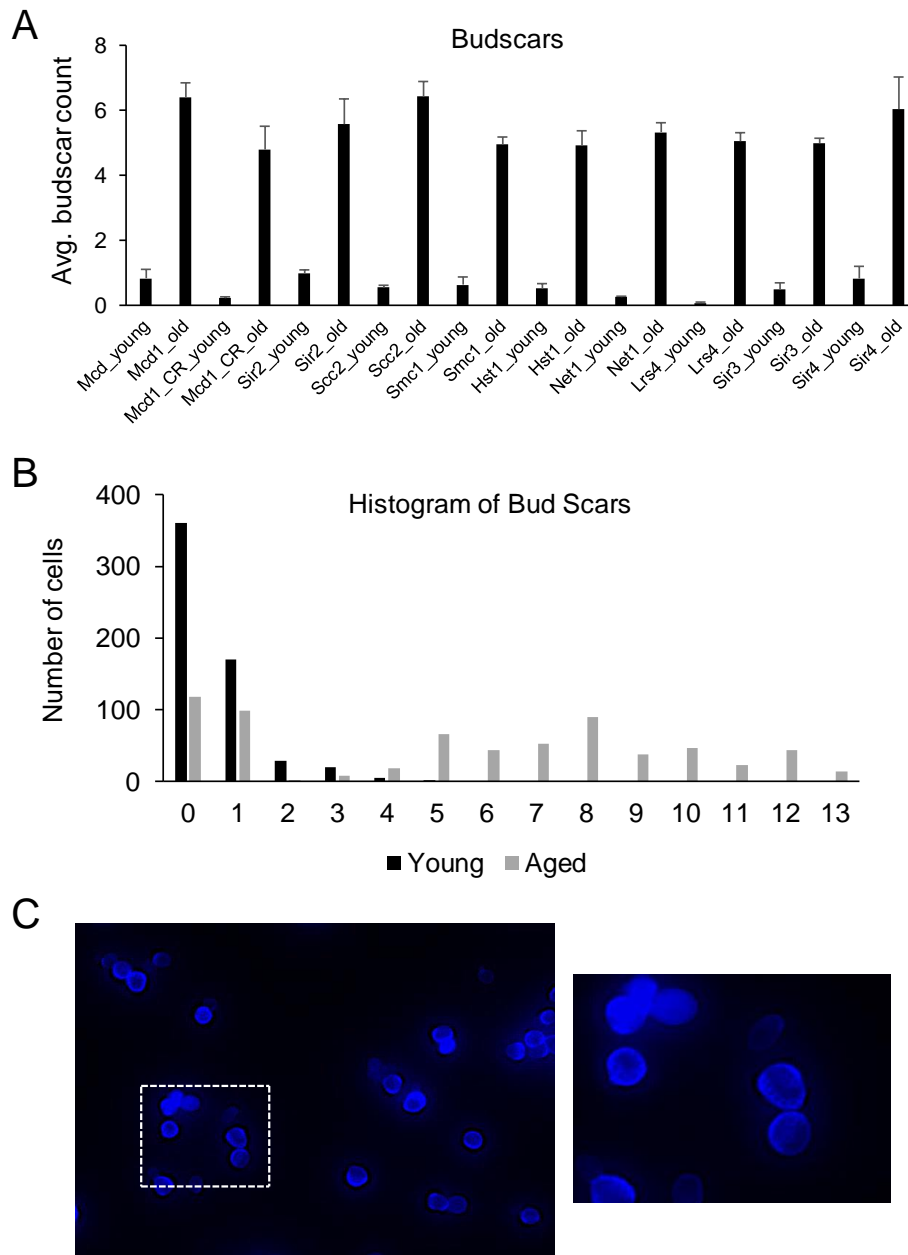


Figure S3.1. Detailed western blot and bud scar count quantification. (A) Bar graph showing average bud scars from young and aged cell populations that were used for western blotting. (B) Histogram of bud scars from young and aged populations used in western blot experiments. (n=584 and 658) (C) Representative image of an enriched aged cell population from the third Lrs4-13xMyc biological replicate. Inset image allows counting of individual bud scars.

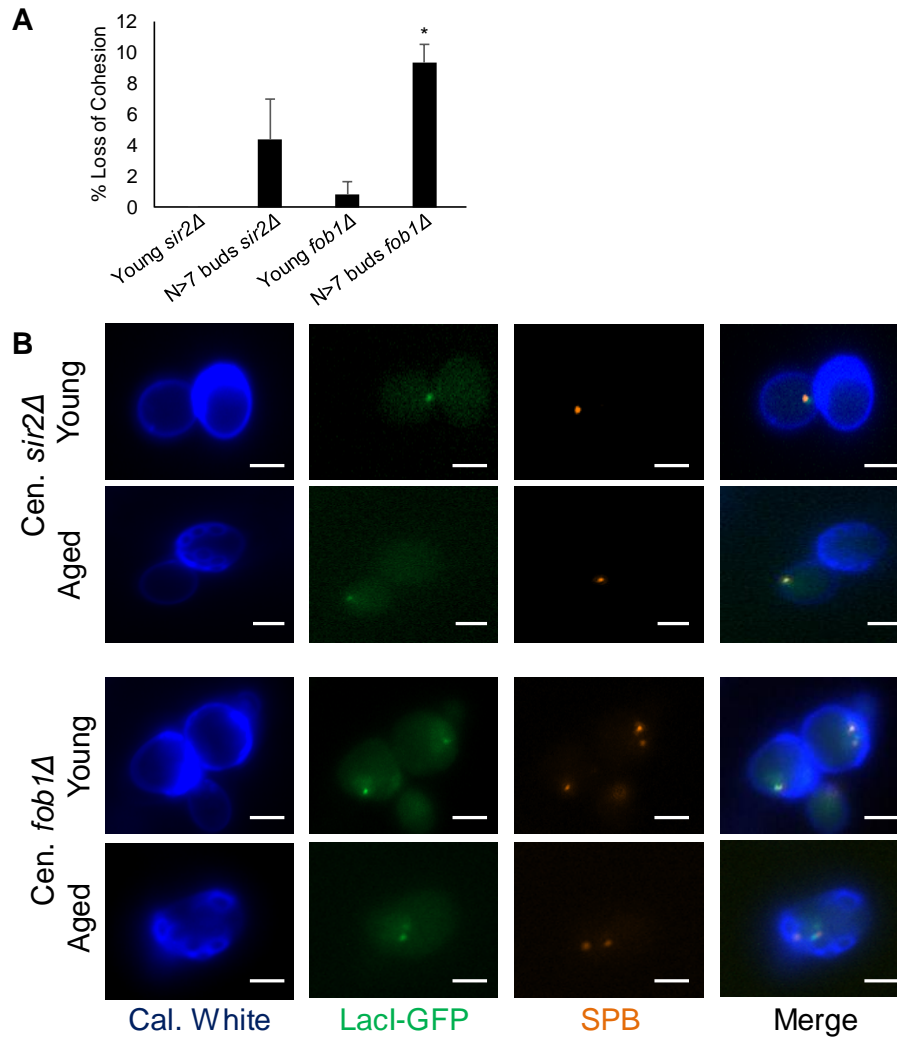


Figure S3.2. rDNA stability does not affect sister chromatid cohesion. (A) Quantification of cells assayed in (B) for loss (2-GFP Dots) of chromatid cohesion. (n=60 cells) (B) Representative screen shots of young (log-phase) or old yeast cells monitoring sister chromatid cohesion 10kb proximal to *CENIV* in *sir2Δ* and *fob1Δ* mutants.

Chapter IV

Conclusions and Future Directions

Our analysis of the statistically overlapping ChIP-seq binding sites of Sir2 and the condensin complex has uncovered a new role for Sir2 in the process of mating-type switching, potentially through transcriptional regulation of the recently discovered gene, *RDT1* (LI *et al.* 2013; WILSON AND MAZEL 2011). Follow up analysis of other overlapping sites has revealed condensin and Sir2 binding at the promoter of *SIR2* (Appendix A, Figure A.1), suggesting the not yet fully understood regulatory mechanism at the *RDT1* promoter may be generalizable to a larger portion of the genome. By using Hi-C analysis, we also observed that deletion of *SIR2* does not change the entirety of yeast 3D genome organization as initially hypothesized (Appendix A, Figure A.2), but rather primarily affects the organization of chromosome III and telomeres through its influence on heterochromatin (Figure 2.8 A; Appendix A, Figure A.2). Of further note, structural alterations of the rDNA array in a *sir2Δ* strain remain a mystery due to its repetitive nature preventing Hi-C analysis. Thus, it will be important to dissect the individual contributions to chromosome III structure by Sir2 (the *SIR* complex) and condensin going forward to gain insight into heterochromatin in general.

In the case of cohesin, the results were less fruitful than anticipated, with Sir2 appearing to have no direct role in facilitating recruitment of cohesin through some general genome-wide mechanism. However, this does not rule out a role for Sir2 within heterochromatic loci, for which there is evidence in the literature for cohesin recruitment at *HMR* and within the rDNA array (KOBAYASHI *et al.* 2004; CHANG *et al.* 2005; WU *et al.* 2011). From our own data, deletion of *SIR2* reduced cohesin binding in the rDNA in asynchronous log-phase cells (Appendix A, Figure A.3), suggesting the loss of Sir2 that we observed in aging cells (Figure 3.1) may be

responsible for the re-distribution seen from the rDNA to centromeres. More importantly, the apparent reduction/loss of numerous rDNA structural protein complexes in aged yeast further suggests stability of the array is the key to maintain healthy aging. Large scale transcriptomics suggests dysregulation is happening at the translation/protein level (JANSSENS *et al.* 2015), so the remaining questions are what is the cause and can it be reverted?

The function of RDT1

While we are certain that Sir2 deacetylase activity is regulating *RDT1*, we have yet to determine a functional role for this gene in the process of yeast mating type switching. Along with the data presented in Figures 2.4 and 2.7, experiments have been performed with overexpression constructs of the putative ORF alone, or a lncRNA version, as defined by RNA-seq data (Figure 2.3). Unfortunately, these experiments have produced only negative results in our standard-mating type switching assay, which leaves a few possibilities. First, we could be simply asking the wrong question with an artificial switching assay. The assay does not take cell-cycle regulation into account, with both *HO* endonuclease and *RDT1* expressed in an asynchronous population, nor does it reflect natural expression of either gene with both under control of highly active inducible promoters. Tetrad dissection of strains that can only switch once due to both donor templates lacking a *HO* cut site (*inc* mutants) could be used in conjunction with colony PCR to reveal subtle *trans* effects (WEILER *et al.* 1995). Additionally, our own mating-type switching assay could be improved by coupling a *MATa*-specific gene promoter (e.g. *STE2*) to an auxotrophic gene (e.g. *ADE2*). Cells can then be pre-cultured in dropout media lacking the auxotrophic nutrient, and inappropriate switching to *MAT α* , leading to

expression of $\alpha 2$ repressor, would kill the cells due to repression of the essential auxotrophic marker.

An alternative possibility is *RDT1* expression regulates mating type switching in *cis*. As shown in figure 2.8, Hi-C data indicates that *HMR* and *HML* are physically close in 3D space, and may be bound together by protein interactions of the *SIR* complex located at each locus, in addition to the telomeres. Eventually, *HML* needs to interact with the *MAT* locus in order to facilitate its usage as a homologous recombination donor template. It could be that *RDT1* expression is used as a mechanism to recruit chromatin remodeling factors, in addition to Pol II machinery, to temporarily disrupt the protein-protein interactions of the *SIR* complex at these loci in order to allow *HML* to associate with the *MAT* locus. If this is indeed the case, effects on mating-type switching and/or Hi-C interaction should be testable with inducible promoters swapped in for the *RDT1* promoter.

SIR loops or lone condensin extrusion?

Returning to Sir2, we cannot currently rule out a structural role, since derepression of the silent mating-type loci by any form of Sir2 inactivation leads to wholesale changes in the *MATa* specific genomic architecture on chromosome III. It is important to determine what role, if any, Sir2 and by extension the *SIR* complex plays in 3D chromatin looping because current data would suggest that condensin is sufficient via the loop extrusion model recently proposed by Haering and colleagues (GANJI *et al.* 2018). In context of chromosome III, condensin would first bind to the RE on the left arm between *HML* and *CEN3* (Appendix A, Figure A.4; top left), and then begin “pumping” DNA in an asymmetric ATP-driven manner, gradually forming an enlarging loop (Figure A.4; top right). This process would continue until the *HM* loci are

physically brought together to oppose the force (Figure A.4; bottom panels). Indeed, condensin function appears to be essential and sufficient for the formation of a chromatin loop on chromosome XII (LAZAR-STEFANITA *et al.* 2017), while a *sir2* Δ had no effect in our hands (Figure 3.12). What is not known, is the “strength” of the respective structures; i.e. is the specialized chromosome III structure more stable than the loop found on chromosome XII? Another possibility is that *SIR* complex acts as an impassable obstacle for the putative condensin pump at the promoter of *RDT1*. If that were true, one could potentially use silencing elements (E and I) that flank the *HM* loci, along with our condensin binding site to create artificial 3D chromatin organization in yeast by moving the silencers to different sites along chromosome III. Strains bearing *HMR* at different locations along chromosome III already exist, so testing this idea should be relatively trivial in combination with high resolution 5C-ID analysis to limit the expense of current methods (WU AND HABER 1996; KIM *et al.* 2018).

Cohibin as condensin loading factor

What is the minimal amount of genetic information needed to encode a condensin binding site? We have extensive evidence (data not shown) suggesting both the nearby *Mcm1* binding site and the condensin/Sir2 binding site, as defined by ChIP-seq, are required for condensin recruitment at the *RDT1* promoter. We were unsure of the role of *Mcm1* until we found a previous report with mass spectrometry data suggesting that it could physically interact with the cohibin complex composed of *Lrs4* and *Csm1* (CHAN *et al.* 2011). As mentioned earlier, *Lrs4* has been shown to deplete condensin binding in the rDNA array when deleted (JOHZUKA AND HORIUCHI 2009; *Chapter I, The condensin complex*). This is intriguing because we have been able to show through ChIP-seq and conformational ChIP-qPCR that deletion of *LRS4* also

eliminates condensin binding at the *RDT1* promoter and the promoter of *SIR2*, in addition to the previously reported rDNA effect (Appendix A, Figure A.1; JOHZUKA AND HORIUCHI 2009). Thus, a direct physical recruitment of condensin by cohibin and, in turn, cohibin by Mcm1 provides the simplest model (Appendix A, Figure A.5). We tested this by Co-IP. As shown in Appendix A Figure A.6, Csm1-flag can be physically pulled out of yeast extracts by immunoprecipitation of Myc-tagged Mcm1. Initial attempts to test cohibin interaction with condensin have not been as successful due to high background, but this can be tested by creating classic *GAL4-DBD* fusions of Lrs4 and Csm1. In short, the chimeric proteins would be expressed in Brn1-13xMyc strains containing either *GAL4* upstream activating sequence (UAS) arrays or empty vector sequence as a negative control. Condensin targeting can then be measured using standard ChIP-qPCR. Given the effects observed to date appear to be occurring outside of heterochromatin, the genomic position of the array should not matter, however, we will initially use *HMRE* as the initial targeting site. While there is a distinct possibility the chimeric fusions will inhibit endogenous Lrs4/Csm1 function, the evidence found thus far warrants further investigation into the potential of cohibin acting as a general condensin loading factor.

Cause and consequences of protein depletion in aging yeast

Our studies of cohesin and Sir2 interplay during yeast RLS has also led to several interesting findings worth following up. We initiated the study with pre-existing knowledge of Sir2 depletion in replicatively aged yeast cells (DANG *et al.* 2009). Our novel contribution was the discovery of depletion of both Sir2 binding partners, Net1 and Sir4, in addition to cohesin depletion, also reported recently by an independent group (Figure 3.1; PAL *et al.* 2018). The proteins tested appear to be depleted at an average “age” of 7 generations (budscars), an early

time that might suggest this phenomenon is a cause of aging in yeast rather than a consequence. Fitting this model, sister chromatid cohesion on chromosome IV is initially well maintained as is at least one of the *SIR* complex's regulated loci, *HML* (MCCLEARY AND RINE 2017). However, a different study using the MEP system has shown that the acidity of the vacuole is reduced around seven generations (HUGHES AND GOTTSCHLING 2014). The vacuole is required to breakdown proteins and store unused basic and neutral amino acids as well as promote mitochondrial homeostasis, which was also disrupted at this early stage (HUGHES AND GOTTSCHLING 2014). It could be the protein depletion that we observe in these early stages is a direct result of either vacuole dysfunction, mitochondrial dysfunction, or both. Further entwining these processes is the forkhead box family member, Hcm1, and Sir2. Hcm1 activates both mitochondrial biogenesis genes and vacuolar acidity (RODRIGUEZ-COLMAN *et al.* 2010; GHAVIDEL *et al.* 2018). Hcm1 also shuttles between the cytoplasm and the nucleus, but requires Sir2's deacetylase activity for the nuclear localization. A previous study has shown that strains with low copy number of rDNA repeats express *SIR2* at a low level and are sensitive to *SIR2* overexpression, suggesting the protein levels of Sir2 are in constant balance with the number of rDNA repeats (MICHEL *et al.* 2005). They further showed that the rDNA can lose as much as 60% of the array size in a single step, when grown in the presence of hydroxyurea. Thus, an early destabilization event of the rDNA during natural aging could lead to a dramatic downregulation of *SIR2* expression and throw the homeostasis of the other two processes out of balance to downregulate protein expression as we have observed (Figures 3.1 and 3.2). Future work should aim to measure the stability of all of these systems in tandem to clarify which process (if any) leads to failure of the other systems. With advances in microscopy and microfluidic-based yeast RLS technologies, such systems-level biology is becoming much more feasible and necessary.

On top of finding the cause of protein depletion, we need to be further certain it has real consequences. Our cohesion maintenance assays showed the critical biological process of sister chromatid cohesion is relatively well maintained during the initial stages of aging, despite a large reduction in cohesin complex compared to young cells (Figure 3.2). Another lab has already shown that cells exhibit chromosome segregation defects in addition to tripartite spindles during the last viable cell division (NEURHOR *et al.* 2018). Interestingly, this study used a LacO array on chromosome I, while another used an array on chromosome XII which showed larger rates of cohesion loss (PAL *et al.* 2018). It has also been speculated that the cells analyzed by PAL *et al.* were actually dead (HENDRICKSON *et al.* 2018). These findings, combined with our own, warrant an investigation into specificity, such as whether or not larger chromosomes lose cohesion and missegregate more often than smaller ones? Or is chromosome XII unique because of the rDNA? Perhaps more importantly, do our current therapeutic strategies of CR, among others, limit such events throughout lifespan or at the end of lifespan? Some of these questions may be studied with current MEP methods, but ideally, they will be answered with less engineered yeast using microfluidics and/or single cell genomic DNA sequencing of aged cells.

If Sir2/Sir4 and Net1 are indeed depleted in aged cells, this should result in loss of silencing at all of the major heterochromatic loci as well as reduced Pol I activity at the rDNA (SHOU *et al.* 2001). Pol I activity could be quickly checked by a simple RT-qPCR of young and aged cell populations. Silencing on the other hand could be tested with use of fluorescent reporter constructs similar to classic Sir2 silencing assays. The Rine lab has already created one such construct dubbed CRASH within the *HML* locus and found no loss of *SIR*-dependent silencing in replicatively aged yeast cells using a microfluidic platform (SCHLISSEL *et al.* 2017). While this result appears to argue against our data, it does not rule out loss of silencing from the

telomeres and the rDNA array. In fact, *HML* and *HMR* silencing is considered much more stable than the telomeres or rDNA. Of course, the telomeres and rDNA will be technically more difficult to study since the telomeres experience variable silencing and the rDNA experiences markers loss at a high rate from unequal recombination. However, we have a unique opportunity with regard to the left flank of the rDNA array that our lab has developed in the past as an indicator of the silencing present throughout the entire array (BUCK *et al.* 2002; BUCK *et al.* 2016). We could do a simple colony sectoring assay of young versus aged populations, as already done with the artificial chromosome III to monitor chromosome missegregation, if a marker such as *ADE2* or GFP are integrated there. As for the telomeres, Sir4 is required for telomere clustering in yeast (BYSTRICKY *et al.* 2005). Thus, we could monitor telomere clustering in old cells with Rap1-GFP using either current MEP methods or a microfluidics approach.

rDNA Destabilization of the other Chromosomes

The final model from our aging study was that the rDNA array acts as a protein sink for factors like Sir2 and cohesin in healthy young cells and upon depletion of total protein levels in old cells, was the first locus to experience loss of these factors, resulting in array instability. Our ChIP-qPCR data supports this with an apparent increase of cohesin binding at centromeres and loss from the rDNA in middle aged cells compared to young cells, as does a study in which Mcd1 proteins levels were artificially reduced (HEIDINGER-PAULI *et al.* 2010). The rDNA array acting in a *trans* manner to destabilize the other chromosomes is based on our Hi-C data, as well as other reports, which revealed the left unique flank of the rDNA array coming into close three-dimensional contact with *CEN12* and thus all centromeres (LAZAR-STEFANITA *et al.* 2017; FINE

et al. 2019). This was further supported by our chromosome missegregation data which revealed that an rDNA stabilizing *foi1Δ* mutation could reduce chromosome loss of a non-rDNA mini-chromosome III (Figure 3.1).

In order to further test this model, it is important to find out how the *CEN12*-left unique rDNA flank contact forms and what it does. An extension of our cohibin hypothesis would suggest the chromosome XII loop will be lost in a *lrs4Δ* strain. This is easily testable by Hi-C. The next prediction of the loop extrusion model suggests that there is a single condensin binding site similar to the one we found on chromosome III between *CEN12* and the left flank of the rDNA (GANJI *et al.* 2018; Figure 2.1). Our ChIP-seq data has revealed dozens of possible sites. Fortunately, data from a recent study in which all of the chromosomes were fused together gives us a hint that the condensin binding site of interest may be within a few kb of *CEN12* since the anaphase loop seems to disappear upon removal of a larger region encompassing *CEN12* (LUO *et al.* 2018). There is a lot of evidence that Ipl1 initiates the process of condensation from the centromeres and may be directly involved in formation of this loop as part of the essential process of condensation maturation of the rDNA (LAVOIE *et al.* 2004; KRUITWAGEN *et al.* 2015; KRUITWAGEN *et al.* 2018). Hence, it may prove prudent to dissect this site using a strain which has removed all but two copies of the rDNA to high expression plasmids (GANLEY *et al.* 2009). This would of course require that the chromosome XII loop be present in this strain, though loss or retention itself would be interesting.

In conclusion, the data presented herein has contributed to the groundwork for an emerging paradigm, where the sirtuins and SMC proteins have independent functions, but ultimately work together to overcome the cellular problems associated with maintaining, replicating, and repairing heterochromatin. The sirtuins establish and maintain silenced

heterochromatin to prevent inappropriate gene expression and disease, such as the pseudo-diploid phenotypes exhibited in Figures 2.1 and 3.1 resulting from *sir2Δ* derepression of the *HML* and *HMR* loci in otherwise haploid strains. In addition to their classic roles in mitosis, the SMCs now appear to provide a means of moving the otherwise stable Sir2-induced heterochromatin structures, which preferentially localize away from the euchromatic interior of the nucleus, towards the euchromatic domains to enable their use in vital processes, such as homologous DNA repair of the *MATa* locus with *HMLα* acting as a donor template during mating-type switching (Chapter II). What remains to be observed is whether or not classic SMC roles in mitosis are achieved through the currently hypothesized loop-extrusion mechanism proposed for their ability to create 3D loops and TADs during interphase. Furthermore, there is a lack of insight into what role (if any) heterochromatin factors may play in establishing the boundaries of such regions, especially in mammalian models. Clearly, the future of sirtuin and SMC overlap will lead to many exciting discoveries as we begin to unravel the mysteries of the highly repetitive domains of heterochromatin.

Appendix A

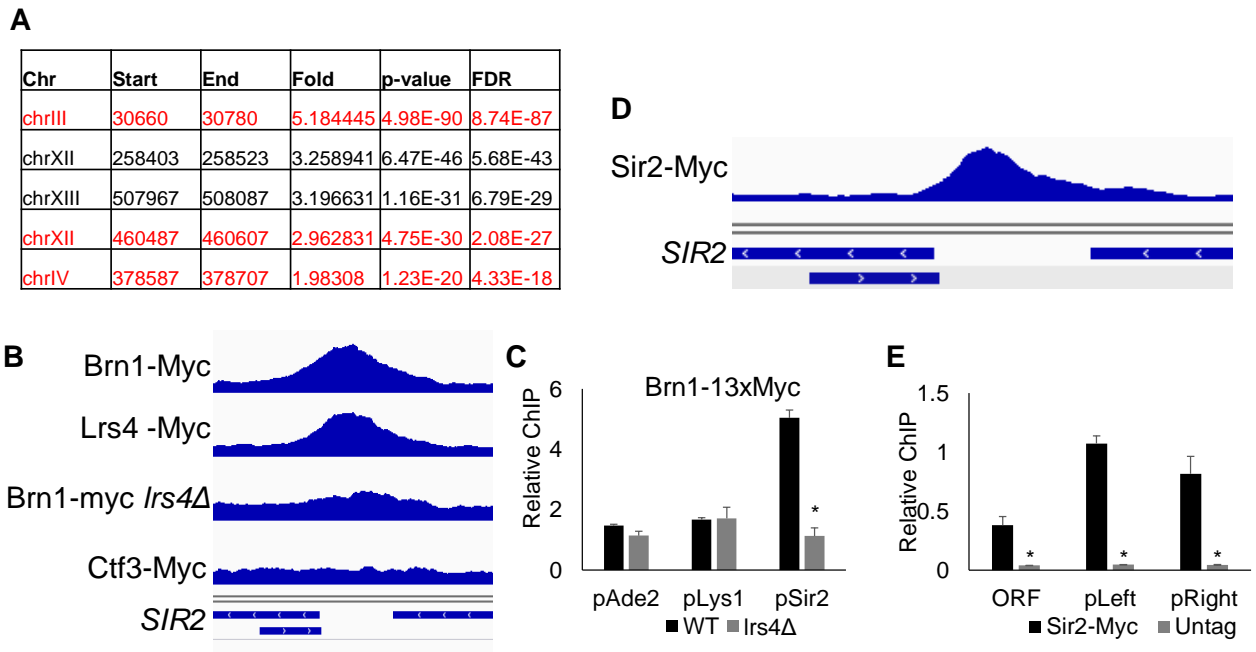


Figure A.1. Cohibin, condensin, and Sir2 genome-wide transcriptional regulation. (A) Table of the top 5 differential binding peaks between Brn1-Myc and Brn1-Myc *lrs4Δ* strains. Starting at the top, the confirmed hits (highlighted in red) include the *RDT1* promoter, rDNA array, and *SIR2* promoter. (B) IGV snapshot of Myc-tagged Brn1 (condensin) and Lrs4 (cohibin) colocalization at the *SIR2* promoter from ChIP-seq data. This also shows Brn1-Myc binding relies on Lrs4 (cohibin). Ctf3-Myc serves as a negative control. (c) ChIP-qPCR confirmation of (B). (D) IGV snapshot of Sir2-Myc binding to its promoter region from ChIP-seq data. (E) ChIP-qPCR confirmation of enriched promoter binding in (D). This data parallels currently unpublished observations (Mingguang Li; personal communication) seen at the *RDT1* promoter, suggesting a more general mechanism of transcriptional regulation.

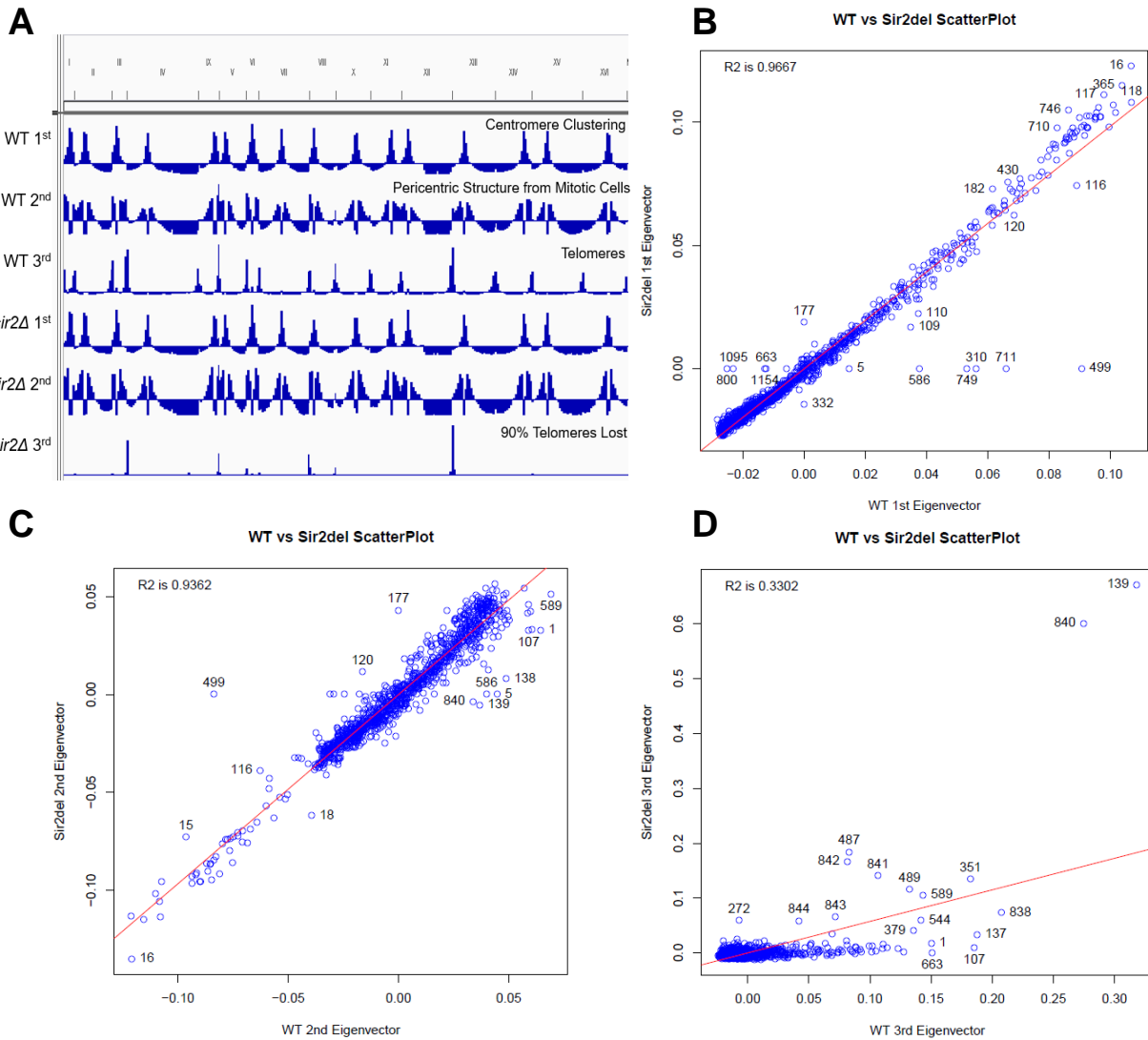


Figure A.2. Deletion of *SIR2* predominantly affects budding yeast heterochromatin structure. (A) IGV snapshot of the first three eigenvectors from iteratively corrected and read normalized Hi-C datasets of WT and *sir2Δ* strains binned at 10kb resolution across the genome. Eigenvectors reveal the dominant structural features of a Hi-C dataset similar to a principle component analysis. (B-D) Scatterplots of the first three eigenvectors from WT and *sir2Δ* Hi-C data (visualized in A) using Pearson correlation coefficient to quantify the differences between the eigenvectors of the two datasets. (B) The first eigenvector represents the 16 yeast centromeres clustering in 3D space and is unchanged by deleting *SIR2*. (C) The second eigenvector corresponds to pericentromeric chromatin from mitotic cells and again is unaltered in a *sir2Δ* strain. (D) Loss of *SIR2* greatly affects the heterochromatic telomeric component (3rd eigenvector) of genome organization ($R^2=0.3302$) and also disrupts the *HML* and *HMR* contact (bin 107), which was extensively analyzed in Chapter III.

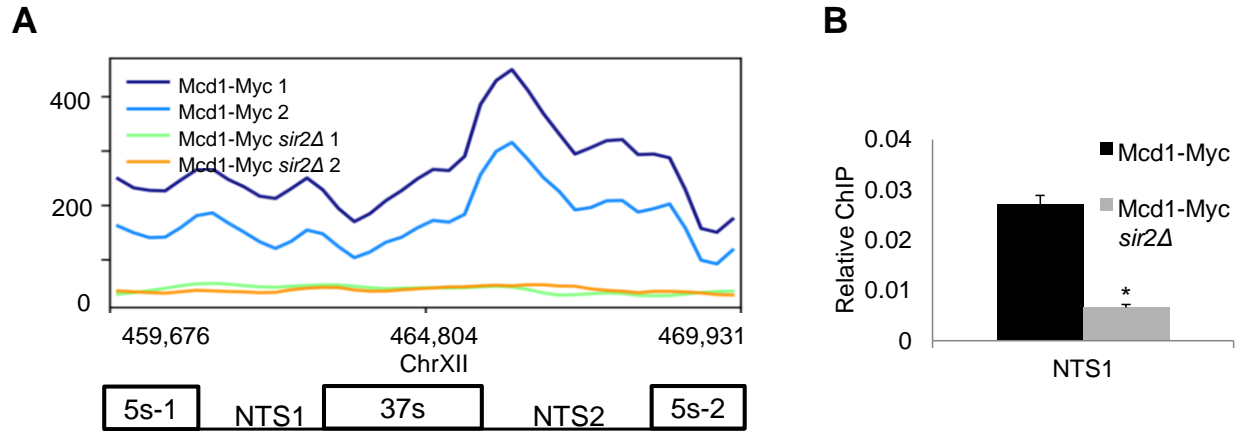


Figure A.3 Sir2 is required for cohesin binding within the rDNA array. (A) 1x coverage composite plot of Mcd1-Myc ChIP-seq in WT and *sir2Δ* backgrounds across 1 copy of the rDNA array repeated in biological duplicate. (B) ChIP-qPCR confirmation of ChIP-seq data in (A) at the NTS1 locus in biological triplicate. (* $p < .05$; two-tailed t-test).

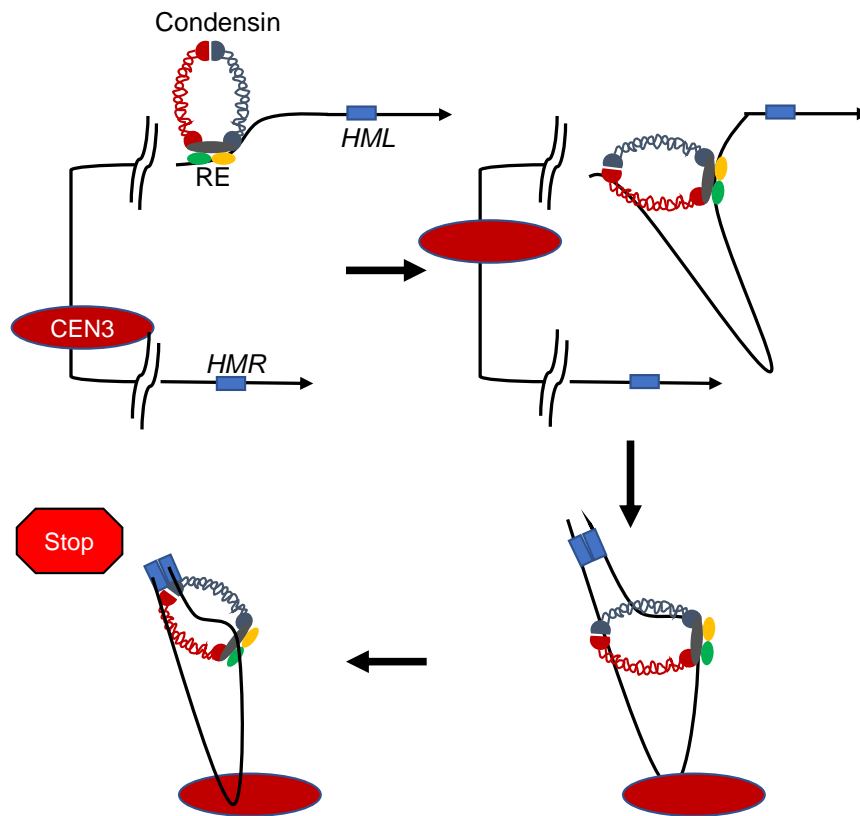


Figure A.4. Model of condensin loop-extrusion at the RE locus on chromosome III. Condensin initially localizes and anchors to the RE (Top Left). The complex then begins utilizing the ATPase activity of the Smc2/Smc4 subunits to extrude DNA in an asymmetric manner (Top Right). This brings *HMR* near *HML* in 3D space, potentially allowing the *SIR* complex at each locus to physically interact and facilitate a stable heterochromatic super structure (Bottom Right). It is not known during which cell-cycle phase this process may occur. Furthermore, Sir2 localization to the RE may only occur after condensin has successfully brought the *HM* loci and RE together in physical space (Bottom Left).

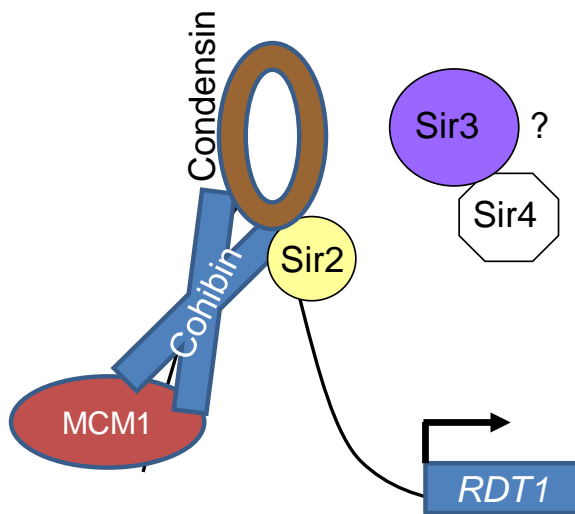


Figure A.5. Model of cohibin recruitment of condensin to the *RDT1* promoter. Mcm1 is a sequence specific DNA binding protein providing specificity to cohibin complex DNA binding through physical recruitment (Figure A.6). Cohibin then recruits the condensin complex. It is currently unknown how Sir2 is recruited, but this may occur in the form of spatial contact with the *SIR* complex (Sir2, Sir3, and Sir4) from the *HM* loci or telomeres.

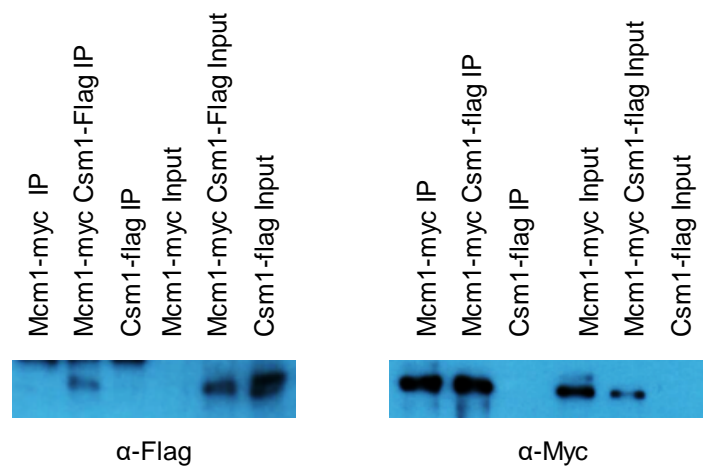


Figure A.6. Cohibin physically interacts with Mcm1. (Right) α -Myc western blot of Co-IP experiment in which α -Myc beads were used to pull out Mcm1-13xMyc from respective yeast cell extracts. (Left) α -Flag western blot from the same Mcm1-13xMyc Co-IP showing 5xflag tagged Csm1 (cohibin) is only precipitated in cells co-expressing Mcm1-13xMyc. Loaded inputs are 5% of cell lysate used for IP.

Acknowledgments

No work of this magnitude can be completed in isolation. We would like to thank all of the members of my thesis committee, Todd Stukenberg, Eyleen O' Rourke, and David Auble, for their countless suggestions, questions, and all too often valid criticisms, which collectively pushed me to be a better scientist than I ever thought possible. We thank Dan Gottschling and all lab members for kindly providing yeast strains and allowing me to visit the lab for initial advice on the MEP system. Stefan Bekiranov, Job Dekker, Jon Belton, Maitreya Dunham, Ivan Liachko, Maxim Imakev, and Anton Goloborodko all provided valuable advice on Hi-C protocols and analysis methods. We thank Doug Koshland for providing the Mcd1 reduction and cohesion assay strains, and Matt Kaerberlein for rDNA marker loss strains. We also thank James Haber, Andrew Murray, Jasper Rine, Jessica Tyler, Alan Hinnebusch, Marc Gartenberg, and Vincent Guacci for kindly providing yeast strains and plasmids. We also thank Jef Boeke, Marc Gartenberg, and Dan Gottschling for providing Sir2 antibodies during a most dire time. Special thanks to Todd Stukenberg for microscopy assistance. Thanks to all the friends and lab mates for support and guidance. Lastly, endless thanks to my amazing mentor, Jeff Smith, for allowing me to join his lab and creating a work environment that made each day a true joy to spend in the laboratory. It makes departing that much harder.

References

- Altemose, N., K. H. Miga, M. Maggioni and H. F. Willard, 2014 Genomic characterization of large heterochromatic gaps in the human genome assembly. *PLoS Comput Biol* 10: e1003628.
- Anderson, D. E., A. Losada, H. P. Erickson and T. Hirano, 2002 Condensin and cohesin display different arm conformations with characteristic hinge angles. *J Cell Biol* 156: 419-424.
- Aparicio, O. M., B. L. Billington and D. E. Gottschling, 1991 Modifiers of position effect are shared between telomeric and silent mating-type loci in *S. cerevisiae*. *Cell* 66: 1279-1287.
- Austriaco, N. R., Jr., and L. P. Guarente, 1997 Changes of telomere length cause reciprocal changes in the lifespan of mother cells in *Saccharomyces cerevisiae*. *Proc Natl Acad Sci U S A* 94: 9768-9772.
- Avalos, J. L., K. M. Bever and C. Wolberger, 2005 Mechanism of sirtuin inhibition by nicotinamide: altering the NAD(+) cosubstrate specificity of a Sir2 enzyme. *Mol Cell* 17: 855-868.
- Baker, D. J., M. M. Dawlaty, T. Wijshake, K. B. Jeganathan, L. Malureanu *et al.*, 2013 Increased expression of BubR1 protects against aneuploidy and cancer and extends healthy lifespan. *Nat Cell Biol* 15: 96-102.
- Baker, D. J., K. B. Jeganathan, J. D. Cameron, M. Thompson, S. Juneja *et al.*, 2004 BubR1 insufficiency causes early onset of aging-associated phenotypes and infertility in mice. *Nat Genet* 36: 744-749.
- Bannister, A. J., P. Zegerman, J. F. Partridge, E. A. Miska, J. O. Thomas *et al.*, 2001 Selective recognition of methylated lysine 9 on histone H3 by the HP1 chromo domain. *Nature* 410: 120-124.
- Bardin, A. J., and A. Amon, 2001 Men and sin: what's the difference? *Nat Rev Mol Cell Biol* 2: 815-826.
- Bedalov, A., M. Hirao, J. Posakony, M. Nelson and J. A. Simon, 2003 NAD⁺-Dependent Deacetylase Hst1p Controls Biosynthesis and Cellular NAD⁺ Levels in *Saccharomyces cerevisiae*. *Molecular and Cellular Biology* 23: 7044-7054.
- Belli, G., E. Gari, L. Piedrafita, M. Aldea and E. Herrero, 1998 An activator/repressor dual system allows tight tetracycline-regulated gene expression in budding yeast. *Nucleic Acids Res* 26: 942-947.
- Belton, J. M., and J. Dekker, 2015 Measuring Chromatin Structure in Budding Yeast. *Cold Spring Harb Protoc* 2015: 614-618.

- Belton, J. M., B. R. Lajoie, S. Audibert, S. Cantaloube, I. Lassadi *et al.*, 2015 The Conformation of Yeast Chromosome III Is Mating Type Dependent and Controlled by the Recombination Enhancer. *Cell Rep* 13: 1855-1867.
- Bhalla, N., S. Biggins and A. W. Murray, 2002 Mutation of YCS4, a budding yeast condensin subunit, affects mitotic and nonmitotic chromosome behavior. *Mol Biol Cell* 13: 632-645.
- Biswas, M., N. Maqani, R. Rai, S. P. Kumaran, K. R. Iyer *et al.*, 2009 Limiting the extent of the RDN1 heterochromatin domain by a silencing barrier and Sir2 protein levels in *Saccharomyces cerevisiae*. *Mol Cell Biol* 29: 2889-2898.
- Bitto, A., A. M. Wang, C. F. Bennett and M. Kaerberlein, 2015 Biochemical Genetic Pathways that Modulate Aging in Multiple Species. *Cold Spring Harb Perspect Med* 5.
- Blank, M. F., S. Chen, F. Poetz, M. Schnolzer, R. Voit *et al.*, 2017 SIRT7-dependent deacetylation of CDK9 activates RNA polymerase II transcription. *Nucleic Acids Res* 45: 2675-2686.
- Bobola, N., R. P. Jansen, T. H. Shin and K. Nasmyth, 1996 Asymmetric accumulation of Ash1p in postanaphase nuclei depends on a myosin and restricts yeast mating-type switching to mother cells. *Cell* 84: 699-709.
- Boddy, M. N., P. Shanahan, W. H. McDonald, A. Lopez-Girona, E. Noguchi *et al.*, 2003 Replication Checkpoint Kinase Cds1 Regulates Recombinational Repair Protein Rad60. *Molecular and Cellular Biology* 23: 5939-5946.
- Boros, J., N. Arnoult, V. Stroobant, J. F. Collet and A. Decottignies, 2014 Polycomb repressive complex 2 and H3K27me3 cooperate with H3K9 methylation to maintain heterochromatin protein 1alpha at chromatin. *Mol Cell Biol* 34: 3662-3674.
- Bose, M. E., K. H. McConnell, K. A. Gardner-Aukema, U. Muller, M. Weinreich *et al.*, 2003 The Origin Recognition Complex and Sir4 Protein Recruit Sir1p to Yeast Silent Chromatin through Independent Interactions Requiring a Common Sir1p Domain. *Molecular and Cellular Biology* 24: 774-786.
- Brachmann, C. B., A. Davies, G. J. Cost, E. Caputo, J. Li *et al.*, 1998 Designer deletion strains derived from *Saccharomyces cerevisiae* S288C: a useful set of strains and plasmids for PCR-mediated gene disruption and other applications. *Yeast* 14: 115-132.
- Brachmann, C. B., J. M. Sherman, S. E. Devine, E. E. Cameron, L. Pillus *et al.*, 1995 The SIR2 gene family, conserved from bacteria to humans, functions in silencing, cell cycle progression, and chromosome stability. *Genes Dev* 9: 2888-2902.
- Brand, A. H., L. Breeden, J. Abraham, R. Sternglanz and K. Nasmyth, 1985 Characterization of a "silencer" in yeast: a DNA sequence with properties opposite to those of a transcriptional enhancer. *Cell* 41: 41-48.

- Brito, I. L., F. Monje-Casas and A. Amon, 2010 The Lrs4-Csm1 monopolin complex associates with kinetochores during anaphase and is required for accurate chromosome segregation. *Cell Cycle* 9: 3611-3618.
- Bryk, M., M. Banerjee, M. Murphy, K. E. Knudsen, D. J. Garfinkel *et al.*, 1997 Transcriptional silencing of Ty1 elements in the RDN1 locus of yeast. *Genes Dev* 11: 255-269.
- Buchwalter, A., and M. W. Hetzer, 2017 Nucleolar expansion and elevated protein translation in premature aging. *Nat Commun* 8: 328.
- Buck, S. W., C. M. Gallo and J. S. Smith, 2004 Diversity in the Sir2 family of protein deacetylases. *J Leukoc Biol* 75: 939-950.
- Buck, S. W., N. Maqani, M. Matecic, R. D. Hontz, R. D. Fine *et al.*, 2016 RNA Polymerase I and Fob1 contributions to transcriptional silencing at the yeast rDNA locus. *Nucleic Acids Res* 44: 6173-6184.
- Buck, S. W., J. J. Sandmeier and J. S. Smith, 2002 RNA polymerase I propagates unidirectional spreading of rDNA silent chromatin. *Cell* 111: 1003-1014.
- Burton, J. N., I. Liachko, M. J. Dunham and J. Shendure, 2014 Species-level deconvolution of metagenome assemblies with Hi-C-based contact probability maps. *G3 (Bethesda)* 4: 1339-1346.
- Bystricky, K., T. Laroche, G. van Houwe, M. Blaszczyk and S. M. Gasser, 2005 Chromosome looping in yeast: telomere pairing and coordinated movement reflect anchoring efficiency and territorial organization. *J Cell Biol* 168: 375-387.
- Bystricky, K., H. Van Attikum, M. D. Montiel, V. Dion, L. Gehlen *et al.*, 2009 Regulation of nuclear positioning and dynamics of the silent mating type loci by the yeast Ku70/Ku80 complex. *Mol Cell Biol* 29: 835-848.
- Canudas, S., and S. Smith, 2009 Differential regulation of telomere and centromere cohesion by the Scc3 homologues SA1 and SA2, respectively, in human cells. *J Cell Biol* 187: 165-173.
- Celic, I., H. Masumoto, W. P. Griffith, P. Meluh, R. J. Cotter *et al.*, 2006 The sirtuins hst3 and Hst4p preserve genome integrity by controlling histone h3 lysine 56 deacetylation. *Curr Biol* 16: 1280-1289.
- Chan, J. N., B. P. Poon, J. Salvi, J. B. Olsen, A. Emili *et al.*, 2011 Perinuclear cohibin complexes maintain replicative life span via roles at distinct silent chromatin domains. *Dev Cell* 20: 867-879.
- Chang, C. R., C. S. Wu, Y. Hom and M. R. Gartenberg, 2005 Targeting of cohesin by transcriptionally silent chromatin. *Genes Dev* 19: 3031-3042.
- Chen, H., M. Fan, L. M. Pfeffer and R. N. Larabee, 2012 The histone H3 lysine 56 acetylation pathway is regulated by target of rapamycin (TOR) signaling and functions directly in ribosomal RNA biogenesis. *Nucleic Acids Res* 40: 6534-6546.

- Chen, S., J. Seiler, M. Santiago-Reichert, K. Felbel, I. Grummt *et al.*, 2013 Repression of RNA polymerase I upon stress is caused by inhibition of RNA-dependent deacetylation of PAF53 by SIRT7. *Mol Cell* 52: 303-313.
- Chen, Y. F., C. C. Chou and M. R. Gartenberg, 2016 Determinants of Sir2-Mediated, Silent Chromatin Cohesion. *Mol Cell Biol* 36: 2039-2050.
- Chi, M. H., and D. Shore, 1996 SUM1-1, a dominant suppressor of SIR mutations in *Saccharomyces cerevisiae*, increases transcriptional silencing at telomeres and HM mating-type loci and decreases chromosome stability. *Mol Cell Biol* 16: 4281-4294.
- Choi, K., B. Szakal, Y. H. Chen, D. Branzei and X. Zhao, 2010 The Smc5/6 complex and Esc2 influence multiple replication-associated recombination processes in *Saccharomyces cerevisiae*. *Mol Biol Cell* 21: 2306-2314.
- Chou, C. C., Y. C. Li and M. R. Gartenberg, 2008 Bypassing Sir2 and O-acetyl-ADP-ribose in transcriptional silencing. *Mol Cell* 31: 650-659.
- Choy, J. S., R. Acuna, W. C. Au and M. A. Basrai, 2011 A role for histone H4K16 hypoacetylation in *Saccharomyces cerevisiae* kinetochore function. *Genetics* 189: 11-21.
- Ciosk, R., M. Shirayama, A. Shevchenko, T. Tanaka, A. Toth *et al.*, 2000 Cohesin's binding to chromosomes depends on a separate complex consisting of Scc2 and Scc4 proteins. *Mol Cell* 5: 243-254.
- Ciosk, R., W. Zachariae, C. Michaelis, A. Shevchenko, M. Mann *et al.*, 1998 An ESP1/PDS1 complex regulates loss of sister chromatid cohesion at the metaphase to anaphase transition in yeast. *Cell* 93: 1067-1076.
- Clarke L. and J. Carbon., 1983 Genomic substitutions of centromeres in *Saccharomyces cerevisiae*. *Nature* 305:23-28.
- Coic, E., G. F. Richard and J. E. Haber, 2006 *Saccharomyces cerevisiae* donor preference during mating-type switching is dependent on chromosome architecture and organization. *Genetics* 173: 1197-1206.
- Corbett, K. D., C. K. Yip, S. S. Ee L *et al.*, 2010 The monopolin complex crosslinks kinetochore components to regulate chromosome-microtubule attachments. *Cell* 142: 556-567.
- Crick, F., 1970 Central dogma of molecular biology. *Nature* 227: 561-563.
- Cuperus, G., and D. Shore, 2002 Restoration of silencing in *Saccharomyces cerevisiae* by tethering of a novel Sir2-interacting protein, Esc8. *Genetics* 162: 633-645.
- D'Ambrosio, C., C. K. Schmidt, Y. Katou, G. Kelly, T. Itoh *et al.*, 2008 Identification of cis-acting sites for condensin loading onto budding yeast chromosomes. *Genes Dev* 22: 2215-2227.
- Dang, W., K. K. Steffen, R. Perry, J. A. Dorsey, F. B. Johnson *et al.*, 2009 Histone H4 lysine 16 acetylation regulates cellular lifespan. *Nature* 459: 802-807.

- Daniloski, Z., K. K. Bisht, B. McStay and S. Smith, 2019 Resolution of human ribosomal DNA occurs in anaphase, dependent on tankyrase 1, condensin II, and topoisomerase IIalpha. *Genes Dev* 33: 276-281.
- Dasgupta, A., K. L. Ramsey, J. S. Smith and D. T. Auble, 2004 Sir Antagonist 1 (San1) is a ubiquitin ligase. *J Biol Chem* 279: 26830-26838.
- Defossez, P. A., R. Prusty, M. Kaeberlein, S. J. Lin, P. Ferrigno *et al.*, 1999 Elimination of replication block protein Fob1 extends the life span of yeast mother cells. *Mol Cell* 3: 447-455.
- Dekker, J., and E. Heard, 2015 Structural and functional diversity of Topologically Associating Domains. *FEBS Lett* 589: 2877-2884.
- Dekker, J., K. Rippe, M. Dekker and N. Kleckner, 2002 Capturing chromosome conformation. *Science* 295: 1306-1311.
- Derbyshire, M. K., K. G. Weinstock and J. N. Strathern, 1996 HST1, a new member of the SIR2 family of genes. *Yeast* 12: 631-640.
- Dheur, S., S. J. Saupe, S. Genier, S. Vazquez and J. P. Javerzat, 2011 Role for cohesin in the formation of a heterochromatic domain at fission yeast subtelomeres. *Mol Cell Biol* 31: 1088-1097.
- Dhillon, N., and R. T. Kamakaka, 2000 A histone variant, Htz1p, and a Sir1p-like protein, Esc2p, mediate silencing at HMR. *Mol Cell* 6: 769-780.
- Dhillon, N., J. Raab, J. Guzzo, S.J. Szyjka *et al.*, 2009 DNA polymerase epsilon, acetylases and remodellers cooperate to form a specialized chromatin structure at a tRNA insulator *EMBO J.*, 28: 2583-2600
- Dillinger, S., T. Straub, and A. Németh, 2017. Nucleolus association of chromosomal domains is largely maintained in cellular senescence despite massive nuclear reorganisation. *PLoS one* 12(6): e0178821.
- Dixon, J. R., S. Selvaraj, F. Yue, A. Kim, Y. Li *et al.*, 2012 Topological domains in mammalian genomes identified by analysis of chromatin interactions. *Nature* 485: 376-380.
- Drinneberg, I. A., D. E. Weinberg, K. T. Xie, *et al.*, 2009 RNAi in budding yeast. *Science* 326:544-550.
- Dodson, A. E., and J. Rine, 2016 Donor preference meets heterochromatin: Moonlighting activities of a recombinational enhancer in *Saccharomyces cerevisiae*. *Genetics* 204: 177-190.
- Downey, M., J. R. Johnson, N. E. Davey, B. W. Newton, T. L. Johnson *et al.*, 2015 Acetylome profiling reveals overlap in the regulation of diverse processes by sirtuins, gcn5, and esal. *Mol Cell Proteomics* 14: 162-176.

- Duan, Z., M. Andronescu, K. Schutz, S. McIlwain, Y. J. Kim *et al.*, 2010 A three-dimensional model of the yeast genome. *Nature* 465: 363-367.
- Dummer, A. M., Z. Su, R. Cherney, K. Choi, J. Denu *et al.*, 2016 Binding of the Fkh1 Forkhead Associated Domain to a Phosphopeptide within the Mph1 DNA Helicase Regulates Mating-Type Switching in Budding Yeast. *PLoS Genet* 12: e1006094.
- Ellahi, A., D. M. Thurtle and J. Rine, 2015 The Chromatin and Transcriptional Landscape of Native *Saccharomyces cerevisiae* Telomeres and Subtelomeric Domains. *Genetics* 200: 505-521.
- Ercan, S., J. C. Reese, J. L. Workman and R. T. Simpson, 2005 Yeast recombination enhancer is stimulated by transcription activation. *Mol Cell Biol* 25: 7976-7987.
- Erjavec, N. and T. Nystrom, 2007 Sir2p-dependent protein segregation gives rise to a superior reactive oxygen species management in the progeny of *Saccharomyces cerevisiae*. *Proc Natl Acad Sci USA*. 104: 10877-81.
- Fabrizio, P., C. Gattazzo, L. Battistella, M. Wei, C. Cheng *et al.*, 2005 Sir2 blocks extreme life-span extension. *Cell* 123: 655-667.
- Felsenstein, J., 2005 PHYLIP (Phylogeny Inference Package) version 3.6. Distributed by the author. Department of Genome Sciences, University of Washington, Seattle.
- Feser, J., D. Truong, C. Das, J. J. Carson, J. Kieft *et al.*, 2010 Elevated histone expression promotes life span extension. *Mol Cell* 39: 724-735.
- Ford, E., R. Voit, G. Liszt, C. Magin, I. Grummt *et al.*, 2006 Mammalian Sir2 homolog SIRT7 is an activator of RNA polymerase I transcription. *Genes Dev* 20: 1075-1080.
- Freeman, L., L. Aragon-Alcaide and A. Strunnikov, 2000 The condensin complex governs chromosome condensation and mitotic transmission of rDNA. *J Cell Biol* 149: 811-824.
- Fudenberg, G., M. Imakaev, C. Lu, A. Goloborodko *et al.* 2016 Formation of chromosomal domains by loop extrusion. *Cell Rep.*, 15:2038-2049
- Gallego-Paez, L. M., H. Tanaka, M. Bando, M. Takahashi, N. Nozaki *et al.*, 2014 Smc5/6-mediated regulation of replication progression contributes to chromosome assembly during mitosis in human cells. 25: 302-317.
- Ganji, M., I. A. Shaltiel, S. Bisht, E. Kim, A. Kalichava *et al.*, 2018 Real-time imaging of DNA loop extrusion by condensin. *Science* 360: 102-105.
- Ganley, A. R., S. Ide, K. Saka and T. Kobayashi, 2009 The effect of replication initiation on gene amplification in the rDNA and its relationship to aging. *Mol Cell* 35: 683-693.
- Ganley, A. R., and T. Kobayashi, 2014 Ribosomal DNA and cellular senescence: new evidence supporting the connection between rDNA and aging. *FEMS Yeast Res* 14: 49-59.

- Gard, S., W. Light, B. Xiong, T. Bose, A. J. McNairn *et al.*, 2009 Cohesinopathy mutations disrupt the subnuclear organization of chromatin. *J Cell Biol* 187: 455-462.
- Gardner, R. G., Z. W. Nelson and D. E. Gottschling, 2005 Degradation-mediated protein quality control in the nucleus. *Cell* 120: 803-815.
- Gartenberg, M. R., and J. S. Smith, 2016 The Nuts and Bolts of Transcriptionally Silent Chromatin in *Saccharomyces cerevisiae*. *Genetics* 203: 1563-1599.
- Gil, R., S. Barth, Y. Kanfi and H. Y. Cohen, 2013 SIRT6 exhibits nucleosome-dependent deacetylase activity. *Nucleic Acids Res* 41: 8537-8545.
- Ghavidel A., M. Prusinkiewicz, C. Swan, Z. R. Belak *et al.*, 2018 Rapid nuclear exclusion of Hcm1 in aging *Saccharomyces cerevisiae* leads to vacuolar alkalization and replicative senescence. *BioRxiv*.
- Girke, P., and W. Seufert, 2019 Compositional reorganization of the nucleolus in budding yeast mitosis. *Mol Biol Cell* 30: 591-606.
- Glynn, E. F., P. C. Megee, H. G. Yu, C. Mistrot, E. Unal *et al.*, 2004 Genome-wide mapping of the cohesin complex in the yeast *Saccharomyces cerevisiae*. *PLoS Biol* 2: E259.
- Gomes, A. P., N. L. Price, A. J. Ling, J. J. Moslehi, M. K. Montgomery *et al.*, 2013 Declining NAD(+) induces a pseudohypoxic state disrupting nuclear-mitochondrial communication during aging. *Cell* 155: 1624-1638.
- Gomes, P., T. Fleming Outeiro and C. Cavadas, 2015 Emerging Role of Sirtuin 2 in the Regulation of Mammalian Metabolism. *Trends Pharmacol Sci* 36: 756-768.
- Gotta, M., S. Strahl-Bolsinger, H. Renauld, T. Laroche, B. K. Kennedy *et al.*, 1997 Localization of Sir2p: the nucleolus as a compartment for silent information regulators. *Embo j* 16: 3243-3255.
- Gottschling, D. E., O. M. Aparicio, B. L. Billington and V. A. Zakian, 1990 Position effect at *S. cerevisiae* telomeres: reversible repression of Pol II transcription. *Cell* 63: 751-762.
- Grob, A., P. Roussel, J. E. Wright, B. McStay, D. Hernandez-Verdun *et al.*, 2009 Involvement of SIRT7 in resumption of rDNA transcription at the exit from mitosis. *J Cell Sci* 122: 489-498.
- Grummt, I., 2013 The nucleolus-guardian of cellular homeostasis and genome integrity. *Chromosoma* 122: 487-497.
- Guacci, V., and D. Koshland, 2012 Cohesin-independent segregation of sister chromatids in budding yeast. *Mol Biol Cell* 23: 729-739.
- Guacci, V., D. Koshland and A. Strunnikov, 1997 A direct link between sister chromatid cohesion and chromosome condensation revealed through the analysis of MCD1 in *S. cerevisiae*. *Cell* 91: 47-57.

- Haber, J. E., 2012 Mating-type genes and MAT switching in *Saccharomyces cerevisiae*. *Genetics* 191: 33-64.
- Haber, J. E., and J. P. George, 1979 A mutation that permits the expression of normally silent copies of mating-type information in *Saccharomyces cerevisiae*. *Genetics* 93: 13-35.
- Haber, J. E., D. T. Rogers and J. H. McCusker, 1980 Homothallic conversions of yeast mating-type genes occur by intrachromosomal recombination. *Cell* 22: 277-289.
- Hachinohe, M., F. Hanaoka and H. Masumoto, 2011 Hst3 and Hst4 histone deacetylases regulate replicative lifespan by preventing genome instability in *Saccharomyces cerevisiae*. *Genes Cells* 16: 467-477.
- Hagstrom, K. A., and B.J. Meyer, 2003 Condensin and cohesin: more than chromosome compactor and glue. *Nat. Rev. Genet.*, 4: 520-534.
- Hahn, M., S. Dambacher and G. Schotta, 2010 Heterochromatin dysregulation in human diseases. *J Appl Physiol* 109: 232-242.
- Hall, I. M., G. D. Shankaranarayana, K. Noma, N. Ayoub, A. Cohen *et al.*, 2002 Establishment and maintenance of a heterochromatin domain. *Science* 297: 2232-2237.
- Halme, A., S. Bumgarner, C. Styles and G. R. Fink, 2004 Genetic and epigenetic regulation of the FLO gene family generates cell-surface variation in yeast. *Cell* 116: 405-415.
- Hecht, A., T. Laroche, S. Strahl-Bolsinger, S. M. Gasser and M. Grunstein, 1995 Histone H3 and H4 N-termini interact with SIR3 and SIR4 proteins: a molecular model for the formation of heterochromatin in yeast. *Cell* 80: 583-592.
- Heidinger-Pauli, J. M., O. Mert, C. Davenport, V. Guacci and D. Koshland, 2010 Systematic reduction of cohesin differentially affects chromosome segregation, condensation, and DNA repair. *Curr Biol* 20: 957-963.
- Heinz, S., C. Benner, N. Spann, E. Bertolino, Y. C. Lin *et al.*, 2010 Simple combinations of lineage-determining transcription factors prime cis-regulatory elements required for macrophage and B cell identities. *Mol Cell* 38: 576-589.
- Heitz E., 1928 Das Heterochromatin derMoose. *Jb. Wiss. Bot.* 69: 728.
- Hendrickson, D. G., I. Soifer, B. J. Wranik, *et al.*, 2018 A new experimental platform facilitates assessment of the transcriptional and chromatin landscapes of aging yeast. *eLife* 7:e39911.
- Herranz, D., M. Muñoz-Martin, M. Cañamero, *et al.*, 2010 Sirt1 improves healthy ageing and protects from metabolic syndrome-associated cancer. *Nat Commun.* 1:3.
- Hickman, M. A., C. A. Froyd and L. N. Rusche, 2011 Reinventing heterochromatin in budding yeasts: Sir2 and the origin recognition complex take center stage. *Eukaryot Cell* 10: 1183-1192.

- Hickman, M. A., and L. N. Rusche, 2007 Substitution as a mechanism for genetic robustness: the duplicated deacetylases Hst1p and Sir2p in *Saccharomyces cerevisiae*. *PLoS Genet* 3: e126.
- Hirano, T., 2016 Condensin-Based Chromosome Organization from Bacteria to Vertebrates. *Cell* 164: 847-857.
- Hoggard, T. A., F. Chang, K. R. Perry, S. Subramanian, J. Kenworthy *et al.*, 2018 Yeast heterochromatin regulators Sir2 and Sir3 act directly at euchromatic DNA replication origins. *PLoS Genet* 14: e1007418.
- Hoppe, G. J., J. C. Tanny, A. D. Rudner, S. A. Gerber, S. Danaie *et al.*, 2002 Steps in Assembly of Silent Chromatin in Yeast: Sir3-Independent Binding of a Sir2/Sir4 Complex to Silencers and Role for Sir2-Dependent Deacetylation. *Molecular and Cellular Biology* 22: 4167-4180.
- Hsu, H. C., C. L. Wang, M. Wang, N. Yang, Z. Chen *et al.*, 2013 Structural basis for allosteric stimulation of Sir2 activity by Sir4 binding. *Genes Dev* 27: 64-73.
- Hu, Z., K. Chen, Z. Xia, M. Chavez, S. Pal *et al.*, 2014 Nucleosome loss leads to global transcriptional up-regulation and genomic instability during yeast aging. *Genes Dev* 28: 396-408.
- Huang, J., I. L. Brito, J. Villen, S. P. Gygi, A. Amon *et al.*, 2006 Inhibition of homologous recombination by a cohesin-associated clamp complex recruited to the rDNA recombination enhancer. *Genes Dev* 20: 2887-2901.
- Huang, J., and D. Moazed, 2003 Association of the RENT complex with nontranscribed and coding regions of rDNA and a regional requirement for the replication fork block protein Fob1 in rDNA silencing. *Genes Dev* 17: 2162-2176.
- Imai, S., C. M. Armstrong, M. Kaeberlein and L. Guarente, 2000 Transcriptional silencing and longevity protein Sir2 is an NAD-dependent histone deacetylase. *Nature* 403: 795-800.
- Imakaev, M., G. Fudenberg, R. P. McCord, N. Naumova, A. Goloborodko *et al.*, 2012 Iterative correction of Hi-C data reveals hallmarks of chromosome organization. *Nat Methods* 9: 999-1003.
- Iyer-Bierhoff, A., N. Krogh, P. Tessarz, T. Ruppert, H. Nielsen *et al.*, 2018 SIRT7-Dependent Deacetylation of Fibrillarin Controls Histone H2A Methylation and rRNA Synthesis during the Cell Cycle. *Cell Rep* 25: 2946-2954 e2945.
- Janssens, G. E., A. C. Meinema, J. Gonzalez, J. C. Wolters, A. Schmidt *et al.*, 2015 Protein biogenesis machinery is a driver of replicative aging in yeast. *Elife* 4: e08527.
- Jensen, R., G. F. Sprague, Jr. and I. Herskowitz, 1983 Regulation of yeast mating-type interconversion: feedback control of HO gene expression by the mating-type locus. *Proc Natl Acad Sci U S A* 80: 3035-3039.

- Jessberger, R., 2012 Age-related aneuploidy through cohesion exhaustion. *EMBO Rep* 13: 539-546.
- Jiang, J. C., E. Jaruga, M. V. Repnevskaya and S. M. Jazwinski, 2000 An intervention resembling caloric restriction prolongs life span and retards aging in yeast. *Faseb j* 14: 2135-2137.
- Johnson, L. M., P. S. Kayne, E. S. Kahn and M. Grunstein, 1990 Genetic evidence for an interaction between SIR3 and histone H4 in the repression of the silent mating loci in *Saccharomyces cerevisiae*. *Proc Natl Acad Sci U S A* 87: 6286-6290.
- Johzuka, K., and T. Horiuchi, 2007 RNA polymerase I transcription obstructs condensin association with 35S rRNA coding regions and can cause contraction of long repeat in *Saccharomyces cerevisiae*. *Genes Cells* 12: 759-771.
- Johzuka, K., and T. Horiuchi, 2009 The cis element and factors required for condensin recruitment to chromosomes. *Mol Cell* 34: 26-35.
- Kaeberlein, M., M. McVey and L. Guarente, 1999 The SIR2/3/4 complex and SIR2 alone promote longevity in *Saccharomyces cerevisiae* by two different mechanisms. *Genes Dev* 13: 2570-2580.
- Kanfi, Y., S. Naiman, G. Amir, *et al.*, 2012 The sirtuin SIRT6 regulates lifespan in male mice. *Nature*. 483: 218–221.
- Kegel, A., and C. Sjogren, 2010 The Smc5/6 complex: more than repair? *Cold Spring Harb Symp Quant Biol* 75: 179-187.
- Kennedy, B. K., N. R. Austriaco, Jr., J. Zhang and L. Guarente, 1995 Mutation in the silencing gene SIR4 can delay aging in *S. cerevisiae*. *Cell* 80: 485-496.
- Kennedy, B. K., M. Gotta, D. A. Sinclair, K. Mills, D. S. McNabb *et al.*, 1997 Redistribution of silencing proteins from telomeres to the nucleolus is associated with extension of life span in *S. cerevisiae*. *Cell* 89: 381-391.
- Kim, J. H., K. R. Titus, W. Gong, J. A. Beagan, Z. Cao *et al.*, 2018 5C-ID: Increased resolution Chromosome-Conformation-Capture-Carbon-Copy with in situ 3C and double alternating primer design. *Methods* 142: 39-46.
- Kimura, A., T. Umehara and M. Horikoshi, 2002 Chromosomal gradient of histone acetylation established by Sas2p and Sir2p functions as a shield against gene silencing. *Nat Genet* 32: 370-377.
- Klar, A. J., S. Fogel and K. Macleod, 1979 MAR1 -a Regulator of the HMa and HMalpha Loci in *SACCHAROMYCES CEREVISIAE*. *Genetics* 93: 37-50.
- Klar, A. J., J. B. Hicks and J. N. Strathern, 1981 Irregular transpositions of mating-type genes in yeast. *Cold Spring Harb Symp Quant Biol* 45 Pt 2: 983-990.

- Klar, A. J., J. B. Hicks and J. N. Strathern, 1982 Directionality of yeast mating-type interconversion. *Cell* 28: 551-561.
- Kobayashi, T., and A. R. Ganley, 2005 Recombination regulation by transcription-induced cohesin dissociation in rDNA repeats. *Science* 309: 1581-1584.
- Kobayashi, T., and T. Horiuchi, 1996 A yeast gene product, Fob1 protein, required for both replication fork blocking and recombinational hotspot activities. *Genes Cells* 1: 465-474.
- Kobayashi, T., T. Horiuchi, P. Tongaonkar, L. Vu and M. Nomura, 2004 SIR2 regulates recombination between different rDNA repeats, but not recombination within individual rRNA genes in yeast. *Cell* 117: 441-453.
- Kogut, I., J. Wang, V. Guacci, R. K. Mistry and P. C. Megee, 2009 The Scc2/Scc4 cohesin loader determines the distribution of cohesin on budding yeast chromosomes. *Genes Dev* 23: 2345-2357.
- Kozak, M. L., A. Chavez, W. Dang, S. L. Berger, A. Ashok *et al.*, 2010 Inactivation of the Sas2 histone acetyltransferase delays senescence driven by telomere dysfunction. *EMBO J* 29: 158-170.
- Kriegenburg, F., V. Jakopec, E. G. Poulsen, S. V. Nielsen, A. Roguev *et al.*, 2014 A chaperone-assisted degradation pathway targets kinetochore proteins to ensure genome stability. *PLoS Genet* 10: e1004140.
- Kruitwagen, T., P. Chymkowitz, A. Denoth-Lippuner, J. Enserink and Y. Barral, 2018 Centromeres License the Mitotic Condensation of Yeast Chromosome Arms. *Cell* 175: 780-795 e715.
- Kruitwagen, T., A. Denoth-Lippuner, B. J. Wilkins, H. Neumann and Y. Barral, 2015 Axial contraction and short-range compaction of chromatin synergistically promote mitotic chromosome condensation. *Elife* 4: e1039.
- Kwan, E. X., E. J. Foss, S. Tsuchiyama, G. M. Alvino, L. Kruglyak *et al.*, 2013 A natural polymorphism in rDNA replication origins links origin activation with calorie restriction and lifespan. *PLoS Genet* 9: e1003329.
- Lacoste, N., R. T. Utley, J. M. Hunter, G. G. Poirier and J. Cote, 2002 Disruptor of telomeric silencing-1 is a chromatin-specific histone H3 methyltransferase. *J Biol Chem* 277: 30421-30424.
- Ladurner, R., V. Bhaskara, P. J. Huis in 't Veld, et al., 2014 Cohesin's ATPase activity couples cohesin loading onto DNA with Smc3 acetylation. *Curr Biol*. 24(19):2228-2237.
- Lamming, D. W., M. Latorre-Esteves, O. Medvedik, S. N. Wong, F. A. Tsang *et al.*, 2005 HST2 mediates SIR2-independent life-span extension by calorie restriction. *Science* 309: 1861-1864.

- Lam Y. T., M.T. Aung-Htut, Y. L. Lim, *et al.*, 2011 Changes in reactive oxygen species begin early during replicative aging of *Saccharomyces cerevisiae* cells. *Free Radical Biol Med.* 50: 963-70.
- Lander, E. S., L. M. Linton, B. Birren, C. Nusbaum, M. C. Zody *et al.*, 2001 Initial sequencing and analysis of the human genome. *Nature* 409: 860-921.
- Landry, J., A. Sutton, S. T. Tafrov, R. C. Heller, J. Stebbins *et al.*, 2000 The silencing protein SIR2 and its homologs are NAD-dependent protein deacetylases. *Proc Natl Acad Sci U S A* 97: 5807-5811.
- Langmead, B., C. Trapnell, M. Pop and S. L. Salzberg, 2009 Ultrafast and memory-efficient alignment of short DNA sequences to the human genome. *Genome Biol* 10: R25.
- Larin, M. L., K. Harding, E. C. Williams, N. Lianga, C. Dore *et al.*, 2015 Competition between Heterochromatic Loci Allows the Abundance of the Silencing Protein, Sir4, to Regulate de novo Assembly of Heterochromatin. *PLoS Genet* 11: e1005425.
- Laurenson, P., and J. Rine, 1991 SUM1-1: a suppressor of silencing defects in *Saccharomyces cerevisiae*. *Genetics* 129: 685-696.
- Lavoie, B. D., E. Hogan and D. Koshland, 2004 In vivo requirements for rDNA chromosome condensation reveal two cell-cycle-regulated pathways for mitotic chromosome folding. *Genes Dev* 18: 76-87.
- Lazar-Stefanita, L., V. F. Scolari, G. Mercy, H. Muller, T. M. Guerin *et al.*, 2017 Cohesins and condensins orchestrate the 4D dynamics of yeast chromosomes during the cell cycle. *Embo j* 36: 2684-2697.
- Li, C., J. E. Mueller and M. Bryk, 2006 Sir2 represses endogenous polymerase II transcription units in the ribosomal DNA nontranscribed spacer. *Mol Biol Cell* 17: 3848-3859.
- Li, J., E. Coic, K. Lee, C. S. Lee, J. A. Kim *et al.*, 2012a Regulation of budding yeast mating-type switching donor preference by the FHA domain of Fkh1. *PLoS Genet* 8: e1002630.
- Li, L., L. Wang, L. Li, Z. Wang, Y. Ho *et al.*, 2012b Activation of p53 by SIRT1 inhibition enhances elimination of CML leukemia stem cells in combination with imatinib. *Cancer Cell* 21: 266-281.
- Li, M., B. J. Petteys, J. M. McClure, V. Valsakumar, S. Bekiranov *et al.*, 2010 Thiamine biosynthesis in *Saccharomyces cerevisiae* is regulated by the NAD⁺-dependent histone deacetylase Hst1. *Mol Cell Biol* 30: 3329-3341.
- Li, M., V. Valsakumar, K. Poorey, S. Bekiranov and J. S. Smith, 2013 Genome-wide analysis of functional sirtuin chromatin targets in yeast. *Genome Biol* 14: R48.
- Li, Q., K. R. Peterson, X. Fang and G. Stamatoyannopoulos, 2002 Locus control regions. *Blood* 100: 3077-3086.

- Li, Y., K. W. Muir, M. W. Bowler, J. Metz, C. H. Haering *et al.*, 2018 Structural basis for Scc3-dependent cohesin recruitment to chromatin. *Elife* 7.
- Lieberman-Aiden, E., N. L. van Berkum, L. Williams, M. Imakaev, T. Ragoczy *et al.*, 2009 Comprehensive mapping of long-range interactions reveals folding principles of the human genome. *Science* 326: 289-293.
- Lin, S. J., M. Kaerberlein, A. A. Andalis, L. A. Sturtz, P. A. Defossez *et al.*, 2002 Calorie restriction extends *Saccharomyces cerevisiae* lifespan by increasing respiration. *Nature* 418: 344-348.
- Lindstrom, D. L., and D. E. Gottschling, 2009 The mother enrichment program: a genetic system for facile replicative life span analysis in *Saccharomyces cerevisiae*. *Genetics* 183: 413-422, 411si-413si.
- Lindstrom, D. L., C. K. Leverich, K. A. Henderson and D. E. Gottschling, 2011 Replicative age induces mitotic recombination in the ribosomal RNA gene cluster of *Saccharomyces cerevisiae*. *PLoS Genet* 7: e1002015.
- Linke, C., E. Klipp, H. Lehrach, M. Barberis and S. Krobitsch, 2013 Fkh1 and Fkh2 associate with Sir2 to control CLB2 transcription under normal and oxidative stress conditions. *Front Physiol* 4: 173.
- Lister, L. M., A. Kouznetsova, L. A. Hyslop, D. Kalleas, S. L. Pace *et al.*, 2010 Age-related meiotic segregation errors in mammalian oocytes are preceded by depletion of cohesin and Sgo2. *Curr Biol* 20: 1511-1521.
- Liszt, G., E. Ford, M. Kurtev and L. Guarente, 2005 Mouse Sir2 homolog SIRT6 is a nuclear ADP-ribosyltransferase. *J Biol Chem* 280: 21313-21320.
- Liu, J., M. H. He, J. Peng, Y. M. Duan, Y. S. Lu *et al.*, 2016 Tethering telomerase to telomeres increases genome instability and promotes chronological aging in yeast. *Aging (Albany NY)* 8: 2827-2847.
- Liu, T., 2014 Use model-based Analysis of ChIP-Seq (MACS) to analyze short reads generated by sequencing protein-DNA interactions in embryonic stem cells. *Methods Mol Biol* 1150: 81-95.
- Longo, V. D., G. S. Shadel, M. Kaerberlein and B. Kennedy, 2012 Replicative and chronological aging in *Saccharomyces cerevisiae*. *Cell Metab* 16: 18-31.
- Loo, S., P. Laurenson, M. Foss, A. Dillin and J. Rine, 1995 Roles of ABF1, NPL3, and YCL54 in silencing in *Saccharomyces cerevisiae*. *Genetics* 141: 889-902.
- Luo, J., X. Sun, B. P. Cormack and J. D. Boeke, 2018 Karyotype engineering by chromosome fusion leads to reproductive isolation in yeast. *Nature* 560: 392-396.
- Lushnikova, T., A. Bouska, J. Odvody, W. D. Dupont and C. M. Eischen, 2011 Aging mice have increased chromosome instability that is exacerbated by elevated Mdm2 expression. *Oncogene* 30: 4622-4631.

- Mallm, J. P., and K. Rippe, 2015 Aurora Kinase B Regulates Telomerase Activity via a Centromeric RNA in Stem Cells. *Cell Rep* 11: 1667-1678.
- Marston, A. L., 2014 Chromosome segregation in budding yeast: sister chromatid cohesion and related mechanisms. *Genetics* 196: 31-63.
- Martin, C. A., J. E. Murray, P. Carroll, A. Leitch, K. J. Mackenzie *et al.*, 2016 Mutations in genes encoding condensin complex proteins cause microcephaly through decatenation failure at mitosis. *Genes Dev* 30: 2158-2172.
- Matecic, M., D. L. Smith, X. Pan, N. Maqani, S. Bekiranov *et al.*, 2010 A microarray-based genetic screen for yeast chronological aging factors. *PLoS Genet* 6: e1000921.
- Matheson, T. D., and P. D. Kaufman, 2016 Grabbing the genome by the NADs. *Chromosoma* 125: 361-371.
- McCleary, D. F., and J. Rine, 2017 Nutritional Control of Chronological Aging and Heterochromatin in *Saccharomyces cerevisiae*. *Genetics* 205: 1179-1193.
- McKinley, K. L., and I. M. Cheeseman, 2016 The molecular basis for centromere identity and function. *Nat Rev Mol Cell Biol* 17: 16-29.
- McNally, F. J., and J. Rine, 1991 A synthetic silencer mediates SIR-dependent functions in *Saccharomyces cerevisiae*. *Mol Cell Biol* 11: 5648-5659.
- Mehta, R., D. Chandler-Brown, F. J. Ramos, L. S. Shamieh and M. Kaeberlein, 2010 Regulation of mRNA translation as a conserved mechanism of longevity control. *Adv Exp Med Biol* 694: 14-29.
- Mekhail, K., J. Seebacher, S. P. Gygi and D. Moazed, 2008 Role for perinuclear chromosome tethering in maintenance of genome stability. *Nature* 456: 667-670.
- Messenguy, F., and E. Dubois, 2003 Role of MADS box proteins and their cofactors in combinatorial control of gene expression and cell development. *Gene* 316: 1-21.
- Michel, A. H., B. Kornmann, K. Dubrana, and D. Shore, 2005 Spontaneous rDNA copy number variation modulates Sir2 levels and epigenetic gene silencing. *Genes Dev.* 19:1199–1210.
- Michishita, E., R. A. McCord, E. Berber, M. Kioi, H. Padilla-Nash *et al.*, 2008 SIRT6 is a histone H3 lysine 9 deacetylase that modulates telomeric chromatin. *Nature* 452: 492-496.
- Miele, A., K. Bystricky and J. Dekker, 2009 Yeast silent mating type loci form heterochromatic clusters through silencer protein-dependent long-range interactions. *PLoS Genet* 5: e1000478.
- Mittal, N., J. C. Guimaraes, T. Gross, A. Schmidt, A. Vina-Vilaseca *et al.*, 2017 The Gcn4 transcription factor reduces protein synthesis capacity and extends yeast lifespan. *Nat Commun* 8: 457.

- Mizuguchi, T., G. Fudenberg, S. Mehta, J. M. Belton, N. Taneja *et al.*, 2014 Cohesin-dependent globules and heterochromatin shape 3D genome architecture in *S. pombe*. *Nature* 516: 432-435.
- Moazed, D., A. Kistler, A. Axelrod, J. Rine and A. D. Johnson, 1997 Silent information regulator protein complexes in *Saccharomyces cerevisiae*: a SIR2/SIR4 complex and evidence for a regulatory domain in SIR4 that inhibits its interaction with SIR3. *Proc Natl Acad Sci U S A* 94: 2186-2191.
- Moradi-Fard, S., J. Sarthi, M. Tittel-Elmer, M. Lalonde, E. Cusanelli *et al.*, 2016 Smc5/6 Is a Telomere-Associated Complex that Regulates Sir4 Binding and TPE. *PLoS Genet* 12: e1006268.
- Moretti, P., K. Freeman, L. Coodly and D. Shore, 1994 Evidence that a complex of SIR proteins interacts with the silencer and telomere-binding protein RAP1. *Genes Dev* 8: 2257-2269.
- Mortimer, R. K., and J. R. Johnston, 1959 Life span of individual yeast cells. *Nature* 183: 1751-1752.
- Mostoslavsky, R., K. F. Chua, D. B. Lombard, W. W. Pang, M. R. Fischer *et al.*, 2006 Genomic instability and aging-like phenotype in the absence of mammalian SIRT6. *Cell* 124: 315-329.
- Nagaoka, S. I., T. J. Hassold and P. A. Hunt, 2012 Human aneuploidy: mechanisms and new insights into an age-old problem. *Nat Rev Genet* 13: 493-504.
- Nakaseko, Y., N. Kinoshita and M. Yanagida, 1987 A novel sequence common to the centromere regions of *Schizosaccharomyces pombe* chromosomes. *Nucleic Acids Res* 15: 4705-4715.
- Nasmyth, K., 1987 The determination of mother cell-specific mating type switching in yeast by a specific regulator of HO transcription. *Embo j* 6: 243-248.
- Nasmyth, K. A., 1982 The regulation of yeast mating-type chromatin structure by SIR: an action at a distance affecting both transcription and transposition. *Cell* 30: 567-578.
- Nestorov, P., M. Tardat, and A. H. Peters, 2013 H3K9/HP1 and Polycomb: two key epigenetic silencing pathways for gene regulation and embryo development. *Curr. Top. Dev. Biol.* 104, 243–291.
- Neurohr, G. E., R. L. Terry, A. Sandikci, K. Zou, H. Li *et al.*, 2018 Deregulation of the G1/S-phase transition is the proximal cause of mortality in old yeast mother cells. *Genes Dev* 32: 1075-1084.
- Niccoli, T., and L. Partridge, 2012 Ageing as a risk factor for disease. *Curr Biol* 22: R741-752.
- Noma, K., T. Sugiyama, H. Cam, A. Verdel, M. Zofall *et al.*, 2004 RITS acts in cis to promote RNA interference-mediated transcriptional and post-transcriptional silencing. *Nat Genet* 36: 1174-1180.

- Nonaka, N., T. Kitajima, S. Yokobayashi, G. Xiao, M. Yamamoto *et al.*, 2002 Recruitment of cohesin to heterochromatic regions by Swi6/HP1 in fission yeast. *Nat Cell Biol* 4: 89-93.
- North, B. J., B. L. Marshall, M. T. Borra, J. M. Denu and E. Verdin, 2003 The human Sir2 ortholog, SIRT2, is an NAD⁺-dependent tubulin deacetylase. *Mol Cell* 11: 437-444.
- North, B. J., M. A. Rosenberg, K. B. Jeganathan, A. V. Hafner, S. Michan *et al.*, 2014 SIRT2 induces the checkpoint kinase BubR1 to increase lifespan. *Embo j* 33: 1438-1453.
- Ohkuni, K., and K. Kitagawa, 2011 Endogenous transcription at the centromere facilitates centromere activity in budding yeast. *Curr Biol* 21: 1695-1703.
- Ono, T., A. Losada, M. Hirano, M. P. Myers, A. F. Neuwald *et al.*, 2003 Differential contributions of condensin I and condensin II to mitotic chromosome architecture in vertebrate cells. *Cell* 115: 109-121.
- Oppikofer, M., S. Kueng, F. Martino, S. Soeroes, S. M. Hancock *et al.*, 2011 A dual role of H4K16 acetylation in the establishment of yeast silent chromatin. *Embo j* 30: 2610-2621.
- Pal, S., S. D. Postnikoff, M. Chavez and J. K. Tyler, 2018 Impaired cohesion and homologous recombination during replicative aging in budding yeast. *Sci Adv* 4: eaaq0236.
- Palacios, J. A., D. Herranz, M. L. De Bonis, S. Velasco, M. Serrano *et al.*, 2010 SIRT1 contributes to telomere maintenance and augments global homologous recombination. *J Cell Biol* 191: 1299-1313.
- Pan, X., P. Ye, D. S. Yuan, X. Wang, J. S. Bader *et al.*, 2006 A DNA integrity network in the yeast *Saccharomyces cerevisiae*. *Cell* 124: 1069-1081.
- Peng, X. P., S. Lim, S. Li, L. Marjavaara, A. Chabes *et al.*, 2018 Acute Smc5/6 depletion reveals its primary role in rDNA replication by restraining recombination at fork pausing sites. *PLoS Genet* 14: e1007129.
- Perkins, A. T., T. M. Das, L. C. Panzera and S. E. Bickel, 2016 Oxidative stress in oocytes during midprophase induces premature loss of cohesion and chromosome segregation errors. *Proc Natl Acad Sci U S A* 113: E6823-e6830.
- Perrod, S., M. M. Cockell, T. Laroche, H. Renauld, A. L. Ducrest *et al.*, 2001 A cytosolic NAD-dependent deacetylase, Hst2p, can modulate nucleolar and telomeric silencing in yeast. *Embo j* 20: 197-209.
- Petes, T. D., 1979 Yeast ribosomal DNA genes are located on chromosome XII. *Proc Natl Acad Sci U S A* 76: 410-414.
- Pidoux, A. L., and R. C. Allshire, 2004 Kinetochore and heterochromatin domains of the fission yeast centromere. *Chromosome Res* 12: 521-534.
- Pillus, L., and J. Rine, 1989 Epigenetic inheritance of transcriptional states in *S. cerevisiae*. *Cell* 59: 637-647.

- Platt, J. M., P. Ryvkin, J. J. Wanat, G. Donahue, M. D. Ricketts *et al.*, 2013 Rap1 relocalization contributes to the chromatin-mediated gene expression profile and pace of cell senescence. *Genes Dev* 27: 1406-1420.
- Porter, D. F., Y. Y. Koh, B. VanVeller, R. T. Raines and M. Wickens, 2015 Target selection by natural and redesigned PUF proteins. *Proc Natl Acad Sci U S A* 112: 15868-15873.
- Pryde, F. E., and E. J. Louis, 1999 Limitations of silencing at native yeast telomeres. *Embo j* 18: 2538-2550.
- Quinlan, A. R., and I. M. Hall, 2010 BEDTools: a flexible suite of utilities for comparing genomic features. *Bioinformatics* 26: 841-842.
- Raab, J. R., J. Chiu, J. Zhu, S. Katzman, S. Kurukuti, *et al.* 2012 Human tRNA genes function as chromatin insulators *EMBO J.*, 31: 330-350.
- Riesen, M., and A. Morgan, 2009 Calorie restriction reduces rDNA recombination independently of rDNA silencing. *Aging Cell* 8: 624-632.
- Rine, J., 1979 Regulation and Transposition of Cryptic Mating Type Genes in *Saccharomyces cerevisiae*, pp. University of Oregon, Eugene, OR.
- Rine, J., and I. Herskowitz, 1987 Four genes responsible for a position effect on expression from HML and HMR in *Saccharomyces cerevisiae*. *Genetics* 116: 9-22.
- Rine, J., J. N. Strathern, J. B. Hicks and I. Herskowitz, 1979 A suppressor of mating-type locus mutations in *Saccharomyces cerevisiae*: evidence for and identification of cryptic mating-type loci. *Genetics* 93: 877-901.
- Rodriguez-Colman, M. J., G. Reverter-Branchat, M. A. Sorolla, J. Tamarit, J. Ros *et al.*, 2010 The forkhead transcription factor Hcm1 promotes mitochondrial biogenesis and stress resistance in yeast. *J Biol Chem* 285: 37092-37101.
- Saksouk, N., E. Simboeck and J. Dejardin, 2015 Constitutive heterochromatin formation and transcription in mammals. *Epigenetics Chromatin* 8: 3.
- Salvi, J. S., J. N. Chan, C. Pettigrew, T. T. Liu, J. D. Wu *et al.*, 2013 Enforcement of a lifespan-sustaining distribution of Sir2 between telomeres, mating-type loci, and rDNA repeats by Rif1. *Aging Cell* 12: 67-75.
- Salvi, J. S., J. N. Chan, K. Szafranski, T. T. Liu, J. D. Wu *et al.*, 2014 Roles for Pbp1 and caloric restriction in genome and lifespan maintenance via suppression of RNA-DNA hybrids. *Dev Cell* 30: 177-191.
- Sasaki, T., B. Maier, A. Bartke and H. Scoble, 2006 Progressive loss of SIRT1 with cell cycle withdrawal. *Aging Cell* 5: 413-422.
- Satoh, A., C. S. Brace, N. Rensing, *et al.*, 2013 Sirt1 extends life span and delays aging in mice through the regulation of Nk2 homeobox 1 in the DMH and LH. *Cell metabolism*. 18: 416-30.

- Schalbetter, S. A., A. Goloborodko, G. Fudenberg, J. M. Belton, C. Miles *et al.*, 2017 SMC complexes differentially compact mitotic chromosomes according to genomic context. *Nat Cell Biol* 19: 1071-1080.
- Schleiffer, A., S. Kaitna, S. Maurer-Stroh, M. Glotzer, K. Nasmyth *et al.*, 2003 Kleisins: A Superfamily of Bacterial and Eukaryotic SMC Protein Partners. *Molecular Cell* 11: 571-575.
- Schlissel, G., M. K. Krzyzanowski, F. Caudron, Y. Barral and J. Rine, 2017 Aggregation of the Whi3 protein, not loss of heterochromatin, causes sterility in old yeast cells. *Science* 355: 1184-1187.
- Schober, H., V. Kalck, M. A. Vega-Palas, G. Van Houwe, D. Sage *et al.*, 2008 Controlled exchange of chromosomal arms reveals principles driving telomere interactions in yeast. *Genome Res* 18: 261-271.
- Shankaranarayana, G. D., M. R. Motamedi, D. Moazed and S. I. S. Grewal, 2003 Sir2 Regulates Histone H3 Lysine 9 Methylation and Heterochromatin Assembly in Fission Yeast. *Current Biology* 13: 1240-1246.
- Shay, J. W., and W. E. Wright, 2000 Hayflick, his limit, and cellular ageing. *Nat Rev Mol Cell Biol* 1: 72-76.
- Shou, W., K. M. Sakamoto, J. Keener, K. W. Morimoto, E. E. Traverso *et al.*, 2001 Net1 stimulates RNA polymerase I transcription and regulates nucleolar structure independently of controlling mitotic exit. *Mol Cell* 8: 45-55.
- Shou, W., J. H. Seol, A. Shevchenko, C. Baskerville, D. Moazed *et al.*, 1999 Exit from mitosis is triggered by Tem1-dependent release of the protein phosphatase Cdc14 from nucleolar RENT complex. *Cell* 97: 233-244.
- Shyian, M., S. Mattarocci, B. Albert, L. Hafner, A. Lezaja *et al.*, 2016 Budding Yeast Rif1 Controls Genome Integrity by Inhibiting rDNA Replication. *PLoS Genet* 12: e1006414.
- Sil, A., and I. Herskowitz, 1996 Identification of asymmetrically localized determinant, Ash1p, required for lineage-specific transcription of the yeast HO gene. *Cell* 84: 711-722.
- Sinclair, D. A., and L. Guarente, 1997 Extrachromosomal rDNA circles--a cause of aging in yeast. *Cell* 91: 1033-1042.
- Smeal, T., J. Claus, B. Kennedy, F. Cole and L. Guarente, 1996 Loss of transcriptional silencing causes sterility in old mother cells of *S. cerevisiae*. *Cell* 84: 633-642.
- Smith, D. L., Jr., C. Li, M. Matecic, N. Maqani, M. Bryk *et al.*, 2009 Calorie restriction effects on silencing and recombination at the yeast rDNA. *Aging Cell* 8: 633-642.
- Smith, J. S., and J. D. Boeke, 1997 An unusual form of transcriptional silencing in yeast ribosomal DNA. *Genes Dev* 11: 241-254.

- Smith, J. S., C. B. Brachmann, I. Celic, M. A. Kenna, S. Muhammad *et al.*, 2000 A phylogenetically conserved NAD⁺-dependent protein deacetylase activity in the Sir2 protein family. *Proc Natl Acad Sci U S A* 97: 6658-6663.
- Smith, J. S., C. B. Brachmann, L. Pillus and J. D. Boeke, 1998 Distribution of a limited Sir2 protein pool regulates the strength of yeast rDNA silencing and is modulated by Sir4p. *Genetics* 149: 1205-1219.
- Smith, J. S., E. Caputo and J. D. Boeke, 1999 A genetic screen for ribosomal DNA silencing defects identifies multiple DNA replication and chromatin-modulating factors. *Mol Cell Biol* 19: 3184-3197.
- Sollier, J., R. Driscoll, F. Castellucci, M. Foiani, S. P. Jackson *et al.*, 2009 The *Saccharomyces cerevisiae* Esc2 and Smc5-6 proteins promote sister chromatid junction-mediated intra-S repair. *Mol Biol Cell* 20: 1671-1682.
- Song, S., and F. B. Johnson, 2018 Epigenetic Mechanisms Impacting Aging: A Focus on Histone Levels and Telomeres. *Genes (Basel)* 9.
- Spencer, F., S. L. Gerring, C. Connelly and P. Hieter, 1990 Mitotic chromosome transmission fidelity mutants in *Saccharomyces cerevisiae*. *Genetics* 124: 237-249.
- Steffen, K. K., B. K. Kennedy and M. Kaeberlein, 2009 Measuring replicative life span in the budding yeast. *J Vis Exp*.
- Steffen, K. K., V. L. MacKay, E. O. Kerr, M. Tsuchiya, D. Hu *et al.*, 2008 Yeast life span extension by depletion of 60s ribosomal subunits is mediated by Gcn4. *Cell* 133: 292-302.
- Stephens, A. D., C. W. Quammen, B. Chang, J. Haase, R. M. Taylor, 2nd *et al.*, 2013 The spatial segregation of pericentric cohesin and condensin in the mitotic spindle. *Mol Biol Cell* 24: 3909-3919.
- Storici F., L. K. Lewis, and M. A. Resnick., 2001 *In vivo* site-directed mutagenesis using oligonucleotides. *Nat Biotechnol.* 19(8):773-6.
- Strahl-Bolsinger, S., A. Hecht, K. Luo and M. Grunstein, 1997 SIR2 and SIR4 interactions differ in core and extended telomeric heterochromatin in yeast. *Genes Dev* 11: 83-93.
- Straight, A. F., W. Shou, G. J. Dowd, C. W. Turck, R. J. Deshaies *et al.*, 1999 Net1, a Sir2-associated nucleolar protein required for rDNA silencing and nucleolar integrity. *Cell* 97: 245-256.
- Strathern, J. N., A. J. Klar, J. B. Hicks, J. A. Abraham, J. M. Ivy *et al.*, 1982 Homothallic switching of yeast mating type cassettes is initiated by a double-stranded cut in the MAT locus. *Cell* 31: 183-192.

- Suka, N., Y. Suka, A. A. Carmen, J. Wu and M. Grunstein, 2001 Highly specific antibodies determine histone acetylation site usage in yeast heterochromatin and euchromatin. *Mol Cell* 8: 473-479.
- Sullivan, B. A., and G. H. Karpen, 2004 Centromeric chromatin exhibits a histone modification pattern that is distinct from both euchromatin and heterochromatin. *Nat Struct Mol Biol* 11: 1076-1083.
- Sun, K., E. Coic, Z. Zhou, P. Durrens and J. E. Haber, 2002 *Saccharomyces* forkhead protein Fkh1 regulates donor preference during mating-type switching through the recombination enhancer. *Genes Dev* 16: 2085-2096.
- Sunshine, A. B., G. T. Ong, D. P. Nickerson, D. Carr, C. J. Murakami *et al.*, 2016 Aneuploidy shortens replicative lifespan in *Saccharomyces cerevisiae*. *Aging Cell* 15: 317-324.
- Sutani, T., T. Sakata, R. Nakato, K. Masuda, M. Ishibashi *et al.*, 2015 Condensin targets and reduces unwound DNA structures associated with transcription in mitotic chromosome condensation. *Nat Commun* 6: 7815.
- Swamy, K. B., C. H. Lin, M. R. Yen, C. Y. Wang and D. Wang, 2014 Examining the condition-specific antisense transcription in *S. cerevisiae* and *S. paradoxus*. *BMC Genomics* 15: 521.
- Szeto, L., and J. R. Broach, 1997 Role of alpha2 protein in donor locus selection during mating type interconversion. *Mol Cell Biol* 17: 751-759.
- Szeto, L., M. K. Fafalios, H. Zhong, A. K. Vershon and J. R. Broach, 1997 Alpha2p controls donor preference during mating type interconversion in yeast by inactivating a recombinational enhancer of chromosome III. *Genes Dev* 11: 1899-1911.
- Taddei A. and S.M. Gasser, 2012 Structure and function in the budding yeast nucleus. *Genetics* 192(1):107-29.
- Takeuchi, Y., T. Horiuchi and T. Kobayashi, 2003 Transcription-dependent recombination and the role of fork collision in yeast rDNA. *Genes Dev* 17: 1497-1506.
- Tamburini, B. A., and J. K. Tyler, 2005 Localized histone acetylation and deacetylation triggered by the homologous recombination pathway of double-strand DNA repair. *Mol Cell Biol* 25: 4903-4913.
- Tanner, K. G., J. Landry, R. Sternglanz and J. M. Denu, 2000 Silent information regulator 2 family of NAD-dependent histone/protein deacetylases generates a unique product, 1-O-acetyl-ADP-ribose. *Proc Natl Acad Sci U S A* 97: 14178-14182.
- Tanno, M., J. Sakamoto, T. Miura, K. Shimamoto and Y. Horio, 2007 Nucleocytoplasmic shuttling of the NAD⁺-dependent histone deacetylase SIRT1. *J Biol Chem* 282: 6823-6832.

- Tanny, J. C., and D. Moazed, 2001 Coupling of histone deacetylation to NAD breakdown by the yeast silencing protein Sir2: Evidence for acetyl transfer from substrate to an NAD breakdown product. *Proc Natl Acad Sci U S A* 98: 415-420.
- Teytelman, L., D. M. Thurtle, J. Rine and A. van Oudenaarden, 2013 Highly expressed loci are vulnerable to misleading ChIP localization of multiple unrelated proteins. *Proc Natl Acad Sci U S A* 110: 18602-18607.
- Thadani, R., F. Uhlmann and S. Heeger, 2012 Condensin, chromatin crossbarring and chromosome condensation. *Curr Biol* 22: R1012-1021.
- Thompson, J. S., X. Ling and M. Grunstein, 1994 Histone H3 amino terminus is required for telomeric and silent mating locus repression in yeast. *Nature* 369: 245-247.
- Tolhuis, B., R.J. Palstra, E. Splinter, F. Grosveld, and W. de Laat, 2002 Looping and interaction between hypersensitive sites in the active beta-globin locus. *Mol. Cell*, 10:1453-1465
- Toselli-Mollereau, E., X. Robellet, L. Fauque, S. Lemaire, C. Schiklenk *et al.*, 2016 Nucleosome eviction in mitosis assists condensin loading and chromosome condensation. *Embo j* 35: 1565-1581.
- Toth, A., R. Ciosk, F. Uhlmann, M. Galova, A. Schleiffer *et al.*, 1999 Yeast cohesin complex requires a conserved protein, Eco1p(Ctf7), to establish cohesion between sister chromatids during DNA replication. *Genes Dev* 13: 320-333.
- Treangen, T. J., and S. L. Salzberg, 2011 Repetitive DNA and next-generation sequencing: computational challenges and solutions. *Nat Rev Genet* 13: 36-46.
- Triolo, T., and R. Sternglanz, 1996 Role of interactions between the origin recognition complex and SIR1 in transcriptional silencing. *Nature* 381: 251-253.
- Trivedi, P., and P. T. Stukenberg, 2016 A Centromere-Signaling Network Underlies the Coordination among Mitotic Events. *Trends Biochem Sci* 41: 160-174.
- Tsang, C. K., H. Li and X. S. Zheng, 2007 Nutrient starvation promotes condensin loading to maintain rDNA stability. *EMBO J* 26: 448-458.
- Tsang, C. K. and X. F. S. Zheng, 2009 Opposing Role of condensin and radiation-sensitive gene RAD52 in ribosomal DNA stability regulation. *J. Biol. Chem.* 284: 21908–21919.
- Uhlmann, F., 2016 SMC complexes: from DNA to chromosomes. *Nat Rev Mol Cell Biol* 17: 399-412.
- Unal, E., J. M. Heidinger-Pauli, W. Kim, V. Guacci, I. Onn *et al.*, 2008 A molecular determinant for the establishment of sister chromatid cohesion. *Science* 321: 566-569.
- Utani, K., and M. I. Aladjem, 2018 Extra View: Sirt1 Acts As A Gatekeeper Of Replication Initiation To Preserve Genomic Stability. *Nucleus* 9: 261-267.

- Valenzuela, L., N. Dhillon and R. T. Kamakaka, 2009 Transcription independent insulation at TFIIC-dependent insulators. *Genetics* 183: 131-148.
- van der Waal, M. S., R. C. Hengeveld, A. van der Horst and S. M. Lens, 2012 Cell division control by the Chromosomal Passenger Complex. *Exp Cell Res* 318: 1407-1420.
- Vaquero, A., M. Scher, D. Lee, H. Erdjument-Bromage, P. Tempst *et al.*, 2004 Human SirT1 interacts with histone H1 and promotes formation of facultative heterochromatin. *Mol Cell* 16: 93-105.
- Vaquero, A., M. B. Scher, D. H. Lee, A. Sutton, H. L. Cheng *et al.*, 2006 SirT2 is a histone deacetylase with preference for histone H4 Lys 16 during mitosis. *Genes Dev* 20: 1256-1261.
- Vas, A. C., C. A. Andrews, K. Kirkland Matesky and D. J. Clarke, 2007 In vivo analysis of chromosome condensation in *Saccharomyces cerevisiae*. *Mol Biol Cell* 18: 557-568.
- Venter, J. C., M. D. Adams, E. W. Myers, P. W. Li, R. J. Mural *et al.*, 2001 The sequence of the human genome. *Science* 291: 1304-1351.
- Verdel, A., S. Jia, S. Gerber, T. Sugiyama, S. Gygi *et al.*, 2004 RNAi-mediated targeting of heterochromatin by the RITS complex. *Science* 303: 672-676.
- Verdin, E., M. D. Hirschey, L. W. Finley and M. C. Haigis, 2010 Sirtuin regulation of mitochondria: energy production, apoptosis, and signaling. *Trends Biochem Sci* 35: 669-675.
- Visintin, R., K. Craig, E. S. Hwang, S. Prinz, M. Tyers *et al.*, 1998 The phosphatase Cdc14 triggers mitotic exit by reversal of Cdk-dependent phosphorylation. *Mol Cell* 2: 709-718.
- Volpe, T. A., C. Kidner, I. M. Hall, G. Teng, S. I. Grewal *et al.*, 2002 Regulation of heterochromatic silencing and histone H3 lysine-9 methylation by RNAi. *Science* 297: 1833-1837.
- Wakeling, L. A., L. J. Ions, S. M. Escolme, S. J. Cockell, T. Su *et al.*, 2015 SIRT1 affects DNA methylation of polycomb group protein target genes, a hotspot of the epigenetic shift observed in ageing. *Hum Genomics* 9: 14.
- Wallrath, L. L. and S. C. Elgin, 1995 Position effect variegation in *Drosophila* is associated with an altered chromatin structure. *Genes. Dev.* 9, 1263-1277.
- Wang, B. D., D. Eyre, M. Basrai, M. Lichten and A. Strunnikov, 2005 Condensin binding at distinct and specific chromosomal sites in the *Saccharomyces cerevisiae* genome. *Mol Cell Biol* 25: 7216-7225.
- Warner, J. R., 1999 The economics of ribosome biosynthesis in yeast. *Trends Biochem Sci* 24: 437-440.
- Wasko, B. M., and M. Kaerberlein, 2014 Yeast replicative aging: a paradigm for defining conserved longevity interventions. *FEMS Yeast Res* 14: 148-159.

- Weiler, K. S., L. Szeto, and J. R. Broach, 1995 Mutations affecting donor preference during mating type interconversion in *Saccharomyces cerevisiae*. *Genetics* 139:1495–1510.
- Wierman, M. B., and J. S. Smith, 2014 Yeast sirtuins and the regulation of aging. *FEMS Yeast Res* 14: 73-88.
- Wiley, E. A., and V. A. Zakian, 1995 Extra telomeres, but not internal tracts of telomeric DNA, reduce transcriptional repression at *Saccharomyces* telomeres. *Genetics* 139: 67-79.
- Wilson, B. A., and J. Masel, 2011 Putatively noncoding transcripts show extensive association with ribosomes. *Genome Biol Evol* 3: 1245-1252.
- Winston, F., C. Dollard and S. L. Ricupero-Hovasse, 1995 Construction of a set of convenient *Saccharomyces cerevisiae* strains that are isogenic to S288C. *Yeast* 11: 53-55.
- Wood, A. J., A. F. Severson and B. J. Meyer, 2010 Condensin and cohesin complexity: the expanding repertoire of functions. *Nat Rev Genet* 11: 391-404.
- Wu, C., K. Weiss, C. Yang, M. A. Harris, B. K. Tye *et al.*, 1998 Mcm1 regulates donor preference controlled by the recombination enhancer in *Saccharomyces* mating-type switching. *Genes Dev* 12: 1726-1737.
- Wu, C. S., Y. F. Chen and M. R. Gartenberg, 2011 Targeted sister chromatid cohesion by Sir2. *PLoS Genet* 7: e1002000.
- Wu, X., and J. E. Haber, 1995 MATa donor preference in yeast mating-type switching: activation of a large chromosomal region for recombination. *Genes Dev* 9: 1922-1932.
- Wu, X., and J. E. Haber, 1996 A 700 bp cis-acting region controls mating-type dependent recombination along the entire left arm of yeast chromosome III. *Cell* 87: 277-285.
- Yang, B., A. Miller and A. L. Kirchmaier, 2008 HST3/HST4-dependent deacetylation of lysine 56 of histone H3 in silent chromatin. *Mol Biol Cell* 19: 4993-5005.
- Yang, B., B. M. Zwaans, M. Eckersdorff and D. B. Lombard, 2009 The sirtuin SIRT6 deacetylates H3 K56Ac in vivo to promote genomic stability. *Cell Cycle* 8: 2662-2663.
- Yang, J., M. A. McCormick, J. Zheng, Z. Xie, M. Tsuchiya *et al.*, 2015 Systematic analysis of asymmetric partitioning of yeast proteome between mother and daughter cells reveals "aging factors" and mechanism of lifespan asymmetry. *Proc Natl Acad Sci U S A* 112: 11977-11982.
- Yang, L., M. O. Duff, B. R. Graveley, G. G. Carmichael and L. L. Chen, 2011 Genomewide characterization of non-polyadenylated RNAs. *Genome Biol* 12: R16.
- Yeung, F., J. E. Hoberg, C. S. Ramsey, M. D. Keller, D. R. Jones *et al.*, 2004 Modulation of NF- κ B-dependent transcription and cell survival by the SIRT1 deacetylase. *EMBO J* 23: 2369-2380.

- Yoshida, K., J. Bacal, D. Desmarais, I. Padioleau, O. Tsaponina *et al.*, 2014 The histone deacetylases sir2 and rpd3 act on ribosomal DNA to control the replication program in budding yeast. *Mol Cell* 54: 691-697.
- Zhang, P., B. Tu, H. Wang, Z. Cao, M. Tang *et al.*, 2014 Tumor suppressor p53 cooperates with SIRT6 to regulate gluconeogenesis by promoting FoxO1 nuclear exclusion. *Proc Natl Acad Sci U S A* 111: 10684-10689.
- Zhang, W., J. Li, K. Suzuki, J. Qu, P. Wang *et al.*, 2015 Aging stem cells. A Werner syndrome stem cell model unveils heterochromatin alterations as a driver of human aging. *Science* 348: 1160-1163.
- Zhu, J., D. Heinecke, W. A. Mulla, W. D. Bradford, B. Rubinstein *et al.*, 2015 Single-Cell Based Quantitative Assay of Chromosome Transmission Fidelity. *G3 (Bethesda)* 5: 1043-1056.
- Zuin, J., J. R. Dixon, M. I. van der Reijden, Z. Ye, P. Kolovos *et al.*, 2014 Cohesin and CTCF differentially affect chromatin architecture and gene expression in human cells. *Proc Natl Acad Sci U S A* 111: 996-1001.